Durham E-Theses

The effect of fluorine substituents on the physical and structural properties of conjugated molecular materials

Collings, Jonathan C.

How to cite:

Collings, Jonathan C. (2002) *The effect of fluorine substituents on the physical and structural properties of conjugated molecular materials*, Durham theses, Durham University. Available at Durham E-Theses Online: http://etheses.dur.ac.uk/4175/

Use policy

University of Durham

The Effect of Fluorine Substituents on the Physical and Structural Properties of Conjugated Molecular Materials

By Jonathan C. Collings

Final Version

A thesis presented to the University of Durham in fulfilment of the thesis requirement for the degree of Doctor of Philosophy in Chemistry

1 2 DEC 2003

Declaration

I hereby declare that the original work presented in this thesis is entirely my own (except where otherwise stated).

I fully authorise the University of Durham to lend this thesis to other institutions or individuals for the purpose of scholarly research.

Dedication

To my parents for their continual love and support

Abstract

A series of selectively fluorinated tolans of the general formulae C_6F_5-$C\equiv C$-C_6H_4X and C_6H_5-$C\equiv C$-C_6F_4X (where X = I, Br, Cl) have been synthesized via homogeneous palladium-catalysed Sonogashira cross-coupling and organolithium chemistry. Several of their crystal structures have been solved from X-ray diffraction data, and their molecular packing is described in terms of arene-perfluoroarene and halogen-halogen interactions.

Diffraction-quality crystals of a number of binary arene-perfluoroarene complexes of hexafluorobenzene and octafluoronaphthalene with several mismatched polyaromatic hydrocarbons have been obtained and their crystal structures solved from X-ray diffraction data. All of the structures have been shown to consist of infinite stacks of alternating components. The individual structures are compared and contrasted in detail, and those of the HFB complexes are found to closely resemble those predicted from *ab initio* DFT calculations, which implies that the interactions are over 90 % electrostatic in nature, in contrast with previous calculations on related complexes.

A number of selectively fluorinated 4,4'-bis(phenylethynyl)tolan (BPET) derivatives containing fluorinated and non-fluorinated phenyl rings, have been synthesized from palladium-catalysed Sonogashira cross-coupling of various tolan-based precursors. They are observed to strongly absorb in the UV range 336 - 342nm, which are directly comparable to the absorptions for similarly fluorinated 1,4-bis(phenylethynyl)benzene derivatives which suggests that an effective conjugation length (ECL) of 3-4 repeat units is applicable for these phenylene ethynylene systems. They are observed to fluoresce very strongly in the range 372 – 410 nm.

The diethynylbenzene derivatives 1,4-diethynyltetrafluorobenzene and 1,4-diethynyl-2,5-difluorobenzene have been synthesized from the hydrodesilation of their trimethylsilylated precursors. Their crystal structures have been solved from X-ray diffraction data, and are described in terms of $C \equiv C\text{-}H \cdots F$ and $C \equiv C\text{-}H \cdots \pi(C \equiv C)$ interactions.

Acknowledgements

First and foremost, I would like to express my sincere gratitude to Prof. Todd B. Marder, who has had the dubious honour of being my supervisor for the past three (and three-quarter) years. Firstly, for allowing me the opportunity to pursue a Ph.D. in his research group, and make use of the excellent facilities in his lab. Secondly, for his continual interest, support, encouragement and strong suggestions, when things were not going as well as they could have been.

I would also like to take the opportunity of thanking my colleagues in the lab, during the above time. Firstly, my fellow Ph.D. students, Jacqui Burke, Ben Coapes, Chris Entwistle and Andy Cox, and the fourth-year project students, Karl Roscoe, Caroline Smith and Joanna Searing. In particular, I would like to reserve a special appreciation to two of our post-doctoral researchers, Dr Edward Robins, who helped me to get started in the lab, and Dr. Rhodri Thomas, who was present during most of my time, and who provided plenty of much-needed advice and encouragement. Also special thanks to Tolu Fasina and Dr. Shigera Shimada, who were visitors from Nigeria and Japan respectively, and who I'm sure are destined for great things.

Finally I would like to thank all of the departmental support staff, particularly those from the NMR and Mass Spectrometry services, Ms Jareka Dostal of the elemental analysis service, and the stores for catering for all my shopping needs. In particular I would like to express my appreciation to the X-ray diffraction service, who were responsible for collecting the data and solving the structures of numerous compounds and complexes, which were an

Table of Contents

Chapter Three: The Synthesis of Ethynyl Arenes via Homogeneous
                Palladium-Catalyzed Cross-Coupling: The Sonogashira
                Reaction

Chapter Four: An Introduction to the Arene-Perfluoroarene Interaction

Chapter Five: The Synthesis and Crystal Structures of Selectively
Halogenated Tolans of Formulae C_6F_5-C≡C-C_6H_4X and
C_6H_5-C≡C-C_6F_4X

Chapter Six: The Arene-Perfluoroarene Interaction in Mismatched Systems:
The Structures of Complexes of Polyaromatic Molecules with
Hexafluorobenzene and Octafluoronaphthalene

Chapter Seven: The Synthesis and Optical Properties of a Series of 4,4'-
bis(Phenylethynyl)tolan Oligomers Containing Fluorinated
and Non-fluorinated Phenyl Rings

Chapter Eight: The Synthesis and Crystal Structures of 1,4-diethynyltetra-
fluorobenzene and 1,4-diethynyl-2,5-difluorobenzene

Chapter Nine: Conclusions and Suggestions for Further Work

List of Figures and Schemes

xv

List of Tables

List of Abbreviations

Å	Angstrom
BPEA	1,4-bis(Phenylethynyl)anthracene
BPEB	1,4-bis(Phenylethynyl)benzene
BPET	4,4'-bis(Phenylethynyl)tolan
CCD	Charge-coupled Device
CT	Charge Transfer
δ	Chemical Shift
DCM	Dichloromethane
DFT	Density Functional Theory
DSC	Differential Scanning Calorimetry
DMF	Dimethylformamide
DMSO	Dimethylsulfoxide

DRAM	Dynamic Random Access Memory
ECL	Effective Conjugation Length
EPR	Electron Paramagnetic Resonance
GC-MS	Gas Chromatography – Mass Spectrometry
HOMO	Highest Occupied Molecular Orbital
HFB	Hexafluorobenzene
HMB	Hexamethylbenzene
HPLC	High Performance Liquid Chromatography
LC	Liquid Crystal
LCD	Liquid Crystal Display
LUMO	Lowest Unoccupied Molecular Orbital
NDR	Negative Differential Resistance
NMR	Nuclear Magnetic Resonance
m	Multiplet
MISFET	Metal Insulator Semiconductor Field Effect Transistor

mmol	Millimoles
mp	Melting Point
OAE	Oligo(aryleneethynylene)
OFN	Octafluoronaphthalene
OLED	Organic Light Emitting Diode
OPE	Oligo(phenyleneethynylene)
OPP	Oligo(para-phenylene)
OPV	Oligo(phenylene-vinylene)
OT	Oligothiophene
PA	Polyacetylene
PAni	Polyaniline
PAE	Poly(aryleneethynylene)
PBD	2-biphenyl-4-yl-5-(4-tert-butylphenyl)-1,3,4-oxadiazole
PE	Phenylene Ethynylene
PPE	Poly(phenyleneethynylene)

PPP	Poly(para-phenylene)
PPV	Poly(phenylenevinylene)
PPy	Polypyrrole
PT	Polythiophene
s	Singlet
SAM	Self Assembled Monolayer
SEC	Size Exclusion Chromatography
SET	Single Electron Transfer
SSH	Schreiffer-Su-Heeger
STM	Scanning Tunnelling Microscopy
TFT	Thin Film Transistor
THF	Tetrahydrofuran
TMS	Trimethylsilyl
TMSA	Trimethylsilylacetylene
XPS	X-ray Photoelectron Spectroscopy

Relevant Publications

'Arene-perfluoroarene interactions in crystal engineering 2: Octafluoro-naphthalene:diphenylacetylene complex (1/1)'

J. C. Collings, A. S. Batsanov, J. A. K. Howard and T. B. Marder, *Acta Crystallogr.* 2001, **C57**, 870.

'Arene-perfluoroarene interactions in crystal engineering. Part 3. Single-crystal structures of 1:1 complexes of octafluoronapthalene with fused-ring polyaromatic hydrocarbons'

J. C. Collings, K. P. Roscoe, R. L. Thomas, A. S. Batsanov, L. M. Stimson, J. A. K. Howard and T. B. Marder, *New J. Chem.*, 2001, **25**, 1410.

'Arene-perfluoroarene interactions in crystal engineering 5: Octafluoro-naphthalene:tetrathiafulvalene complex (1/1)'

A. S. Batsanov, J. C. Collings, J. A. K. Howard, T. B. Marder and D. F. Perepichka, *Acta Crystallogr.*, 2001, **C57**, 1306.

'Arene-perfluoroarene interactions in crystal engineering 6: Octafluoro-naphthalene:1,8-diaminonaphthalene complex (1/1)'.

A. S. Batsanov, J. C. Collings, J. A. K. Howard and T. B. Marder, *Acta Crystallogr.*, 2001, **E57**, 950.

'Arene-perfluoroarene interactions in crystal engineering 7: Single-crystal structures of 1:1 complexes of octafluoronaphthalene and hexafluorobenzene with acenaphthene'

J. C. Collings, A. S. Batsanov, J. A. K. Howard and T. B. Marder, *Cryst. Eng.* 2002, **5**, 37.

Conferences Attended

33rd Annual Universities of Scotland Inorganic Club Meeting

Heriot–Watt University, Edinburgh   September 20-21, 1999.

16th International Symposium on Fluorine Chemistry

University of Durham, UK.   July 16-21, 2000.

13th European Symposium on Fluorine Chemistry

University of Bordeaux, France,   July 15-20, 2001.

Chapter One

An Introduction to Conjugated Materials

1.1 Introduction to Conjugated Systems

Covalent bonds in molecules are formed by the contribution of atomic orbitals into molecular orbitals. Most molecular orbitals, such as σ-orbitals are confined to two adjacent atoms in a molecule. However, some molecular orbitals, such as π-orbitals, can be extended over more than two atomic centres. This extension is called delocalisation. Perhaps the most familiar examples of delocalised molecules are the arenes, in which the π-electrons are delocalised over all six carbons atoms of the benzene ring. However, conjugation is not merely confined to cyclic aromatic species, as many non-aromatic species are also conjugated. A simple example is butadiene. Although this is formally represented as two carbon-carbon double bonds linked by a single carbon-carbon bond, Hückel theory predicts that the π-orbitals from the highest occupied molecular orbital (HOMO) and the lowest unoccupied molecular orbital (LUMO) are actually delocalised over the entire molecule, including the formal single bond. This delocalisation is present in all molecules with alternating single and double bonds and is known as

1

conjugation. As the number of double bonds increases, the energy gap between the ground state HOMO and LUMO orbitals decreases. This means that π-electrons can be easily promoted into the LUMO orbitals by the action of UV radiation or even visible light, which is what happens in many natural light absorbers, such as the carotenes.

1.2 Conjugated Polymers

1.2.1 Introduction

It was predicted that an infinite polymer consisting of alternating double and single carbon-carbon bonds, as is shown in Figure 1.1, would have no HOMO-LUMO gap, just a half filled band, and would therefore be a conductor.[2] Much effort was devoted to the synthesis of the polymer, which is known as a polyacetylene (PA), and it was first prepared by polymerising acetylene gas. The initial synthesis resulted in a black, insoluble and intractable solid, but the synthetic procedure was later modified to produce PA films.[3] In contrast with theory, polyacetylene was found to be a semiconductor, with a band gap of 1.4 eV.[4] This required a modification of the original simplistic theory. A more rigorous treatment takes into the account the fact that single and double bonds have slightly differing bond lengths, which doubles the length of the repeat unit of the polymer.[5] This induces a gap in the band, dividing it into two bands: a valence band, which is fully occupied at absolute zero, and a conduction band, empty at the same temperature, which is the situation for inorganic semiconductors. A similar result was predicted theoretically several years earlier for one-dimensional conductors, and is known as the Peierl's distortion.[6]
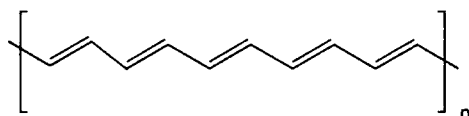
Figure **1.1** The Structure of Polyacetylene

The conductivity that had hitherto eluded the researchers was discovered when PA films were doped with small amounts of electron donating and accepting species such as sodium, iodine and arsenic pentafluoride.[7] Initial conductivities of up to 10^3 S cm^{-1} were obtained at room temperature, and the current record for the conductivity of doped PA is of the same magnitude as conductive metals (10^5 S cm^{-1}). Typically, the onset of high conductivity occurs for dopant concentrations in excess of 1 mole percent. For this, and other subsequent work, the originators Heeger, McDiarmid and Shirakawa were awarded the 2001 Nobel Prize for Chemistry.[8] Many other conjugated polymers have been synthesized and shown to be conducting upon doping, including poly-para-phenylene (PPP), polythiophene (PT), polypyrrole (PPy) and polyaniline (PAni), as shown in Figure **1.2**. Although all of these are based on an alternating double and single bond motif they have the advantages of being more stable than PA, and can also be rendered soluble in organic solvents for processing by substituting the aromatic rings with alkyl or alkyoxy substituents. These substituents can have a profound effects on the properties and morphology of the polymers, which was emphasised recently when a regioregularly substituted polythiophene was shown to become superconducting at low temperature.[9] Over the last two decades a tremendous amount of work has been carried out on these conjugated polymers. This has focused upon the synthesis, properties, theoretical aspects and potential applications of conjugated polymers and has

encompassed the efforts of both physicists and chemists. The section below presents a brief overview of the theory and applications of conjugated polymers. For a much more detailed review, the interested reader is referred to some of the comprehensive literature on the subject.[10]
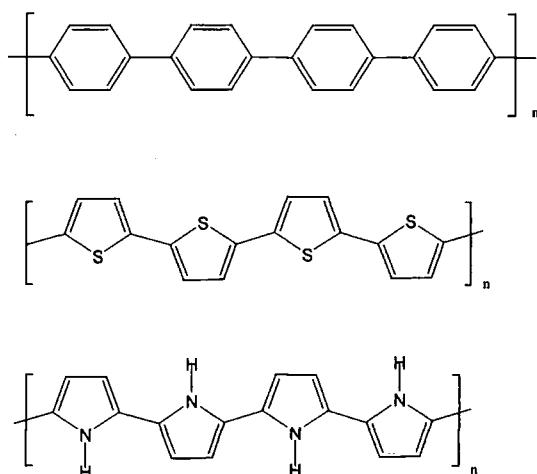
Figure **1.2** Examples of conjugated polymers

1.2.2 Theoretical Work

Several theories have been proposed to explain the dramatic increase in conductivity that takes place upon doping. It became clear from the outset that the doping was not the same as that for doped inorganic semiconductors, in which the dopants supply either free electrons to the conduction band or holes to the valence band, when it was shown by electron spin resonance (ESR) spectroscopy that, under moderate doping, the concentration of free spins in the polymer is too low to account for the degree of conductivity.[11] Only at large doping levels does the conduction mechanism begin to resemble that of

metals. A sophisticated theory was developed to model the structure of PA, which is known as Shrieffer-Su-Heeger (SSH) theory, after its originators.[12] They proposed that dopants create localised regions of positive or negative charge on the PA chain, which are known as charged solitons, as they are closely related to soliton waves. These solitons can be envisaged as a defect in the PA chain, in which the phase of the bond alternation is reversed.[13] Solitons are associated with a localised energy level, at the mid point of the band gap, and exist in two forms: negative solitons, in which the energy level is populated by a pair of electrons, and positive solitons, for which it is empty. The solitons and their energy level diagrams are shown in Figure **1.3**. Solitons are free to travel along the polymer chain at very little energy cost. As the doping level increases, so does the density of solitons, and above a certain concentration they begin to interfere with one another, and eventually merge into a partially filled band, which is responsible for the onset of metal-like conductivity.[14]
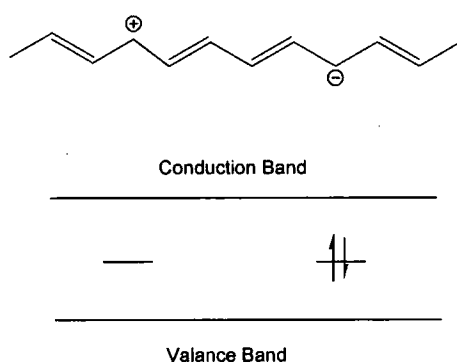
Figure **1.3**   Positive and negative solitons in Polyacetylene and their localised energy level diagrams

According to the theory, solitons are only stable in PA, in other conjugated polymers, doping induces entities known as polarons in the polymer chains. A polaron can be thought of as a charge, surrounded by a distortion in the

polymer chain, which is analogous to the situation when a small conjugated molecule becomes a radical ion.[15] A polaron in PT is shown in Figure **1.4**. Although the formation of a polaron requires energy to distort the conjugation, this is compensated for by a reduction in the ionisation energy required to produce it. Polarons occupy discrete energy levels in the forbidden gap, often close to the valence and conduction band edges. An increase in doping can result in one of two possibilities: more polarons can be formed, or more electrons are removed from or added to the existing polarons, to form what are termed bipolarons. It transpires that it requires less energy to form bipolarons. It is these bipolarons that are believed to be the active participants in the conduction process in doped polymers as they do not possess any spin. Experimental evidence supporting the existence of polarons and bipolarons has been obtained from optical spectra.[16] As with solitons, increasing levels of doping leads to polaron energy bands, and metallic conductivity.
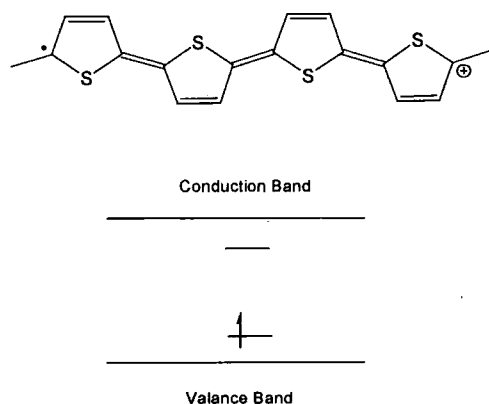
Figure **1.4**   The structure and energy level digram of a positive polaron in polythiophene

The exact mechanism of charge transportation in the conjugated polymers has been the subject of some controversy. Thus, it is not sufficient to consider only transport along the chains; interchain transport must also be considered.

This has been postulated to take place either by hopping[17] or tunnelling.[18] It appears that in contrast with inorganic materials, conjugated polymers have large regions of disorder. This means that the conduction properties of the polymers have a large degree of dependence on the polymer microstructure. This was proven when it was found that stretched PA films have a conductivity two orders of magnitude higher than unstretched ones.[19] Stretched films have been shown to have improved lateral packing and interchain co-ordination. The disorder of the polymers can be substantially reduced by the synthesis of regioregularly substituted polymers, such as regioregular poly(3-alkylthiophene). It was recently proposed that the conducting form of PAni contains crystalline regions surrounded by amorphous regions, the crystalline regions being conducting.[20]

1.2.3 Applications

The most obvious application of conjugated polymers is for plastic conductors. Unlike metals, they are semi-transparent, which makes their films of use for transparent electrodes,[21] and in antistatic coatings and electro-chromic windows. One important property of some conjugated polymers which has come to light over the last decade is that of electro-luminescence. The first report came in 1990, with the discovery that a thin film of undoped poly-para-phenylene vinylene, (PPV), prepared from a soluble sulphonium precursor, emitted green light when placed between an aluminium cathode and transparent indium tin oxide anode.[22] Such a device is known as an organic light emitting diode (OLED). Over the past decade, a large volume of literature on the subject has built up, which has been reviewed several times.[23] The main objectives of this research have been to increase the efficiencies of the

devices to obtain maximum brightness and minimum drive voltage, to change the colour of emission, and to improve the conditions for commercial fabrication. This can all be achieved by incorporating alkyl side chains on the polymer main chain. This renders the polymers soluble in most organic solvents for ease of fabrication, and can also shift the emission wavelength, and increase the efficiency. There is no need for a soluble precursor polymer and the substituted polymers are easily prepared by various condensation polymerisation reactions.[24] A particularly well-studied PPV derivative with branched side-groups is the orange emitter MEH-PPV.[25]

The simplistic theoretical model of the device operation consists of electrons being injected from the cathode and holes from the anode, although these are actually negative and positive polarons respectively. These 'electrons' and 'holes' can re-combine in the polymer layer, a process which can result in the emission of a photon. In most polymers, it is easier to inject holes than electrons, which leads to a lowering of the potential efficiency. This situation can be ameliorated by the use of a lower work function cathode such as calcium, although these are susceptible to atmospheric degradation. Another alternative is to sandwich a layer of an electron transporting material between the cathode and the polymer. One commonly used compound is the molecular material 2-biphenyl-4-yl-5-(4-tert-butylphenyl)-1,3,4-oxadiazole (PDB).[26] This can be sublimed onto the cathode under vacuum, which is undesirable for commercial fabrication, or spin coated as a dispersion in a polymer matrix. One can also increase the electron affinity of the polymer by incorporating cyano groups, efficiencies of 4 % have been reported for these devices.[27] Commercial polymeric OLEDs have recently become available.[28]

The opposite process to light emission is photo-induced electron transfer, which occurs when the OLED is in reverse bias. An incident photon generates an electron-hole pair of charge carriers, which are available for conduction; in

this way the OLED acts as a photocell.[29] However, this effect is very weak in films of instrinsic PPV. Later it was found that a substituted PPV, with a layer of a fullerene derivative as an acceptor, is much more efficient.[30] Dramatic increases in efficiency were made when the fullerene was incorporated directly into the polymer composition, which is known as a bulk heterojunction structure. Similar results were achieved with a mixture of acceptor conjugated polymers in conjunction with PPV.[31] It is remarkable in that the quantum efficiency for charge separation approaches unity, and the charge-transfer state is metastable. This work has paved the way for large-area photo-voltaic cells with efficiencies comparable to those of silicon based devices.[32]

1.2.4 Fluorinated Polymers

There has been comparatively little work carried out on fluorinated conjugated polymers. Partially fluorinated PPV co-polymers containing perflourinated and non-fluorinated phenylene groups have been prepared. The UV-vis absorption spectra of the polymers were observed to be strongly shifted to the blue region with increasing fluorine content. The polymers have been used in OLEDs, where a slight blue shift in the electro-luminescence of the more highly fluorinated polymers was noted.[33] PPV containing mono-fluorinated groups showed a similar blue shift, however, the di-fluorinated PPV derivative showed a substantial red-shift.[34] The quantum efficiencies of these OLEDs were observed to be a factor of ten higher than the non-fluorinated devices, although the threshold voltages were higher.[35]

1.3 Conjugated Oligomers

1.3.1 Introduction

Conjugated polymers are made by random statistical processes, which has several adverse affects on their homogeneity. Firstly, the polymers are composed of chains of varying lengths, the extent of which is quantified by the term polydispersity, which approaches unity as the chains become more uniform in length. Secondly, polymers can contain numerous structural defects, as well as impurities. Thirdly, although conjugated polymers are more crystalline than most polymers, they contain amorphous regions. These facts make it difficult to obtain reliable structure / property information from conjugated polymers. Despite advances in well-controlled living polymerisations, precise control of conjugated polymer homogenenity is unobtainable at the present time. However, well-defined, defect-free, monodisperse conjugated oligomers, which are composed of fewer repeat units, can be obtained through careful synthesis, and can serve as species for reliable structure / property correlation.[36] Homologous series of conjugated oligomers can be synthesised and their properties mapped out as function of their number of repeat units. Often, the properties will tend asomptopically towards those of their respective polymer. Oligomers can also reveal information about the packing as they often crystallise in a uniform manner, although it is often difficult to obtain crystals which are suitable for single-crystal X-ray diffraction. Conjugated oligomers are also potentially useful materials in their own right, and have been employed in several applications.

There are two main approaches to oligomer synthesis. The random approach is analogous to condensation polymerisation, except that the polymerisation is prevented from going to completion, either by moderating the reaction conditions, using a non-stoichiometric mixture of monomers, or by the introduction of end-capping reagents. This approach affords mixtures of oligomers with a statistical distribution of molecular weights, which can be separated by chromotographic techniques such as size exclusion chromatography (SEC) or high-performance liquid chromotography (HPLC). The other is the step-by-step approach, which affords well-defined oligomeric products, that are usually isolated at each step. A sub-category of this is the modular iterative approach, which has the advantage of an exponential growth in molecular weight. During the course of the last century, several conjugated oligomers, or species containing oligomeric moieties, have been synthesized or isolated as natural products, such as the carrotenoids.[37] However, it is only in recent years that the systematic synthesis of several series of conjugated oligomers has been attempted, with a view to establishing structure / property relationships.

Oligomers based upon polyacetylene are known as oligoenes. Series of these have been synthesized by both random and step-by-step approaches. They are usually synthesized with alkyl end groups to confer stability.[38] Oligo-para-phenylenes (OPPs) have also been synthesised by random approaches, and a modular approach, in which the length of the oligomer doubles with each step.[39] Although, unlike the oligoenes, they are not inherently unstable, and the phenylene rings are usually alkylated in order to impart solubility. However, this alkylation can sterically compromise the planarity of the rings, which interferes with the conjugation. A strategy for planarising of the phenylene rings, and therefore increasing the conjugation, is to synthesise ladder-type oligophenylenes, with methylene bridges between phenylene rings.[40] There has also been considerable interest in oligo-phenylene-

vinylenes (OPVs) which can model the PPV polymers used in OLEDs. Oligomers of up to eight repeat units have been synthesised in various step-wise approaches, including a modular orthogonal one, in which non-interacting coupling reactions are used to form the carbon-carbon double bonds.[41]

Oligothiophenes (OTs) represent the conjugated oligomer in which there has been the most intense interest in recent years.[42] Most are linked at the 2,5-positions, and are known as α-OTs. Some of the rings are usually substituted with alkyl groups to soublize the longer oligomers, and stabilise the reactive terminal positions. Substituted oligothiophenes up to the dodecamer have been synthesized, through the use of step-wise methodologies, and subsequently characterised.[43] An OT containing 27 repeat units represents the longest conjugated oligomer to have been synthesized thus far.[44] Special techniques have been used to synthesize regioregularly substituted OTs of up to 16 repeat units, which show superior properties compared to non-regioregularly substituted ones.[45]

1.3.2 Physical Properties

UV-vis absorption spectroscopy can give valuable information about the energy gap between the HOMO and LUMO levels of these oligomers. The lowest-energy absorption maximum is equal to the energy gap. A comparison of the absorption spectra of conjugated oligomers of increasing length reveals few differences, except for red-shifts in the absorption maxima. A plot of the lowest-energy absorption maximum against inverse oligomer chain length

(1/n) is shown in Figure **1.5**. For the shorter oligomers it is linear, and an extrapolation to the y-axis was thought to give the band gap of the corresponding polymer. However, these extrapolated values are usually found to be of lower energy than the ones obtained experimentally from the polymers. This discrepancy was initially thought to be due incomplete conjugation due to defects in the polymer. However, a deviation from linearity is also observed for the higher-order oligomers, which are defect-free, indicating that it is a fundamental property of the conjugated systems. An effective conjugation length (ECL) can be defined for the each polymer as the number of repeat units of the corresponding oligomer which has an extrapolated absorption energy equal (or closest) to that observed for the polymer. For most conjugated polymers, the ECL is about ten repeat units.[46] It was thought that the low conjugation lengths were due to twisting of some of the rings, which would break conjugation; however, the ECL of the rigorously planar ladder-PPP, was also found to be around ten repeat units.[47]
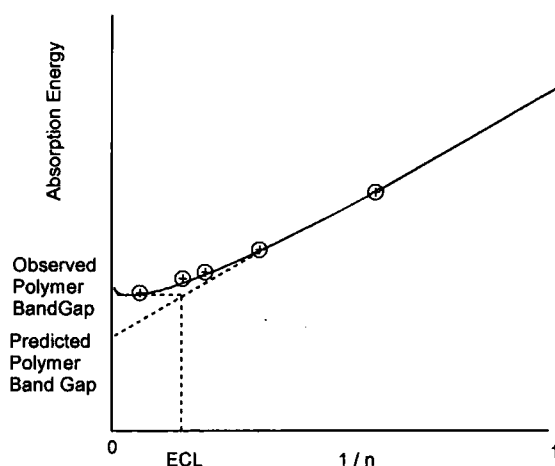
Figure **1.5**   Plot of the maximum absorption versus inverse chain length for a series of conguated oligomers

There has been much interest in the electrochemical properties of conjugated

oligomers, as the anions and cations produced are thought to be closely related to the polarons and bipolarons that have been held responsible for the conductive properties of conjugated polymers. Thin films of conjugated OPVs and α-OTs have been investigated by cyclic voltammetry.[48] Systematic studies were later carried out on a series of these oligomers, often substituted by terminal end groups to prevent side-reactions. In general, the potentials of the first oxidation were found to decrease almost linearly with inverse chain length.[49] In the longer oligomers, a second oxidation peak appears, which also decreases with inverse chain length. The potential difference between the first and second oxidation potentials decreases with increasing chain length as a result of increased separation between the charges. Single two-electron oxidation steps were observed for the longer oligomers, consistent with the formation of two polarons, which is in agreement with theoretical calculations.[50] The radical cations of OTs and oligopyrroles in certain solvents show very weak electron-paramagnetic resonance (EPR) in solution, which has been suggested to be a result of the formation of π-stacked dimers,[51] a view that has recently been confirmed by crystallographic studies.[52] These dimers have been proposed as an alternative to bipolarons, as the charge carriers in heavily doped conjugated polymers.[53]

It is usual to think of all molecular materials as insulators, in which the electrons are confined to localised orbitals in the molecules, and there are no available charge carriers. However, most conjugated oligomers are in fact p-type semiconductors, although with low conductivities if sufficiently pure. The explanation for this is two-fold. Firstly, in the solid state there is a small interaction between the orbitals of neighbouring molecules, which leads to a slight dispersion of the molecular energy levels into narrow bands.[54] In most organic molecules this is negligible; however, in those with extensive π-systems, such as conjugated oligomers, it is significant. In solid state physics

parlance, the HOMO becomes the valence band, and the LUMO the conduction band. The width of the bands is proportional to the resonance integrals and is strongly anisotropic. Secondly, conjugated oligomers have a relatively small HOMO-LUMO energy gap, which is a requirement for efficient semiconductors. The presence of trace acceptor impurities leads to an excess of holes in the valence band, therefore, most oligomers are p-type semiconductors. The exact method of conduction of these holes is still not fully understood. Measurement of the mobilities of the charge carriers, can lead to an understanding of the processes involved, which are believed to be dependant on temperature.[55] At low temperatures, high mobilities are observed, which is typical of band-type conduction. However, at room temperature, the mobilities are significantly lower, which indicates charge transport by a hopping mechanism from neighbouring localised sites, which are thought to be similar to radical ions.

Oligothiophenes have been doped with materials such as iodine, which results in conductivities close to those of conducting polymers.[56] It is only recently that reliable measurements have been made on ultra-pure samples obtained by zone refinement. Impurities can act as both dopants and charge traps, which strongly affect the electrical conductivity. Both the conductivity of doped oligomers and the mobility of undoped oligomers have been shown to be strongly anisotropic. This is a result of the anisotropic nature of their packing in the solid state.[57] The crystal structures of most oligomers have shown the molecules to be arranged in layers, with a herringbone packing. The sexithiophenes have two stable polymorphs, a high temperature one and a low temperature one. These have very similar structures, but differ slightly in the amount of overlap between the π-orbitals.[58] A similar situation was observed for quaterthiophene.[59] The band structure of the high temperature polymorph of sexithiophene has been determined by extended Hückel calculations.[60]

1.3.3 Oligomeric Devices

The fact that conjugated oligomers are semiconducting means that they can be used in various electronic devices, particularly those where their properties are superior to those of undoped conjugated polymers, due to their higher charge carrier mobility, the best example of which is the thin film transistor (TFT).[61] This is a type of metal-insulator-semiconductor field–effect transistor (MISFET), in which a thin film of semiconducting material provides the active layer. Such devices are envisaged as key large-area components for both display drivers and memory elements in transaction cards and identification tags.[62]

A MISFET consists of a layer of semi-conducting material on top of an insulator layer, between two terminals called the source and drain, and a third terminal called the gate, isolated from the semiconducting layer by the insulator. Applying a sufficient voltage to the gate attracts minority charge carriers to the interface of the semiconductor and insulator layers. This is known as inversion, and gives rise to a conduction channel between the drain and source, and the FET is said to be in an 'on' state. If, however, the gate voltage is removed or reversed, the charge carriers are expelled from the interface, forming a depletion region, which is not conducting and thus there is no conduction channel between the drain and source, and the FET is in the 'off' state.[63] FETs are characterised by their 'on' / 'off' current ratio, which is a measure of the conductivity in the 'on' state compared to the 'off' state. To be of use in practical application, this ratio must be higher than 10^7. In order to achieve this, the semiconductor must have low intrinsic conductivity but high

16

charge carrier mobility. Measurement of the electrical properties of the FET allows accurate determination of the field-effect mobility of the charge carriers in the oligomer.

Initial attempts at organic TFTs were based on undoped polythiophenes. However, it was found that the device performance was poor due to the conductivity in the 'off' state being too high, probably because of the presence of residual dopants from their polymerisation.[64] Later, much better results were achieved using regioregular polythiophenes, which should have important industrial uses.[65] It was suggested instead that OTs be used, as these have very low conductivities if sufficiently pure. Early devices based on unsubstituted sexithiophene displayed poor performance, which was probably a result of low purity of the sample.[66] Improved purification procedures gave large improvements in performance, and other conjugated oligomers have been used.[67] It was found that device performance is also very dependent on the conditions used in the sublimation step. Films made under low sublimation rates and high substrate temperatures tended to exhibit better device performance.[68] The morphology of these films was studied by X-ray diffraction, polarised UV-vis spectroscopy and scanning electron microscopy (SEM),[69] which showed better ordering of the oligomers in the low-temperature films. The oligomers tended to be aligned perpendicular to the substrate, so the current from drain to source is transmitted through the closely packed π-orbitals, which leads to higher mobilities. End-group substituted sexithiopenes are soluble enough to allow film deposition by spin coating during the manufacture of the devices.[70] Very efficient FETs have also been based on single crystals of sexithiophene.[71]

Congugated oligomers have been used extensively in OLEDs, especially as they can be sublimed or, if soluble, spin-coated into amorphous films. They are generally not as efficient as their polymeric counterparts, and deteriorate

more rapidly, which has been attributed to their crystallisation. OPVs have been used in single-layer OLEDs which resulted in devices of lower intensity emission and lower efficiency than the corresponding polymers.[72] A homologous series of OPVs was synthesed which showed a large emission range.[73] Blue-emitting sexi-para-phenylenes have also been used.[74] OTs generally result in devices with very low efficiencies, which has been ascribed to their poor electron transporting characteristics. However, several efficient devices based upon their β-substituted derivatives have recently been created.[75] OTs have also been used in photo-voltaic applications such as solar cells. Devices based on octathiophene have been obtained with solar conversion efficiencies of 0.6%.[76]

1.3.4 Fluorinated Oligomers

There have been few instances of fluorinated conjugated oligomers reported in the literature, which is surprising in view of the fact that they are electron-deficient and could be suitable candidates for use as electron-transporting materials in OLEDs. A homologous series of perfluorinated OPPs has been synthesized, for such an application.[77] The devices created were shown to have increased luminescence and lower operating voltages than ones without the layers of such molecules. Perfluorinated sexithiophene has also been synthesized by similar methods.[78] Several partially fluorinated OPVs and OPPs containing perfluorinated phenylene groups have been synthesized and used as electron transporting layers in OLEDs.[79] In all cases, the quantum efficiencies of the devices were increased by the oligomer layers. The properties of several partially fluorinated distyrylbenzene derivatives have been examined.[80] It was found that increased fluorine substitution does not

alter the HOMO-LUMO gap of these compounds, but does reduce their first reduction potentials. These and related compounds are being explored for possible use in optical applications such as OLEDs and other devices.

1.4 References

1.   a) P. W. Atkins, *Physical Chemistry*, 5th Ed., Oxford University Press, Oxford, p. 493; b) L. Salem, *The Molecular Orbital Theory of Conjugated Systems*, Benjamin, New York, 1966.

2.   J. C. W. Chien, *Polyacetylene: Chemistry, Physics and Materials Science*, Academic Press, London, 1984.

3.   T. Ito, H. Shirakawa and S. Ikeda, *J. Polym. Sci., Polym. Chem. Ed.*, 1974, **12**, 11.

4.   H. Shirakawa, T. Ito and S. Ikeda, *Polym. J.*, 1973, **4**, 460.

5.   M. Hatano, S. Kambara and S. Okamoto, *J. Polym. Sci.*, 1961, **51**, S26.

6.   R. Peierls, *Quantum Theory of Solids*, Oxford University Press, Oxford, 1955, p. 108.

7.   a) C. K. Chiang, C. Z. Fincher, Y. W. Park, A. J. Heeger, H. Shirakawa, E. J. Louis, S. C. Gau and A. G. MacDiarmid, *Phys. Rev. Lett.*, 1977, **39**, 1098;
        b) H. Shirawaka, E. J. Louis, A. G. MacDiarmid, C. K. Chiang, and A. J. Heeger, *J. Chem. Soc., Chem. Commun.*, 1977, 578.

8.   R. F. Service, *Science*, 2000, **290**, 425.

9.   J. H. Schon, A. Dodabalapur, Z. Bao, C. Kloc, O. Schenker and B. Batlogg, *Nature*, 2001, **410**, 189.

10.   a) *Conjugated Polymers*, J.-L. Bredas and R. Silbey, Eds., Kluwer, Dordrecht, 1991, p. 211; b) *Handbook of Conducting Polymers*, T. A. Skothiem, R. L. Elsenbaumer and J. R. Reynolds, Eds., Marcel Dekker, New York, 1998; c) *Molecular Electronics*, G. J. Ashwell, Ed., Wiley, 1992; d) A. P. Monkman in *Introduction to Molecular Electronics*, M. C. Petty, M. R. Bryce and D. Bloor, Eds., Edward Arnold, London, 1995.

11.   S. Ikehata, J. Kaufer, T. Woerner, A. Pron, M. A. Druy, A. Sivak, A. J. Heeger and A. G. McDiarmid, *Phys. Rev. Lett.*, 1980, **45**, 423.

12.   a) W.-P. Su, J. R. Schrieffer and A. J. Heeger, *Phys. Rev. Lett.*, 1979, **42**, 1698; b) W.-P. Su, J. R. Schrieffer and A. J. Heeger, *Phys. Rev. B.*, 1980, **22**, 2099; erratum, 1983, **28**, 1138.

13.   H. Thomann, L. R. Dalton, Y. Tomkiewicz, N. S. Shiren and T. C. Clarke, *Phys. Rev. Lett.*, 1983, **50**, 533.

14.   A. J. Heeger, S. Kivelson, J. R. Schrieffer and W.-P. Su, *Rev. Mod. Phys.* 1988, **60**, 781.

15.   J.-L. Bredas and G. B. Street, *Acc. Chem. Res.*, 1985, **18**, 309.

16.   J. H. Kaufmann, N. Colaneri, J. C. Scott, G. B. Street, *Phys. Rev. Lett.* 1984, **53**, 1005.

17. a) S. Kivelson, *Phys. Rev. B.*, 1982, **25**, 3798; b) R. R. Chance, J.-L. Bredas and R. Silbey, *Phys. Rev. B.*, 1984, **29**, 4491.

18. P. Sheng, B .Abeles and Y. Arie, *Phys. Rev. Lett.*, 1973, **31**, 44.

19. a) Y. Cao, P. Smith, A. J. Heeger, *Polymer*, 1991, **32**, 1210; b) S. Tokito, P. Smith, and A. J. Heeger, *Polymer*, 1991, **32**, 464.

20. M. I. Salkalu and S. A. Kivelson, *Phys. Rev. B*, 1994, **50**, 13962.

21. a) Y. Cao, G. M. Treacy, P. Smith, A. J. Heeger, *Appl. Phys. Lett.* 1992, **60**, 2711; b) G. Gustafsson, Y. Cao, G. M. Treacy, F. Klavetter, N. Colaneri, A. J. Heeger, *Nature*, 1992, **357**, 477.

22. J. H. Burroughes, D. D. C. Bradley, A. R. Brown, R. N. Marks, K. Mackay, R. H. Friend, P. L. Burn and A .B. Holmes, *Nature*, 1990, **347**, 539.

23. a) A. Kraft, A. C. Grimsdale and A. B. Holmes, *Angew. Chem. Int. Ed. Engl.*, 1998, **37**, 402; b) L. Dai, B. Winkler, L. Dong, L. Tong, A. W. H. Mau, *Adv. Mater.*, 2001, **13**, 915; c) U. Mitschke and P. Bauerle, *J. Mater. Chem.*, 2000, **10**, 1471.

24. a) S. Doi, M. Kuwabara, T. Noguchi and T. Ohnishi, *Synth. Met.*, 1993, **57**, 4147; b) G. J. Sarnecki, P. L. Burn, A. Kraft, R. H. Friend and A. B. Holmes, *Synth. Met.*, 1993, **55**, 914.

25. D. Braun and A. J. Heeger, *Appl. Phys. Lett.*, 1991, **58**, 1982.

26. M. Berggren, M. Granstrom, O. Inganas and M. Andersson, *Adv. Mater.*, 1995, **7**, 900.

27. N. C. Greenham, S. C. Moratti, D. D. C. Bradley, R. H. Friend and A. B. Holmes, *Nature*, 1993, **365**, 628.

28. R. F. Service, *Science*, 1996, **273**, 878.

29. a) N. S. Sarifitci, L. Smilowitz, A. J. Heeger and F. Wudl, *Science*, 1992, **258**, 1474; b) N. S. Sarifitci, D. Braun, C. Zhang, V. Srdanov, A. J. Heeger, G. Stucky and F. Wudl, *Appl. Phys. Lett.*, 1993, **62**, 585.

30. G. Yu, J. Gao, J. C. Hummelen, F. Wudl and A. J. Heeger, *Science*, 1995, **270**, 1789.

31. J. J. M. Halls, C. A. Walsh, N. C. Greenham, E. A. Marseglia, R. H. Friend, S. C. Moratti and A. B. Holmes, *Nature*, 1995, **376**, 498.

32. C. J. Brabec, N. S. Saricifci and J. C. Hummelen, *Adv. Funct. Mater.*, 2001, **11**, 15.

33. I. Benjamin, E. Z. Faraggi, Y. Avny, D. Davidov and R. Neumann, *Chem. Mater.*, 1996, **8**, 352.

34. R. M. Gurge, A. M. Sarker, P. M. Lahti, B. Hu and F. E. Karasz, *Macromolecules*, 1997, **30**, 8286.

35. I.-N. Kang, H.-K. Shim and T. Zyung, *Chem. Mater.*, 1997, **9**, 746.

36. a) K. Mullen and G. Wegner, Eds., *Electronic Materials: The Oligomer Approach,* Wiley-VCH, Wienheim, 1998; b) R. E. Martin and F. Diederich, *Angew. Chem. Int. Ed. Engl.*, 1999, **38**, 1350.

37. a) O. Isler, Ed., *Carotenoids*, Birkhauser Verlag, Basel, 1971.
b) G. Britton and T. W. Goodwin, Eds., *Carotenoid Chemistry and Biochemistry*, Pergamon Press, London, 1982.

38. a) K. Knoll and R. R. Schrock, *J. Am. Chem. Soc.* 1989, **111**, 7989.
b) A. Kiehl, A. Eberhardt, M. Adam, V. Enkelmann and K. Mullen, *Angew. Chem. Int. Ed. Engl.*, 1992, **31**, 1588.

39. a) A. Bohnen, W. Heitz, K. Mullen, H.-J. Rader and R. Schenk, *Makromol. Chem.*, 1991, **192**, 1679; b) P. Galda and M. Rehahn, *Synthesis*, 1996, 614;
c) P. Liess, V. Hensel and A.-D. Schluter, *Liebegs Ann.*, 1996, 1037.

40. a) U. Scherf and K. Mullen, *Makromol. Chem. Rapid Commun.*, 1994, **12**, 489; b) J. Grimme, M. Kreyenschmidt, F. Uckert and K. Mullen, *Adv. Mater.*, 1995, **7**, 3.

41. a) R. Schenk, H. Gregorius, K. Meerholz, J. Heinze and K. Mullen, *J. Am. Chem. Soc.*, 1991, **113**, 2635; b) K. Meerholz, H. Gregorius, K. Mullen and J. Heinze, *Adv. Mater.* 1994, **6**, 671; c) U. Stalmach, H. Kolshorn, I. Brehm and H. Meier, *Liebigs Ann.*, 1996, 1449; d) T. Maddox, W. Li and L. Yu, *J. Am. Chem. Soc.*, 1997, **119**, 844.

42. a) D. Fichou, Ed., *Handbook of Oligo- and Polythiophenes*, Wiley-VCH, Weinheim, 1999.

43. a) D. Delabouglise, M. Hmyene, G. Horowitz, A. Yassar and F. Garnier, *Adv. Mater.*, 1992, **4**, 107; b) A. Yassar, D. Delabouglise, M. Hmyene, B. Nessak, G. Horowitz and F. Garnier, *Adv. Mater.*, 1992, **4**, 490; c) W. ten Hoeve, H. Wynberg, E. E. Havinga and E. W. Meijer, *J. Am. Chem. Soc.*, 1991, **113**, 5887; d) E. E. Havinga, I. Rotte, E. W. Meijer, W. ten Hoeve and H. Wynberg, *Synth. Met.*, 1991, **41-43**, 473.

44. H. Nakaanishi, N. Sumi, Y. Aso and T. Otsubo, *J. Org. Chem.*, 1998, **63**, 863.

45. a) P. Bauerle, F. Pfau, H. Schlup et al, *J. Chem. Soc. Perkin Trans. 2*, 1993, 489; b) P. Bauerle, T. Fischer, B. Bidlingaier, A. Stabel and J. P. Rabe, *Angew. Chem. Int. Ed. Engl.*, 1995, **34**, 303.

46. H. Meier, U. Stalmach and H. Kolshorn, *Acta Polym.*, 1997, **48**, 379.

47. J. Grimme, M. Kreyenschmidt, F. Uckert, K. Mullen and U. Scherf, *Adv. Mater.*, 1995, **7**, 292.

48. P. Bauerle, *Adv. Mater.*, 1992, **4**, 102.

49. J. Guay, P. Kasai, A. Diaz, R. Wu, J. Tour and L. H. Dao, *Chem. Mater.*, 1992, **4**, 1097.

50. J. A. E. H. van Haare, E. E. Havinga, J. L. J. van Dongen, R. A. J. Janssen, J. Cornil and J.-L. Bredas, *Chem. Eur. J.*, 1998, **4**, 1509.

51. a) M. G. Hill, J. F. Penneau, B. Zinger, K. P. Mann and L. C. Miller, *Chem. Mater.*, 1992, **4**, 1106; b) P. Bauerle, U. Segelbacher, A. Maier and M. Mehring, *J. Am. Chem. Soc.*, 1993, **115**, 10217; c) G. Zotti, G.

Shiavan, A. Berlin and G. Pagnini, *Chem. Mater.*, 1993, **5**, 620; d) P. Hapiot, P. Audenbert, K. Mourier,, J. M. Pernaut and P. Garcia, *Chem. Mater.*, 1994, **6**, 1549; e) J. A. E. H. van Haare, L. Groenedaal, E. E. Havinga, R. A. J. Janssen and E. W. Meijer, *Angew. Chem. Int. Ed. Engl.*, 1996, **35**, 638.

52.   D. D. Graf, R. G. Dunn, J. P. Campbell, L. L. Miller and K. R. Mann, *J. Am. Chem. Soc.*, 1997, **119**, 5888.

53.   L. L. Miller and K. R. Mann, *Acc. Chem. Res.*, 1996, **29**, 417.

54.   J. K. Burdett, *Chemical Bonding in Solids*, Oxford University Press, Oxford, 1995.

55.   M. Pope, C. E. Swenberg, *Electronic Processes in Organic Crystals*, Clarendon Press, Oxford, 1982.

56.   a) E. E. Havinga, I. Rotte, E. W. Meijer, W. ten Hoeve and H. Wynberg, *Synth. Met.*, 1991, **41-43**, 473; b) D. M. deLeuw, *Synth. Met.*, 1993, **55-57**, 3597.

57.   S. Hotta and K. Waragai, *Adv. Mater.*, 1993, **5**, 896.

58.   a) G. Horowitz, B. Bachet, A. Yassar, P. Lang, F. Demanze, J.-L. Fave, F. Garnier, *Chem. Mater.*, 1995, **7**, 1337; b) T. Siegrist, R. M. Fleming, R. C. Haddon, R. A. Laudise, A. J. Lovinger, H. E. Katz, P. Bridenbaugh and D. D. Davis, *J. Mater Res.*, 1995, **10**, 2170.

59.   a) L. Antolini, G. Horowitz, F. Kouki and F. Garnier, *Adv. Mater.*, 1998, **10**, 379; b) T. Siegrist, C. Kloc, R. A. Laudise, H. E. Katz and R. C. Haddon, *Adv. Mater.*, 1998, **10**, 382.

60.   R. C. Haddon, T. Siegrist, R. M. Fleming, P. M. Bridenbaugh and R. A. Laudise, *J. Mater. Chem.*, 1995, **5**, 1719.

61.   a) G. Horowitz, *Adv. Mater.*, 1998, **10**, 365; b) H. E. Katz, *J. Mater. Chem.*, 1997, **7**, 369; c) F. Garnier, in *Electronic Materials: The Oligomer Approach*, K. Mullen and G. Wegner, Eds., Wiley-VCH, Weinheim, 1996, p. 559.

62.   a) C. P. Jarrett, R. H. Friend, A. R. Brown and D. M. deLeuw, *J. Appl. Phys.*, 1995, **77**, 6289; b) A. R. Brown, A. Pomp, C. M. Hart and D. M. deLeuw, *Science*, 1995, **270**, 972; c) H. Klauk, D. J. Gundlach, J. A. Nichols and T. N. Jackson, *IEEE Trans. Electron. Devices*, 1999, **46**, 1258.

63.   G. Horowitz, *Adv. Mater.*, 1990, **2**, 376.

64.   A. Tsumura, H. Koezuka and T. Ando, *Appl. Phys. Lett.*, 1986, **49**, 1210.

65.   a) Z. Bao, A. Dodabalapur and A. J. Lovinger, *Appl. Phys. Lett.*, 1996, **69**, 4108; b) H. Sirringhaus, N. Tessler and R. H. Friend, *Science*, 1998, **280**, 1741.

66. a) G. Horowitz, D. Fichou, X. Z. Peng, Z. Xu and F. Garnier, *Solid State Chem.*, 1989, **72**, 381; b) G. Horowitz, D. Fichou, X. Peng and F. Garnier, *Synth. Met.*, 1989, **41-43**, 1127.

67. a) F. Garnier, G. Horowitz, X. Z. Peng and D. Fichou, *Synth. Met.*, 1991, **45**, 163; b) G. Horowitz, F. Deloffre, F. Garnier, R. Hajlaoui and M. Hmyene, *Synth. Met.*, 1993, **54**, 435.

68. a) B. Servet, G. Horowitz, S. Ries, O. Lagorsse, P. Alnot, A. Yassar, F. Deloffre, P. Srivastava, R. Hajlaoui, P. Lang and F. Garnier, *Chem. Mater.*, 1994, **6**, 1809; b) A. Dodabalapur, L. Torsi and H. E. Katz, *Science*, 1995, **268**, 270; c) A. Dodabalapur, A. J. Lovinger, H. E. Katz, R. Ruel, D. D. Davis and K. W. Baldwin, *Chem. Mater.*, 1995, **7**, 2247.

69. H. Egalhaaf, P. Bauerle, K. Bauer, V. Hoffman and D. Oelkrug, *J. Mol. Struct.*, 1993, **293**, 249.

70. a) F. Garnier, A. Yasser, R. Hajlaoui, G. Horowitz, F. Deloffre, B. Servet, S. Reis and P. Alnot, *J. Am. Chem. Soc.*, 1993, **115**, 8716; b) H. E. Katz, A. Dodabalapur, L. Torsi and D. Elder, *Chem. Mater.*, 1995, **7**, 2238.

71. G. Horowitz, B. Bachet, A. Yassar, P. Lang, F. Demanze, J. L. Fave and F. Garnier, *Chem. Mater.*, 1995, **7**, 1337.

72. a) T. Goodson, W. Li, A. Gharavi and L. Yu, *Adv. Mater.*, 1997, **9**, 639; b) M. Halim, J. N. G. Pilow, I. D. W. Samuel and P. L. Burn, *Adv. Mater.*, 1999, **11**, 371.

73.   V. Gebhardt, A. Bacher, M. Thelakkat, U. Stalmach, H. Meier, H.-W. Schmidt and D. Haarer, *Adv. Mater.*, 1999, **11**, 119.

74.   a) S. Tasch, C. Brandstatter, F. Meghdadi, G. Leising, G. Froyer and L. Athouel, *Adv. Mater.*, 1997, **9**, 33.

75.   G. Barbarella, L. Favaretto, G. Sotgiu, M. Zambianchi, V. Fattori, M. Cocchi, F. Cacialli, G. Gigli and R. Cingolani, *Adv. Mater.*, 1999, **11**, 1375.

76.   P. Noma, T. Tsuzuki and Y. Shirota, *Adv. Mater.*, 1995, **7**, 647.

77.   S. B. Heidenhain, Y. Sakamoto, T. Suzuki, A. Miura, H. Fujikawa, T. Mori, S. Tokito and Y. Taga, *J. Am. Chem. Soc.*, 2000, **122**, 10240.

78.   Y. Sakamoto, S. Komatsu and T. Suzuki, *J. Am. Chem. Soc.*, 2001, **123**, 4643.

79.   B. Winkler, F. Meghdadi, S. Tasch, R. Mullner, R. Resel, R. Saf, G. Leising and F. Stelzer, *Opt. Mater.*, 1998, **9**, 159.

80.   a) M. L. Renak, G. P. Bartholomew, S. Wang, P. J. Ricatto, R. J. Lachicotte and G. C. Bazan, *J. Am. Chem. Soc.*, 1999, **121**, 7787; b) B. Strehmel, A. M. Sarker, J. H. Malpert, V. Strehmel, H. Seifert and D. C. Neckers, *J. Am. Chem. Soc.*, 1999, **121**, 1226.

Chapter Two

An Introduction to the Synthesis, Properties and Applications of Systems Based Upon Arylene Ethynylene Motifs

2.1 Poly(arylene-ethynylene)s

2.1.1 Synthesis

One important class of conjugated polymers are the poly(arylene-ethynylenes) (PAEs). Their structures have an alternating arrangement of aryl and ethynyl moieties in the main chain, which is illustrated in Figure **2.1**. Whilst they have not received as much attention as other conjugated polymers, such as poly(phenylene-vinylene) (PPV) and its derivatives, a substantial body of literature has been built up around them, which has been subject to two comprehensive recent reviews.[1] PAEs containing phenylene groups constitute the vast majority of PAEs and are known as poly(phenylene-ethynylenes) (PPEs), although polymers containing pyridine, thiophene and anthracene groups have been synthesized. Most PPEs are linear, with substitution at the para-positions of the phenylene groups; however, several non-linear PPEs have been synthesized. Due to their rigid structures, unsubstituted PAEs are completely insoluble and intractable in all solvents, which limits the maximum degree of polymerisation, and hampers their characterisation. The first report of a moderately soluble high molecular

weight PAE came with the preparation of a PPE derivative containing long chain alkoxy substituents at the 2,5 positions.[2] Alkoxy groups remain the most widely used substituents, although other substituents have been used, including simple alkyl groups[3] and aliphatic amides, which lead to polymers with a high degree of polymerisation.[4]
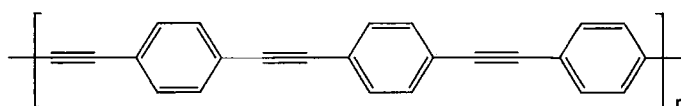
Figure **2.1** The structure of linear poly(phenylene-ethynylene) (PPE)

There are several reported routes for the synthesis of PAEs, which include the self-polymerisation of tin and cuprous acetylides, the electrochemical reduction of para-xylene derivatives, the dehydobromination of PPV derivatives, and the polycondensation of arylhalides with disodium acetylide.[1b] However, the most commonly used method is the condensation co-polymerisation of diethynylarene and dihaloarene derivatives, using homogenous palladium catalysis.[5] Although the reaction conditions have been optimized,[6] there remain several problems associated with this cross coupling methodology, particularly in the formation of defect- containing and low-molecular weight species due to competing hydrodehalogenation and oxidative homocoupling side reactions. It is also difficult to separate the polymer from the catalyst residues and ammonium salts generated during the reaction. An alternative method of synthesizing PAEs has recently been devised based upon alkyne metathesis using molybdenum or tungsten carbyne complexes as catalysts at elevated temperatures in carefully dried solvents and oxygen free conditions.[7] It was found that simple catalysts like molybdenum(0) hexacarbonyl are able to function in non-dried, off-the-shelf

solvents at elevated temperatures under a nitrogen gas purge.[8] This is shown in Scheme **2.1**. Polymers made under these conditions are usually obtained in almost quantitative yield and with a very high degree of polymerisation. The catalyst can be easily removed by acid and base washes. This methodology may replace palladium catalysis as the method of choice for the synthesis of PPEs, although it is less tolerant of heterocyclic groups.
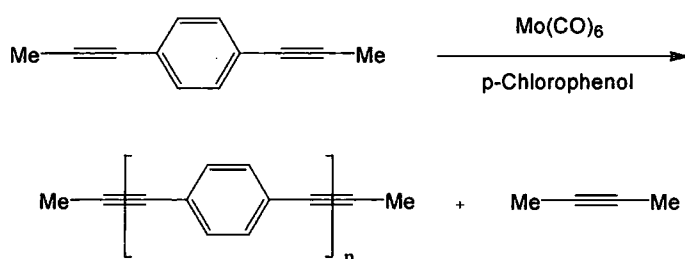
Scheme **2.1** Synthesis of PPE via alkyne metathesis polymerisation

2.1.2 Properties

Linear PAEs are coloured, because they strongly absorb in the visible region, the position of the absorption maximum being dependent on the substituents.[9] Electron-donating substituents, such as alkyl and alkyoxy groups, tend to lead to considerable bathochromic shifts in the absorption spectra, whereas the effect of electron-withdrawing ones is negligible. Close examination of the position of the absorption maximum allows a determination of the band gap to be made. These are close to the theoretically calculated value for PPE of 3.4

eV.[10] Non-linear PPEs are not as effectively conjugated and absorb in the UV-region.[11] Incorporation of the polymers into thin films generally red-shifts the absorption compared to solution measurements, but interestingly, this does not appear to occur in PPEs with chiral substituents.[12] The exact shift and bandwidth is dependent upon whether the film was spin-cast or cast from solution, and subsequent annealing results in sharper absorption bands. This suggests that the absorption spectra are dependent on the amount of disorder in the films. The red-shift has been postulated to have two causes: either the aggregation induced adoption of co-planarity by the aryl rings in the solid state, or possibly due to π-stacking of the phenylene rings. Recent work based on theoretical and structural information has suggested that it is primarily due to the former.[13]

The bulk structures of PPEs has been analysed using powder X-ray diffraction and electron microscopy, in combination with force-field calculations.[14] The solid state ordering of PPEs generally obeys Neher's rule, which states that conjugated polymers with alkyl and alkoxy side chains adopt different structural types depending on the number of solublizing side chains per repeat unit.[15] If every ring is substituted by side chains, a lamellar or double lamellar structure results, in which the packing of the polymers is almost entirely governed by the packing of the long alkyl side-chains. If only alternating rings are substituted, a structure results in which the side-chains of neighbouring polymers are interdigitated. In the case of PPEs, both lamellar and indigitated structures have been observed,[16] which result in differing spacings between the main chains. It is believed that the phenyl rings of the main chains in one layer lie below the triple bonds in the adjacent layer, which minimses π-π stacking between the rings.[17]

PAEs also show a marked luminescence. Detailed spectroscopic measurements have been carried out, in which it was noted that the solution

state, fluorescence quantum yields can approach unity in some polymers,[18] which means that almost all absorbed photons are re-emitted. This was attributed to the lack of alternative relaxation paths in the excited state, due to the rigid nature of the polymer. The emission efficiency is very sensitive to impurities. Fluorescence also occurs in the solid-state, with much reduced quantum yields in a range 0.1-0.3, and substantial red-shifts. The shifts have been postulated to arise from the formation of excimers in the solid state. Incorporation of anthracene moieties into the main-chain decreases the quantum yield and low-energy electronic transition, and lower wavelength emission bands associated with the anthracene unit appear in the fluoresence spectra.[19] In cases where the polymers have terminal anthracene groups the polymers are able to absorb optical energy and transfer it to the end groups for luminscence with an efficiency greater than 95%.[20]

PPE has been doped with several dopants and then tested for conductivity. After doping with arsenic pentafluoride or iodine, conductivities of 10^{-3} to 10^{-2} S cm^{-1} have been measured.[21] These conductivities are much lower than those of other doped conjugated polymers, and it is unlikely that PPE will find practical application as an electrically conducting polymer. The conductivity has been shown to be dependent on the morphology of the polymer, suggesting that higher conductivity is associated with lower long-range order in the films, but shows little dependence on the average chain length of the polymers.[22]

2.1.3 Applications

The use of fluorescent PPEs in chemical sensors has recently been pioneered. It takes advantage of the fact that that their high fluorescence can

be quenched by low concentrations of analytes, which attach themselves to binding groups on the main-chain, and disrupt the conjugation and therefore dramatically lower the quantum yield. These binding sites are usually cyclophanes, which can act as hosts for molecules such as paraquat.[23] Porous PPEs containing pentictytene groups have also been used as detectors for TNT, and function in much the same way.[24] Films of substituted PPEs have also been used as emitting layers in organic light emitting diodes. Most alkyloxy-substituted PPEs give a yellow emission,[25] but a white light emitting device has been synthesized using a PAE with alternating perylene groups.[26] Although electron injection from the cathode has been to shown to be more efficient in PPE devices with aluminium cathodes than in analogous PPV devices due to their lower energy LUMOs, hole injection is less efficient, because of the energy mismatch between the anode and the HOMO, thus their overall efficiency is lower and PPEs are not expected to be used in commercial devices.[27] However, the ordering of PPE films means that they could be potentially used as polarisers. Films of PPE dissolved in high molecular weight polyethene have been drawn out on a hot shoe, and shown to have very narrow emission ranges and large dichroic ratios, making them ideal for use as photoluminscent polarisers for use in liquid crystal displays (LCDs), to produce devices with much increased brightness and contrast.[28] A patent has also been taken out which describes the use of PPE as an anti-static agent, photoelectric transducing element and storage battery.[29]

2.2 Oligo(arylene-ethynylene)s

2.2.1 Synthesis

Oligo(arylene-ethynylene)s (OAEs), have been the focus of increasing attention in recent years. They are known more colloquially as rigid-rods and molecular wires, due to their rigidly linear conformations and their recently demonstrated electrical conductivity. Many OAEs have been prepared, and most have been collated in a recent review.[30] As the length of the oligomers increases they quickly become insoluble in most solvents, thus, as with PAEs, flexible alkoxy side-chains are incorporated in order to make them soluble.

OAEs are usually prepared by an iterative divergent/convergent modular approach using palladium catalysed cross-coupling methodology.[31] The starting material is often a halogenated ethynylarene monomer. Although both the halogen and ethynyl groups are capable of participating in cross-coupling reactions, they can be protected and deprotected independently of each other. A typical synthetic procedure is as follows: the doubly-protected monomer is divided into two equal portions. Each portion has one of its protecting groups removed, then the two portions are brought together for the coupling step. As the resulting product will contain the same protected end groups as the monomer the whole process can be repeated in the next step. In this way, the length of the oligomer is doubled with each iteration, as is shown in Scheme **2.2**. This fact makes separation of the product from any unreacted starting materials easier. A variation on this methodology has been developed whereby one of the monomers couples at both ends during each step.[32] This method has the advantage of not requiring the isolation of oxidatively-unstable terminal alkyne intermediates.

The scope of this methodology has been extended by the use of solid-supported catalyst syntheses, which enable the syntheses and subsequent purifications to be streamlined and possibly automated. The first example used a polystyrene support.[33] For later ones, Merrifield's resin was chosen as the solid support phase, from which the oligomers are cleaved in the final step.[34] This technique enables the oligomers to be grown from both ends,[35] which could not occur in the original methodology due to polymerisation, and can also be used for the preparation of alternating block co-oligomers.[36]
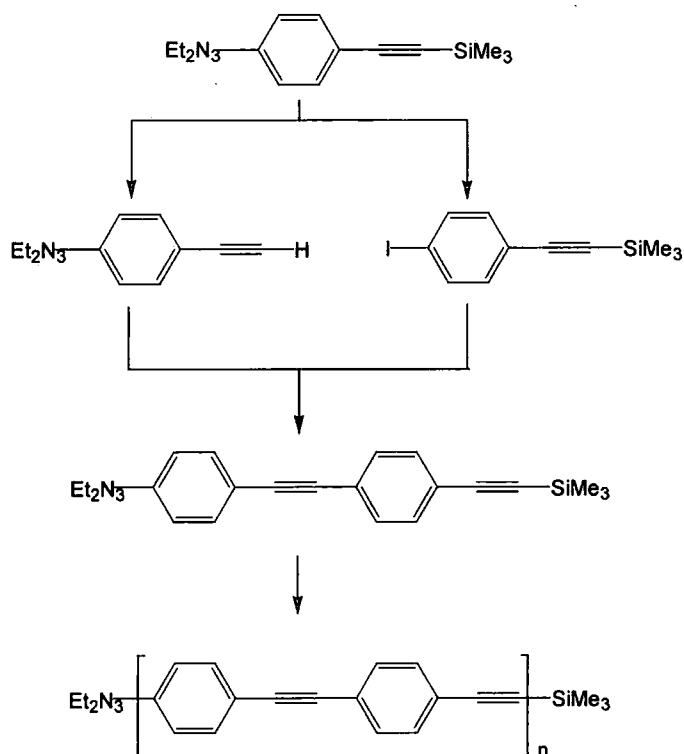
Scheme **2.2** Iterative/divergent coupling methodology for the synthesis of OPEs

In addition to these linear OPEs, a variety of other differently substituted OPEs have been prepared. Ortho-linked OPEs are in general more soluble than the para-OPEs and so do not require the incorporation of alkyl side chains. The crystal structures of some of them have been obtained.[37] Meta-linked OPEs have been studied in detail. Even though these are not rigid rods they do possess a shape persistent architecture, which can adopt many different conformations. In certain solvents, they coil into helices, to minimize interaction with the solvent, which mimics the folding of proteins in biological systems.[38]

2.2.2 Molecular Wires

A selection of linear OPEs with thiol and thioester end-groups have been synthesized by the above approach.[39] They were then exposed to gold surfaces, upon which they form self-assembled monolayers (SAMs).[40] Several techniques, such a ellipsometry, contact angle measurement, X-ray photo-electron spectroscopy, (XPS), scanning tunnelling microscopy (STM) and grazing angle IR measurements have shown that the molecules arrange themselves nearly perpendicular to the surface, and exhibit a reasonable degree of order. This holds true for molecules up to 50 Å in length, above which it becomes difficult to obtain densely packed, well-ordered monolayers. These OPEs are also able to insert themselves into SAMs of alkyl thiols. The OPE protrudes above the SAM and can be detected using the tip of a scanning tunnelling microscope.[41] This has conclusively demonstrated that individual OPEs are electrically conducting over distances of up to 100 Å.

Quantitative measurements of the current passing through the molecules were made using a nanopore arrangment, consisting of a defect-free SAM of around 1000 molecules, topped with a coating of gold, established that the current varied almost linearly with applied voltage, which suggest that the individual oligomers behave as molecular wires.[42] The conductivity of the wires was found to be dependent upon the temperature, which was attributed to changes in molecular conformation of the phenyl rings. A subsequent theoretical study has concluded that conductivity is at a maximum when the phenyl rings are all in plane, and a minimum when they are perpendicular.[43] Further methods have been developed to insert molecules at controlled rather than random locations. This was achieved by applying controlled voltage pulses to specific locations in an alkanethiolate SAM, under a solution of molecular wires. This resulted in precise placement of bundles of around ten molecules at specific sites in the SAM.[44]

2.2.3 Molecular Electronics

With the proof that certain OPEs can act as molecular wires, came the realisation that others should be able to function as individual electronic devices, such as transistors and diodes. At present, electronic devices are based largely on inorganic semiconductors, such as silicon. Large numbers of these devices are integrated into microchips, using lithographic techniques, for use in computers. Over the past few decades, technological advances have led to the number of devices that can be incorporated onto a single chip, doubling every 18 months, which has led to ever more powerful computers.

However, this trend cannot continue indefinitely, as increased miniaturisation leads to an increased likelihood of inconsistencies in individual devices due to quantum mechanical effects such as tunnelling.[45]

In theory, molecular devices could operate over much smaller dimensions as the electrons in the orbitals of molecules are tightly bound and are less likely to interfere with one another, and thus enable unprecedented numbers of devices to be incorporated into single chips. Molecules are easy to synthesize and tailor to device specifications. However, there are several major challenges inherent in creating devices based on molecules. The most pertinent is the question of positioning and addressing every molecule individually. It would be very unpractical to attempt to manipulate individual molecules using an STM probe. A better method would be to use SAMs, although these would be laden with defects, which would impair overall performance. Another problem is how to dissipate the intense heat generated by such densely packed devices. At present, none of these design challenges can be said to have been solved to a suitable degree of satisfaction, and computers based on molecular devices remain a remote possibility. However, several inroads have already been made.

In theory, a molecular device can be constructed from any molecule which has a non-linear current/voltage profile. Various potential molecular devices have been synthesized based on OPEs.[46] Several linear molecules have been synthesized based on OPEs containing either methylene or porphyrin moieties.[47] Other molecular devices which have three and four terminals have been synthesized, which are the molecular analogues of simple junctions, switches and logic gates.[48] Some of these are shown in Figure **2.2**. In addition, orthogonally fused derivatives have been prepared for switch-like applications.[49] However, the electronic properties of none of these devices

have yet been established due to the unfeasibility of producing multiprobe testing arrays, over such small dimensions.
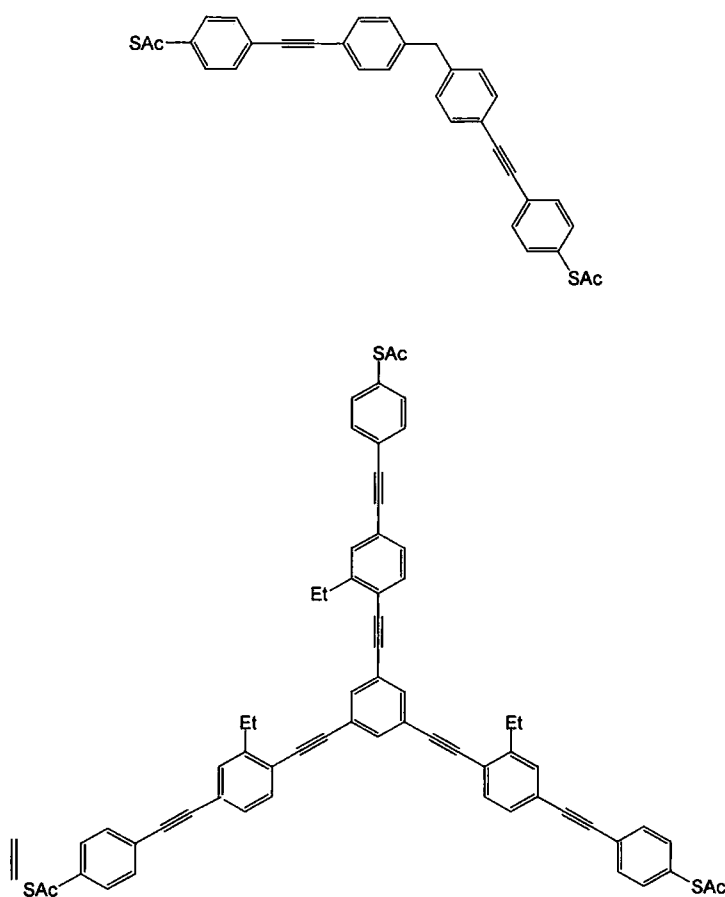
Figure **2.2** Potential molecular devices with multiple terminals

However, the electronic properties of linear OPEs containing nitro and aniline groups, as shown in Figure **2.3,** have been tested, in a nanopore SAM arrangement. These showed current-voltage graphs containing a pronounced spike, a phenomenon known as negative differential resistance (NDR).[50] This means that it could potentially be used as a diode. Theoretical studies have suggested that this effect is based on dramatic changes in the LUMO upon

charging.[51] The same molecules also display current storage properties, which have been shown to have an application in dynamic random access memory (DRAM) devices, in which a voltage pulse is used to write, read and erase the high conductivity state.[52]
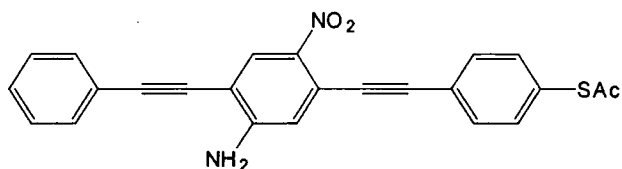
Figure **2.3** A molecular device for use as a diode and in dynamic random access memories

2.3 Shape-Persistent Architectures

The rigid structure of the phenylene ethynylene unit makes it an ideal candidate for incorporation in molecules designed to have what is termed a shape-persistent architecture. Numerous examples of phenylene ethynylene species with rigid architectures have been synthesized, and these have been recently reviewed.[53] One such molecule has been proposed as a rigid tip for scanning tunnelling microscopes (STMs).[54] A good example of a phenylene-ethynylene network is a carbon allotrope consisting of planar sheets made up of benzene ring and triple bonds. This has been given the name graphyne, and has been postulated to have interesting physical and electronic properties. Although graphyne itself remains a synthetic challenge, several

molecules which could act as its potential precursors have been synthesized.[55]
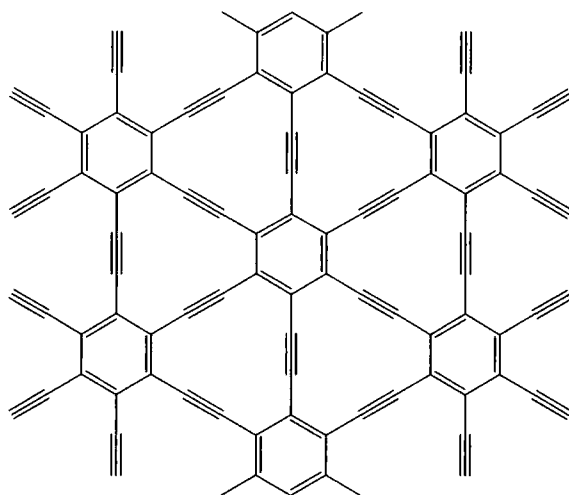
Figure **2.4** The structure of graphyne

2.3.1 Dendrimers

Dendrimers are molecules which branch out from a central core. The first examples were synthesized in the mid-1980's.[56] Their synthesis takes place over a number of stages or generations. This can occur divergently, where each step radiates outwards from the core, or convergently, in which a new core is created in each synthetic step.[57] The phenylene-ethynylene (PE) motif provides an ideal basis for the construction of dendrimers that possess a highly defined three-dimensional structure. PE dendrimers have been synthised by both divergent and convergent methods, and are currrently the only examples of fully conjugated dendrimers in existence. Initial attempts at convergent PE dendrimer synthesis were hampered by the decreasing solubility of the dendrimers with increasing size.[58] This problem was

43

overcome by the use of reagents with tert-butyl substituents, which formed dendrimers whose solubility actually increased with increasing size, with the higher generation dendrimers even being soluble in pentane.[59]

A convergent approach was used to synthesize a fourth-generation dendrimer containing 31 phenylene ethynylene units. Attempts to produce further generations via the same methodology as the first ones failed, probably as a result of the steric crowding that would be manifest in these higher generation dendrimers. However, a dendrimer containing 94 units was synthesized by reacting three equivalents of the 31-unit dendrimer with one of a 1,3,5-triiodobenzene core. The resulting dendrimer was characterised by various mass spectrometry techniques.[60] Another approach was used to prepare a dendrimer composed of 127 units, which spans over 125 Å, with an open core to reduce steric hindrance.[61] A method for synthesising even larger dendrimers is known as double exponential dendrimer growth, in which protecting groups are employed for the iodo groups, as well as the ethynyl groups, much in the same manner as the iterative divergent/convergent process used in the synthesis of OPE (vide supra). The number of units in dendrimers synthesized by this method is proportional to the generation numbers, raised to a power of power, which means that very large dendrimers, of up to 255 units (verified by MALDI-MS) can be synthesized in relatively few steps.[62] This dendrimer possesses much larger conjugation lengths at the centre than at the periphery, meaning that it possesses an electronic energy gradient that decreases from the perimeter to the core. This in turn means that it should direct any excitation energy towards its core, making it potentially of use as a convergent and directional antenna and energy funnel.[63]

Such dendrimers could have a variety of other applications. Recently, smaller dendrimers have been developed with long aliphatic chains instead of tert-

butyl groups. These were shown to form stablized columnar liquid crystalline phases at room temperature.[64] PE dendrimers containing a central core based on anthracene and peripheral diphenyl amine units have been synthesized and used as emissive layers in organic LEDs.[65] PE dendrimers with a binaphthol core have also been synthesized with an intent to use them as enantioselective fluorescence sensors for rapid optical determination of the stereochemistry of certain chiral compounds, particularly amino alcohols. These dendrimers have also been observed to catalyse asymmetric reactions.[66] A [60]Fullerene unit has recently been used as a core in some dendrimers.[67]

2.3.2 Macrocycles

Similar methods to the ones outlined above have been used to create macrocycles. They can be synthesized from the intramolecular cyclisation of OPEs containing alternate meta and para linkages by the palladium cataylzed cross-coupling of the unprotected end groups.[68] Similar cyclisations have been carried out with branched OPEs in order to create bicyclic,[69] and even tricyclic, structures.[70] Several of these macrocycles have very convoluted topologies,[71] whilst others are geometrically rigid, but exhibit conformational bistabilty, meaning that they can act as molecular turnstiles.[72] The rate of the rotation has been shown by NMR studies to be sluggish at low temperatures but fast at high temperatures. Many of the simpler macrocycles, such as cyclo-hexakis(phenylene-ethynylene), form aggregates in solution.[73] It is strongly believed that this manifests itself in stacked structures,[74] which has been confirmed by X-ray diffraction studies.[75] Such stacked aggregates are able to display discotic liquid crystalline phases.[76] These macrocycles have been modified by the incorporation of substituents which allow the

macrocycles to function amphiphilically, and enables them to form monolayer films on the surface of water, or on various substrates.[77]
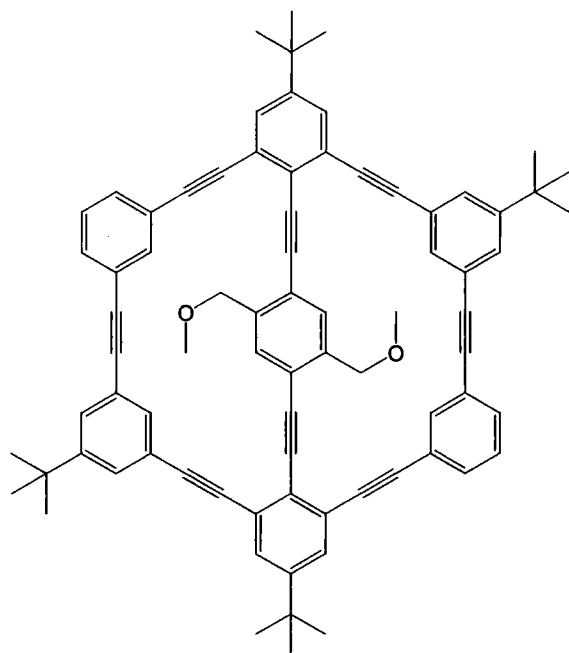
Figure **2.5** A molecule turnstyle macrocycle

2.4 References

1.   a) U. H. F. Bunz, *Chem. Rev.*, 2000, **100**, 1605; b) R. Giesa, *J. Mater. Soc. Rev. Macromol. Chem. Phys.*, 1996, **C36**, 631.

2.   R. Giesa and R. C. Schultz, *Macromol. Chem. Phys.*, 1990, **191**, 857.

3.   V. Franke, T. Mangel and K. Mullen, *Macromolecules*, 1998, **31**, 2447.

4.   Q. Zhou and T. M. Swager, *J. Am. Chem. Soc.*, 1995, **117**, 12593.

5.   K. Sanecheka, T. Yamamoto and A. Yamamoto, *Bull. Chem. Soc. Jpn.*, 1984, **57**, 752.

6.   V. Percec, C. Pugh, E. Cramer, S. Okita and R. Weiss, *Makromol. Chem., Macromol. Symp.*, 1992, **54/55**, 113.

7.   K. Weiss, A. Michel, E. M. Auth, U. H. F. Bunz, T. Mangel and K. Mullen, *Angew. Chem. Int. Ed. Engl.*, 1997, **36**, 506.

8.   N. G. Pschirer and U. H. F. Bunz, *Tetrahedron Lett.*, 1999, **40**, 2481.

9.   H. Li, D. R. Powell, R. K. Hayashi and R. West, *Macromolecules*, 1998, **31**, 52.

10.   J.-L. Bredas, R. R. Chance, R. H. Baughman and R. Silbey, *J. Chem. Phys.*, 1982, **76**, 3673.

11.   Y. Pang and J. Li, *Macromolecules*, 1998, **31**, 6730.

12.   R. Feisel and U. Scherf, *Macromol. Rapid Commun.*, 1998, **19**, 427.

13.   T. Miteva, L. Palmer, L. Koppenburg, D. Neher and U. H. F. Bunz, *Macromolecules*, 2000, **33**, 652.

14.   M. Moroni, J. LeMoigne and S. Luzzati, *Macromolecules*, 1994, **27**, 562.

15.   D. Neher, *Adv. Mater.*, 1995, **7**, 691.

16.   J. M. Rodriguez-Parada, R. Duran and G. Wegner, *Macromolecules*, 1989, **22**, 2507.

17.   U. H. F. Bunz, V. Enkelmann, L. Kloppenburg, D. Jones, K. D. Shimizu, J. B. Claridge, H. C. zur Loye and G. Leisser, *Chem. Mater.*, 1999, **11**, 1416.

18.   a) C. Weder, M. S. Wrighton, R. Spreiter, C. Bosshard and P. Gunter, *J. Phys. Chem.*, 1996, **100**, 18931; b) C. E. Halkyard, M. E. Rampey, L. Kloppenburg, S. L. Studer-Martinez and U. H. F. Bunz, *Macromolecules*, 1998, **31**, 8655.

19.   a) C. Weder, M. J. Wagner and M. S. Wrighton, *Mater. Res. Soc. Symp. Proc.*, 1996, **413**, 77; b) C. Weder and M. S. Wrighton, *Macromolecules*, 1996, **29**, 5157.

20.   T. M. Swager, C. J. Gil and M. S. Wrighton, *J. Chem. Phys.*, 1995, **99**, 4886.

21. M. V. Lakshmikantham, J. Vartikar, K.-Y. Jen, M. P. Cava, W. S. Huang and A. G. McDiarmid, *Polym. Prep.*, 1983, **24**, 75.

22. D. Ofer, T. M. Swager and M .S. Wrighton, *Chem. Mater.*, 1995, **7**, 418.

23. a) Q. Zhou and T. M. Swager, *J. Am. Chem. Soc.*, 1995, **117**, 12593; b) T. M. Swager, *Acc. Chem. Res.*, 1998, **31**, 201; c) I. A. Levitsky, J. S. Kim and T. M. Swager, *J. Am. Chem. Soc.*, 1999, **121**, 1273.

24. a) J. S. Yang and T. M. Swager, *J. Am. Chem. Soc.*, 1998, **120**, 5321; b) J. S. Yang and T. M. Swager, *J. Am. Chem. Soc.*, 1998, **120**, 11864.

25. a) L. S. Swanson, F. Lu, J. Shinar, Y. W. Ding, T. J. Barton, *Proc. SPIE Int. Soc. Opt. Eng.*, 1993, **1910**, 101; b) L. S. Swanson, J. Shinar, Y. W. Ding, T. J. Barton, *Synth. Met.*, 1993, **55**, 1; c) M. Hirohata, K. Tada, T. Kawei, M. Onoda and K. Yoshino, *Synth. Met.*, 1997, **85**, 1273; d) H. Hager and W. Heitz, *Chem. Phys.*, 1998, **199**, 1821.

26. S. Tasch, E. J. W. List, O. Ekstrom, W. Graupner, G. Leising, P. Schliching, U. Rohr, Y. Geerts, U. Scherf, K. Mullen, *Appl. Phys. Lett.*, 1997, **71**, 2883.

27. A. Montali, P. Smith and C. Weder, *Synth. Met.*, 1998, **97**, 123.

28. a) C. Weder, C. Sarwa, C. Bastiaansen and P. Smith, *Adv. Mater.*, 1997, **9**, 1035; b) C. Weder, C. Sarwa, A. Montali, G. Bastiaansen and P. Smith, *Science*, 1998, **279**, 835; c) A. Montali, G. Bastiaansen, P. Smith and C. Weder, *Nature*, 1998, **392**, 261.

29. Mitsubushi Chem. Industries, JP-Patent 59 102,912 [84, 102,914] *Chem. Abstr.*, 1984, **101**, 172649.

30. J. M. Tour, *Chem. Rev.*, 1996, **96**, 537.

31. J. S. Schumm, D. L. Pearson and J. M. Tour, *Angew. Chem. Int. Ed. Engl.*, 1994, **33**, 1360.

32. S. Huang and J. M. Tour, *Tetrahedron Lett.*, 1999, **40**, 3347.

33. J. K. Young, J. C. Nelson and J. S. Moore, *J. Am. Chem. Soc.*, 1994, **116**, 10841.

34. a) D. M. Pearson and J. M. Tour, *J. Org. Chem.*, 1997, **62**, 1376.
    b) L. Jones II, J. S. Schumm and J. M. Tour, *J. Org. Chem.*, 1997, **62**, 1388.

35. S. Huang and J. M. Tour, *J. Am. Chem. Soc.*, 1999, **121**, 4908.

36. S. Huang and J. M. Tour, *J. Org. Chem.*, 1999, **64**, 8898.

37. R. H. Grubbs and D. Kratz, *Chem. Ber.*, 1993, **126**, 149.

38. a) J. Zhang, J. S. Moore, Z. Xu and R. A. Aguirrre, *J. Am. Chem. Soc.*, 1992, **114**, 2273; b) R. B. Prince, J. G. Saven, P. G. Wolynes and J. S. Moore, *J. Am. Chem. Soc.*, 1999, **121**, 3114; c) P.-J. Prest, R. B. Prince and J. S. Moore, *J. Am. Chem. Soc.*, 1999, **121**, 5933; d) M. J. Mio, R. B. Prince, J. S. Moore, C. Kuebel and D. C. Martin, *J. Am. Chem. Soc.*, 2000, **122**, 6134; e) S. Lahiri, J. L. Thompson and J. S. Moore, *J. Am. Chem. Soc.*, 2000, **122**, 11315.

39. a) D. Pearson, J. S. Schumm and J. M. Tour, *Macromolecules*, 1994, **27**, 2348; b) J. S. Schumm, L. Jones II, D. L. Pearson, R. Hara and J. M. Tour, *Polym. Prep. (Am. Chem. Soc. Div. Polym. Chem.)*, 1994, **35**, 687.

40. a) J. M. Tour, L. Jones II, D. L. Pearson, J. S. Lamba, T. P. Burgin, G. W. Whitesides, D. L. Allara, A. N. Parikh and S. V. Atre, *J. Am. Chem. Soc.*, 1995, **117**, 9529; b) A.-A. Dhirani, R. W. Zehner, R. P. Hsung, P. Guyot-Sionnest and L. R. Sita, *J. Am. Chem. Soc.*, 1996, **118**, 3319.

41. a) L. A. Bumm, J. J. Arnold, M. T. Cygan, T. D. Dunbar, T. P. Burgin, L. Jones II, D. L. Allara, J. M. Tour and P. S. Weiss, *Science*, 1996, **271**, 1705; b) M. T. Cygan, T. D. Dunbar, J. J. Arnold, L. A. Bumm, N. F. Shedlock, T. P. Burgin, L. Jones II, D. L. Allara, J. M. Tour and P. S. Weiss, *J. Am. Chem. Soc.*, 1998, **120**, 2721.

42. C.-W. Zhou, M. R. Deshpande, M. A. Reed, L. Jones II and J. M. Tour, *Appl. Phys. Lett.*, 1997, **71**, 611.

43. J. M. Seminario, A. G. Zarcarius and J. M. Tour, *J. Am. Chem. Soc.*, 1998, **120**, 3970.

44. M. A. Reed, C.-W. Zhou, C. J. Muller, T. P. Burgin, and J. M. Tour, *Science*, 1997, **278**, 252.

45. J. M. Seminario, J. M. Tour, in *Molecular Electronics, Science and Technology*, ed. A. Aviram and M. Ratner, New York Academy of Sciences, New York, 1998, p. 68.

46.   a) M. A. Reed, *Proc. IEEE*, 1999, **87**, 652; b) J. M. Tour, *Acc. Chem. Res.*, 2000, **33**, 791; c) J. M. Tour, A. M. Rawlett, M. Kozaki, Y. Yao, R. C. Jagessar, S. M. Dirk, D. W. Price, M. A. Reed, C.-W. Zhou, J. Chen, W. Wang and I. Campbell, *Chem. Eur. J.*, 2001, **7**, 5118.

47.   R. C. Jagessar and J. M. Tour, *Org. Lett.*, 2000, **2**, 111.

48.   J. M. Tour, M. Kozaki and J. M. Seminario, *J. Am. Chem. Soc.*, 1998, **120**, 8486.

49.   R. Wu, J. S. Schumm, D. L. Pearson and J. M. Tour, *J. Org. Chem.*, 1996, **61**, 6906.

50.   J. Chen, M. A. Reed, A. M. Rawlett and J. M. Tour, *Science*, 1999, **286**, 1550.

51.   a) J. M. Seminario, A. G. Zacarias, and J. M. Tour, *J. Am. Chem. Soc.*, 2000, **122**, 3015; b) J. M. Seminario, A. G. Zacarias and P. A. Derosa, *J. Phys. Chem. A.*, 2001, **105**, 791.

52.   M. A. Reed, J. Chen, A. M. Rawlett, D. W. Price and J. M. Tour, *Appl. Phys. Lett.*, 2001, **78**, 3735.

53.   J. S. Moore, *Acc. Chem. Res.*, 1997, **30**, 402.

54.   A. V. Rukavishnikov, A. Phadke, M. D. Lee, D. H. LaMunyon, P. A. Petukhov and J. F. W. Keana, *Tetrahedron Lett.*, 1999, **40**, 6353.

55.   a) M. M. Haley, *Synlett.*, 1998, 557; b) C. Eickmeier, H. Junga, A. J. Matzger, F. Scherhag, M. Shim and K. P. C. Vollhardt, *Angew. Chem. Int. Ed. Engl.*, 1997, **36**, 2103.

56.   G. R. Nekome, Z.-Q. Yao, G. R. Baker and V. K. Gupta, *J. Org. Chem.*, 1985, **50**, 2033.

57.   C. J. Hawker and J. M. J. Frechet, *J. Am. Chem. Soc.*, 1990, **112**, 7638.

58.   J. S. Moore and Z. Xu, *Macromolecules*, 1991, **24**, 5893.

59.   Z. Xu and J. S. Moore, *Angew. Chem. Int. Ed. Engl.*, 1993, **32**, 246.

60.   Z. Xu, M. Kuhr, K. L. Walker, C. L. Wilkins and J. S. Moore, 1994, **116**, 4537.

61.   Z. Xu and J. S. Moore, *Angew. Chem. Int. Ed. Engl.*, 1993, **32**, 1354.

62.   T. Kawaguchi, K. L. Walker, C. L. Wilkins and J. S. Moore, *J. Am. Chem. Soc.*, 1995, **117**, 2159.

63.   a) C. Devadoss, P. Bharathi, J. S. Moore, *J. Am. Chem. Soc.*, 1996, **118**, 9635; b) R. Kopelman, M. Shortreed, Z.-Y. Shi, W. Tan, Z. Xu and J. S. Moore, *Phys. Rev. Lett.*, 1997, **78**, 1239.

64.   D. J. Pesak and J. S. Moore, *Angew. Chem. Int. Ed. Engl.*, 1997, **36**, 1636.

65.   P.-W. Wang, Y.-J. Liu, C. Devadoss, P. Bharathi and J. S. Moore, *Adv. Mater.*, 1996, **8**, 237.

66.   a) Q.-S. Hu, V. Pugh, M. Sabat and L. Pu, *J. Org. Chem.*, 1999, **64**, 7528.
       b) V. J. Pugh, Q.-S. Hu and L. Pu, *Angew. Chem. Int. Ed. Engl.*, 2000, **39**, 3638.

67.   A. G. Avent, P. R. Birkett, F. Paolucci, S. Roffia, R. Taylor and N. K. Wachter, *J. Chem. Soc., Perkin Trans. 2*, 2000, 1409.

68.   J. S. Moore and J. Zhang, *Angew. Chem. Int. Ed. Engl.*, 1992, **31**, 922.

69.   J. Zhang, D. J. Pesak, J. J. Ludwick and J. S. Moore, *J. Am. Chem. Soc.*, 1994, **116**, 4227.

70.   Z. Wu, S. Lee and J. S. Moore, *J. Am. Chem. Soc.*, 1992, **114**, 8730.

71.   Z. Wu and J. S. Moore, *Angew. Chem. Int. Ed. Engl.*, 1996, **35**, 297.

72.   T. C. Bedard and J. S. Moore, *J. Am. Chem. Soc.*, 1995, **117**, 10662.

73.   Z. Zhang and J. S. Moore, *J. Am. Chem. Soc.*, 1992, **114**, 9701.

74.   A. S. Shetty, Z. Zhang and J. S. Moore, *J. Am. Chem. Soc.*, 1996, **118**, 1019.

75.   D. Venkataraman, S. Lee, J. Zhang and J. S. Moore, *Nature*, 1994, **371**, 591.

76. J. Zhang and J. S. Moore, *J. Am. Chem. Soc.*, 1994, **116**, 2657.

77. A. S. Shetty, P. R. Fischer, K. F. Stork, P. W. Bohn and J. S. Moore, *J. Am. Chem. Soc.*, 1996, **118**, 9409.

Chapter Three

The Synthesis of Ethynyl Arenes via Homogenous Palladium-catalyzed Cross-coupling: The Sonogashira Reaction

3.1 The Development of the Reaction

3.1.1 The Discovery of the Reaction

The synthesis of molecules containing arylene ethynylene moieties from commercially available starting materials usually requires the formation of carbon-carbon single bonds, between the aryl and ethynyl units.[1] Although this step is thermodynamically feasible, it is hampered by a large kinetic barrier. This means that the terminal alkyne has to undergo prior conversion into a nucleophilic synthon, such as a copper acetylide, which can be coupled to aryl halides in refluxing pyridine in the absence of air as shown in Scheme 3.1.[2] Although this reaction gives high yields of products, it requires stoichiometric amounts of copper acetylides which are potentially explosive if isolated. In addition, although the reaction is tolerant of many other functional groups, the presence of nucleophilic substituents at the ortho-position of the aryl halide resulted in exclusive cyclisation to the corresponding heterocycle. Some years later, it was demonstrated that less dangerous copper (I) salts can promote the reaction of aryl halides with terminal alkynes directly, but

here too a stoichiometric quantity of copper salt is required.[3] Several years later, a catalytic reaction was developed using copper iodide, triphenylphosphine and potassium carbonate in DMF or DMSO which was reported to give good yields.[4] More recently, the coupling of halogenoalkynes to aryl stananes has been achieved in the presence of 10 mol% copper iodide in DMF.[5]
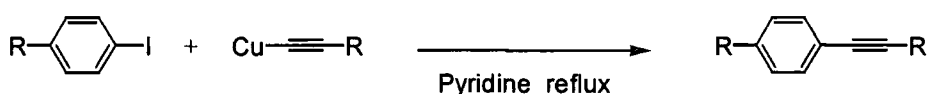
Scheme **3.1** The Stephens-Castro cross-coupling reaction

The inherent difficulties associated with these methods, led to the search for other catalytic routes to the formation of ethynyl arenes. One of the most promising areas was the field of homogeneous catalysis by transition metals, particular those in Group 10 of the periodic table. The most commonly used catalysts are palladium species, which have the ability to selectively catalyse an enormous range of reactions.[6] Many of the most widely utilised reactions are named after their originators, such as the Heck reaction, used to couple aryl or vinyl halides to terminal alkenes,[7] and the Stille[8] and Suzuki-Miyaura[9] reactions, which couple aryl and vinyl halides to organo-tin and organo-boron compounds respectively. Numerous palladium salts and complexes are used in these reactions. Often certain catalysts or catalyst systems have been found to perform better in some reactions than others. For example, one of the most widely used catalysts for the Heck reaction is palladium(II) acetate, which is routinely used in acetonitrile solution in the presence of phosphine and tertiary amine. However, in the Suzuki-Miyaura reaction, much better results are obtained with tetrakis-(triphenylphosphine)palladium(0).

Over the course of many years, various transition metal acetylides have been coupled to aryl halides, through the use of palladium catalysed cross-coupling reactions.[10] These include tin,[11] zirconium,[12] lithium,[13] and magnesium acetylides (alkynyl Grignard reagents).[14] Alkynyl boranes have also been used to synthesize ethynyl arenes under Suzuki-Miyaura conditions.[15] While the reactions utilising these reagents are often very efficient and high yielding, there are drawbacks associated with their preparation. As with copper acetylides, many acetylide species are expensive, toxic, air-sensitive, or potentially explosive. In order to circumvent these drawbacks, a search was undertaken in the mid-1970s to find a catalytic system which would couple aryl halides directly to terminal alkynes, without the need for the preparation of these, or any other, acetylide species beforehand.

An important observation was that tetrakis(triphenylphosphine)nickel(0) is able to couple aryl halides to terminal alkynes in the presence of base. However, the products were found to remain co-ordinated to the nickel centre, necessitating their removal with hydrochloric acid. This leaves the nickel in the (+2) oxidation state, and therefore unable to undergo any further reactions with the substrate, meaning that the reaction is not catalytic. However, a similar reaction using tetrakis-(triphenylphospine)palladium(0) was found to be catalytic.[16] Similar reactions were found to proceed using bis(triphenylphosphine)palladium(II) diacetate in triethylamine at 100 °C.[17] A major breakthrough came shortly after, when it was discovered that a combination of catalytic amounts of the air-stable bis(triphenylphosphine)palladium(II) dichloride complex and copper(I) iodide in an organic amine solvent, was able to couple aryl iodides to terminal alkynes in high yields at low temperatures, often at room temperature[18] as shown in Scheme **3.2**. This reaction is widely referred to as the Sonogashira reaction after one of its discoverers. The active catalytic species is believed to

be formed *in situ* during the reaction, from the palladium(II) precursor complex.

$$R-\langle\bigcirc\rangle-I \quad + \quad H-\!\!\equiv\!\!-R \quad \xrightarrow[NR_3]{(PPh_3)_2PdCl_2, \ CuI} \quad R-\langle\bigcirc\rangle-\!\!\equiv\!\!-R$$
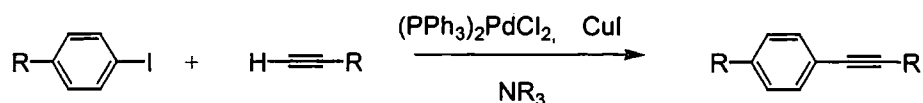
Scheme **3.2**   The Sonogashira cross-coupling reaction

Although the catalyst precursors are air-stable, the actual catalytic species are not and, as a consequence, the reaction must take place in the absence of air, or more specifically oxygen. The amines are usually distilled under nitrogen beforehand to remove any traces of oxygen from them, which would otherwise impair the reaction.   If any oxygen is present during the reaction, it leads to the formation of butadiyne species, created by the oxidative coupling of two terminal alkyne species. This is known as Glasser coupling.[19] Sometimes competing side-reactions involving hydrodehalogenation of the aryl halide have been found to occur.[20] This can be avoided through the use of aryl triflates.[21] It was found that most aryl iodides and aryl triflates will react at room temperature, whereas aryl bromides usually require elevated temperatures. It was also found that electron-withdrawing groups at the para position of the aryl bromide increase the reactivity, whereas electron-donating ones decrease it. Most aryl chlorides are completely unreactive, although those activated by several nitro-groups and aromatic heterocyclic chlorides will react under refluxing conditions[22] These observations are consistent with most other palladium catalyzed cross-coupling reactions.

3.2.2 Some Modifications of the Reaction

There have been many developments made to the Sonogashira reaction in subsequent years, which have been reviewed several times.[23] However, the most important of these will be summarised below. The palladium complex can be synthesized easily, and in almost quantitative yields from palladium(II) dichloride, via the bis(benzonitrile) palladium (II) complex or otherwise.[24] However, many other variations of catalyst system have been tried. It was found that other palladium(II) complexes can catalyse the reaction, such as bis(triphenylphosphine(II) diacetate,[25] or simply palladium(II) salts, such as palladium(II) diacetate in the presence of free phosphine.[26] The activity is high with a palladium to phosphine ratio of 2:1, but decreases significantly if the phosphine is present in excess.[27] Palladium(0) complexes, such as tetrakis(triphenylphosphine)palladium(0) or bis(dibenzylidenacetone)-palladium(0) can also be used in the presence of phosphine, which removes the possibility of diyne formation if air is rigorously excluded.[28] Recently, dramatic results have been achieved with equimolar mixtures of bis(benzonitrile)palladium(II)dichloride and tri(tert-butyl)phosphine, which can cataylse reactions of the normally unreactive aryl bromides at room temperature.[29] There have also been reports of the use of palladacycles[30] and palladium carbene complexes,[31] which are able to catalyse the reaction in the absence of copper salts. Palladium on activated glass or charcoal has also been shown to be an effective catalyst.[32] Similar modifications have been made to the copper co-catalyst. It was found that copper(I) bromide can be substituted for the iodide, although the use of copper(I) chloride precipitates copper acetylides.[33] It has been demonstrated recently that the co-catalyst need not be copper iodide as both zinc chloride and sodium iodide have been used, giving good yields and reasonable rates.[34] However, the most commonly used catalyst system remains the original one.

Amines are commonly used as solvents for the reaction, although the reaction will take place in other solvents if stoichiometric quantities of amine are present. The nature or basicity of the amine appears to have little effect on the reaction. An interesting recent observation is that the reaction can take place at ambient temperature without a copper co-catalyst if piperidine or pyrrolidine are used as solvents.[35] It has also been found that aryl bromides can react at room temperature in solvents such as THF with only 1.5 equivalents of added amine, giving yields comparable to those obtained in refluxing amine.[36] Several promising developments have been made in reactions which take place in aqueous solvents. These are potentially important from both an environmental and economic standpoint. The first attempts were made using water-soluble palladium catalysts, in water / acetonitrile mixures, without a copper co-catalyst, in the presence of amine.[37] More recently, couplings have been reported to proceed in aqueous potassium carbonate solutions, in the presence of small amounts of amine, using the original catalysts.[38]

The major disadvantage of homogeneous transition metal-catalyzed reactions such as the Sonogashira reaction is the necessity to remove the metal species from the products after the reaction. In the laboratory this is usually accomplished with the use of small columns of silica gel. However, this is impractical for industrial processes, and leads to it being disfavoured by industry. It was with this in mind that several groups began to look at alternative solvent systems, particularly biphasic ones, which allow for easy separation of the products from the metallic waste. One potential method of overcoming this is to use fluorous biphasic catalysis, employing a mixture of hydrocarbons with perfluorocarbons. These are miscible at high temperatures, which the reaction mixtures would require to react, but separate upon cooling to facilitate the easy separation of the products from the catalysts. This has recently been applied to several palladium catalyzed cross-coupling reactions, but not as yet to the Sonogashira reaction. However, reactions in supercritical

carbon dioxide have been attempted. The products can be isolated simply by a change in pressure, which allows the two phases to separate.[39] Recently, an entirely solventless coupling has been developed based on palladium-doped alumina, in the presence of phosphine, copper iodide and microwave radiation.[40]

3.2 The Reaction Mechanism

3.2.1 The Catalytic Cycle

A basic mechanism for the reaction was proposed by its originators, and is outlined in Scheme **3.3**.[18] It can be divided into two parts: a catalytic cycle, and an initiation step. In common with most other palladium reactions, the first step of the catalytic cycle is the oxidative addition of the aryl halide to a palladium(0) species. This is followed by a transmetallation step, in which the halogen from the oxidative addition is replaced by an acetylide group. This is followed by a trans-cis isomerisation, after which the acetylide is coupled to the aryl group in a reductive elimination, which also regenerates the original palladium(0) species, making it available to participate in further catalytic cycles. The initiation of the reaction requires the formation of the active palladium(0) species from the air-stable palladium(II) precursor complex. This reduction of the palladium can be achieved either through the use of nucleophiles,[41] or by independent reducing agents.[42] In the case of the Sonogashira reaction, it is believed that the nucleophile is a copper(I) acetylide species. Two of these can undergo transmetallation with the palladium(II) complex, in which the original chloride ligands are substituted by acetylide ones. The two acetylide ligands then reductively eliminate to afford the catalytically active bis(triphenylphosphine) palladium(0) species. The side-product of this elimination is a butadiyne species. In the absence of oxygen, one mol equivalent is produced per mol catalyst.[20a] However, any oxygen that is present can re-oxidise the palladium(0) species to palladium(II), which is able to repeat the initiation step again, to generate more diyne. The fact that this redox cycle is often faster than the cross-coupling, leads to the potential for large quantities of diyne being produced at the expense of product and makes the exclusion of air essential.
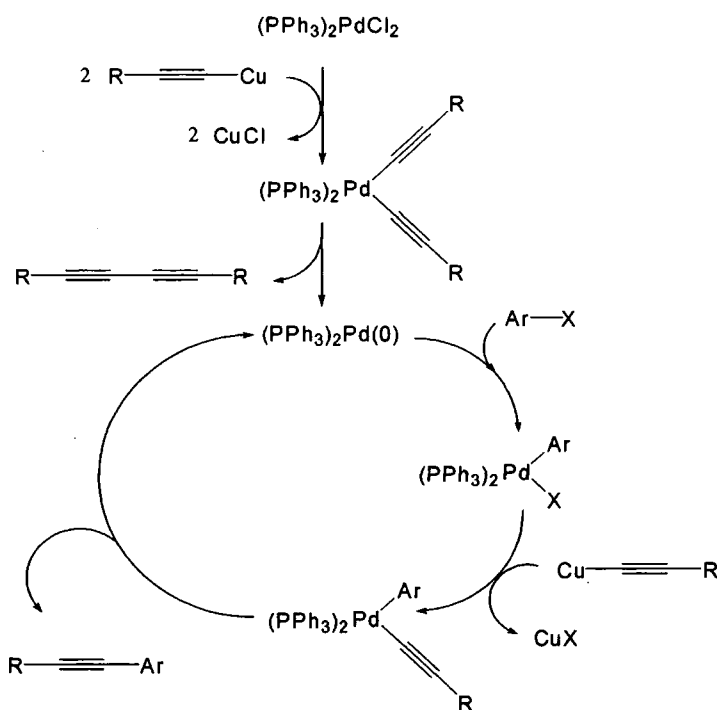
Scheme **3.3**   The proposed initiation step and catalytic cycle of the Sonogashira reaction

Each step of the catalytic cycle has been studied in detail, both in the context of the Sonogashira reaction and other catalytic cycles for similar reactions. Oxidation addition of aryl halides to low valent metal centres, has been thoroughly reviewed.[43] Generally, aryl iodides are more reactive than aryl bromides, and aryl chlorides will only react if the metal has electron-donating ligands which make it more nucleophilic.[44] It has been observed to proceed via three separate processes, as shown in Scheme **3.3**, nucleophilic aromatic substitution; a single electron transfer (SET) process in which an electron is transferred from the metal to the aryl halide, followed by the collapse of the electron pair of the carbon-halogen bond; or a three-centred concerted pathway.   In the nucleophilic substitution and SET processes, the rate is increased by electron-withdrawing substituents on the aryl halide, which

stabilise the transition states. However, in the three-centre concerted pathway, the transition state is stablised by electron-donating substituents.
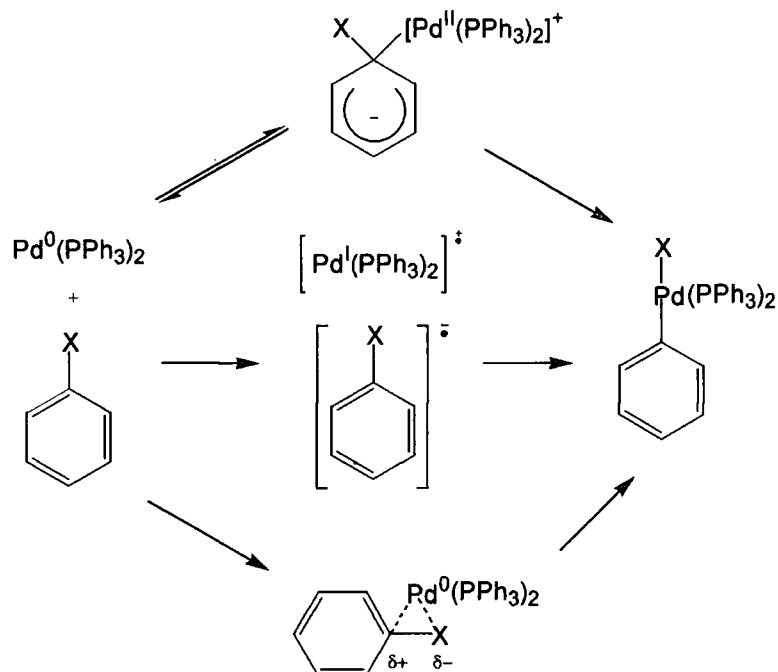
Scheme **3.4** Suggested pathways for oxidative addition of aryl halide to palladium: nucleophilic aromatic substitution (top); single electron transfer (centre); three centre concerted pathway (bottom)

The oxidative addition of aryl halides to tetrakis(triphenylphosphine) palladium(0) has been subject to a number of studies.[45] It was that found that generally aryl iodides are the most reactive, usually reacting at room temperature. Aryl bromides will also undergo oxidative addition at high temperature generated under refluxing conditions, whereas aryl chlorides are usually inert to oxidative addition, except when activated by electron withdrawing groups at the para position. The oxidative addition of aryl iodides to palladium centres has been studied by electrochemical methods.[46] It was found the rate of oxidative addition was first order in both palladium and aryl iodide, and inversely proportional to the amount of free phosphine ligand. It

was then suggested from a Hammett plot that the mechanism was one of aromatic nucleophilic substitution, by a bis(phosphine)palladium(0) complex, formed from a rapid dissociation of phosphine ligands. Since all of these trends are observed in the Sonogashira reaction, it has been suggested that oxidative addition is usually the rate-limiting step. After oxidative addition, the complex is usually in the trans-form.[47]

The next stage is transmetallation, which is the key step in a number of cross coupling reactions. It occurs when a main group (or pseudo-main group) organometallic transfers its organic moiety to a transition metal.[48] Although it has generally been much less well studied than oxidative addition, it has been found to be an equilibrium, which, in order to proceed with any great efficiency, must result in an energy gain for both metals, which means that the main group organometallic metal must be more electropositive than the transition metal. In the case of the Sonogashira reaction, the organometallic is believed to be a copper(I) acetylide species, which is formed from the copper-assisted abstraction of the proton on the terminal alkyne by the amine. This transmetallation has been studied in some detail, and it is found that it generally occurs with a retention of the trans-configuration of the complex.[49]

Reductive elimination is the final step of the cycle, which generates the coupled product. It can only take place if the ligands being eliminated are cis to each other, as was demonstrated by the failure of complexes containing the transphos ligand, shown in Figure 3.1, to reductively eliminate.[50] The ligand is sterically required to chelate in the trans position, and therefore forces the other ligands to remain trans to each other in a square planar complex. The rate of reductive elimination has been found to be dependent upon the nature of the phosphine ligands on the palladium centre.[51]
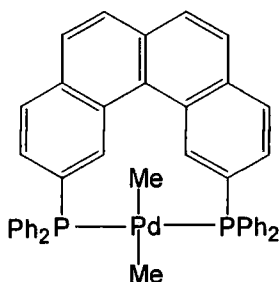
Figure **3.1** The structure of a palladium transphos complex unable to reductively elminate ethane

Following on from this, additional work has been carried out on the kinetics of the Sonogashira reaction as a whole. However, some conflicting results have been obtained. It was shown that the reaction is zero-order with respect to both aryl.bromides and 1-heptyne,[52] with a rate constant that increases with increasing electron-withdrawing power of the para-substituents. However, this was in contrast to later reports that it is first order in both aryl halides and TMSA.[53] The difference in the two studies may be due to the fact that the former employed tetrakis(triphenylphosphine)palladium(0), whereas the latter used bis(triphenylphosphine)-palladium(II) dichloride. It was also found that the effect that the para-subtituents on aryl iodides have on the rate was more complicated. Whilst the largest rate constants occur for the most electron-withdrawing groups, the constants for electron-donating groups are all very similar. This suggests that two mechanistic pathways are involved: nucleophilic aromatic substitution for the electron-withdrawing substituents, and a concerted three-centre associative step for the electron-donating substituents. In the latter case, there may be a build up of positive charge at the C(ipso) of the transition state, which is stabilized by the electron-donating substituents and by the 'soft' iodide ligand. A similar argument was made previously in order to explain the rate dependence of Heck reactions of para-

substituted aryl iodides, although these were made under ligandless conditions.[54]

3.2.2 Recent Developments

The validity of the proposed catalytic cycle has come under increasing scepticism in recent years. This is because the overall rate of the reaction has been shown to be faster than the oxidative addition to the palladium(0) which was reputed to be the rate limiting step in the proposed mechanism. There was concern that, although many of the proposed catalytic intermediates have been shown to form stable complexes, they may not be the ones formed during the catalytic cycle. This led to a major investigation of the reaction mechanism by modern techniques. It has been shown by cyclic voltammetry and ^{31}P-NMR that bielectronic reduction of the palladium(II) precursor produces three anionic species, which exist in equilibrium. The major species is a three-coordinate anion, which is similar to the palladium(0) proposed in the original mechanism, but it is co-ordinated by a chloride ligand.[55] The other species are a four-coordinate dianion with two chloride ligands, and an anionic, chloride-bridged palladium dimer, as is shown in Scheme 3.5. These are both believed to undergo oxidative addition, the dimer being even more reactive than the three-coordinate species, but are present in such small quantities as to not significantly affect the overall catalytic cycle. The relative proportion of these species is dependent on both the palladium and chloride concentrations. These species have also been generated chemically by bases in the presence of metal cations, which increases their reactivity towards oxidative addition, due to the interaction of the metal cations with the chloride

ligands, which is believed to result in a less well coordinated species that is more reactive.[56] Similar reductions performed on the same complexes with bromide and iodide ligands gave species with dramatically different ^{31}P chemical shifts suggesting that the halogen is involved in the complex.

$(PPh_3)_2PdCl_2$

$\downarrow$ +2e$^-$

$\left[(PPh_3)_2Pd^0\text{—}Cl \right]^{\ominus}$ $\xrightarrow{+Cl^-}$ $\left[(PPh_3)_2Pd^0\underset{Cl}{\overset{Cl}{\diagup}} \right]^{2-}$

$\left[(PPh_3)_2Pd^0\underset{Cl}{\overset{Cl}{\diagup\diagdown}}Pd^0(PPh_3)_2 \right]^{2-}$
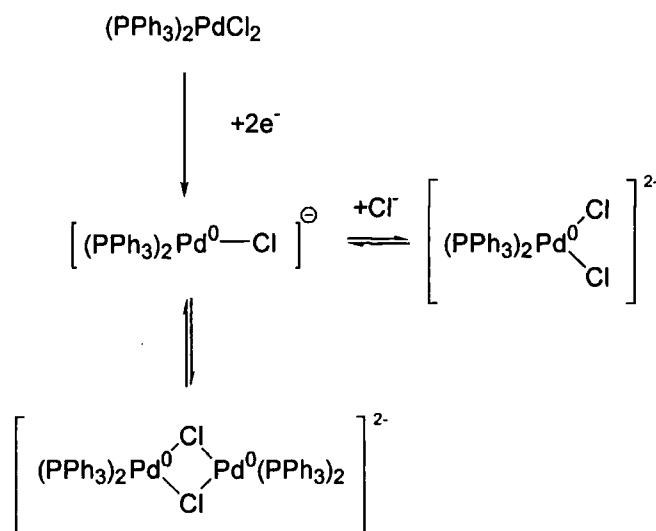
Scheme **3.5** The anionic species formed upon reduction of the palladium(II) precursor

Upon the oxidative addition of aryl halides an 18-electron anionic five-coordinate species is formed, which has been detected by its oxidation peaks in a cyclic voltammogram.[57] These species are short-lived and decay to a neutral species by replacement of the chloride ion by a solvent molecule. This solvent molecule then departs to leave the four co-ordinate oxidative addition complex as generated in the original reaction scheme. This step is inhibited by chloride ions, and indeed, their concentration exerts a considerable influence on the formation of these species and hence the rate of reaction. Even though the four-coordinate palladium species generated by this sequence are able to undergo transmetallation with nucleophiles, these reactions are slower than the overall catalytic reaction, which rules them out

as reactive intermediates in the catalytic cycle. Instead the acetylide nucleophiles are believed to attack the five-coordinate solvated species. The reaction then proceeds via anionic species in a new catalytic cycle. The adjacent acetylide and aryl ligand reductively eliminate to generate the cross-coupled product and the original chloride-ligated palladium(0) ligand species, which is then available to catalyse further turnovers.[58]

However, several complicating factors have recently been brought to light. As the reaction proceeds, halide ions are released. These may be free or ion-paired, and this has a considerable effect on the reaction. If the ions are paired, it reduces the probability of the formation of anionic complexes, leaving the reaction with no alternative other than to proceed through the original slower catalytic route. However, whenever free ions are available, as is the case in most solvents including amines, the faster anionic mechanism is expected to dominate. However, towards the end of the reaction, the acetylide begins to get used up. This increases the probability of the five-coordinate solvated species transforming irreversibly to the four-coordinate species. This is then able to react with the nucleophile in a subsidiary cycle similar to the one originally proposed. After having reductively eliminated the product it then rejoins the main cycle.[59] This is illustrated in Scheme **3.6**.
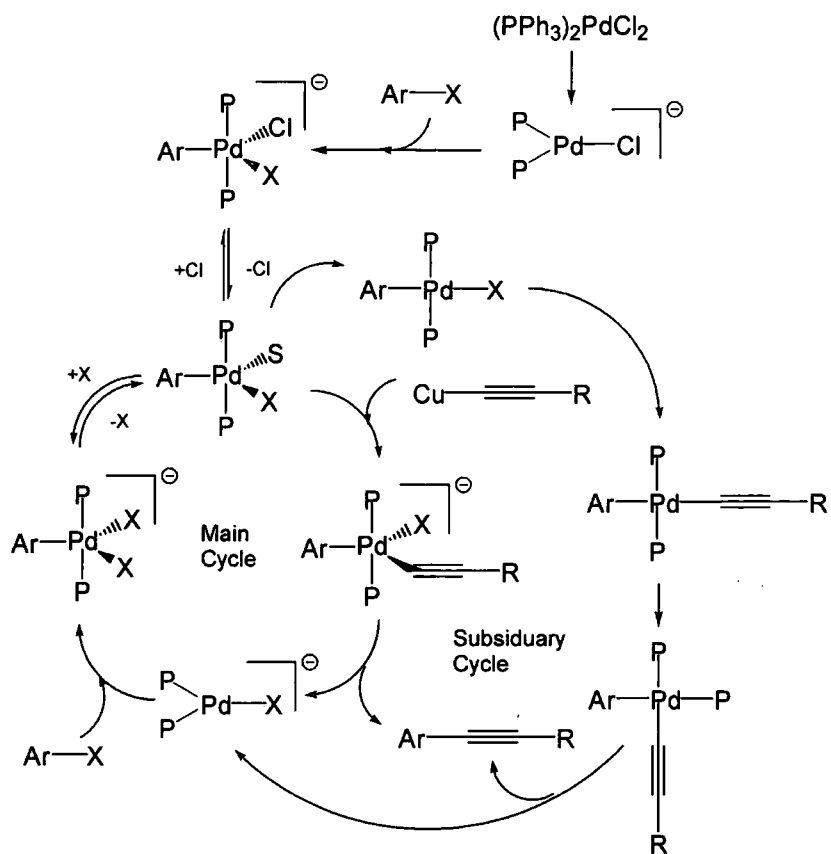
Scheme **3.6** The revised catalytic cycle for the Sonogashira reaction

3.3 References

1. K. Sonogashira, in *Comprehensive Organic Synthesis,* series ed. B. M. Trost and I. M. Fleming, Vol. 3, ed. G. Pattenden, Pergamon, Oxford, 1990, p. 521.

2. R. D. Stephens and C. E. Castro, *J. Org. Chem.*, 1963, **28**, 3313.

3. T. Ogawa, K. Kusume, M. Tanaka, K. Hayami and H. Suzuki, *Synth. Commun.*,1989, **19**, 2199.

4. a) K. Okuro, M. Furune, M. Miura and M. Nomura, *Tetrahedron Lett.* 1992, **37**, 5363; b) K. Okuro, M. Furune, M. Enna, M. Miura and M. Nomura, *J. Org. Chem.*, 1993, **58**, 4716.

5. a) S. K. Kang, J. S. Kim and S. C. Choi, *J. Org. Chem.*, 1997, **62**, 4208; b) S. K. Kang, W. Y. Kim and X. G. Jiao, *Synthesis*, 1998, **9**, 1252.

6. a) L. S. Hegedus, *Transition Metals in the Synthesis of Complex Organic Molecules*, University Science Books, Mill Valley, CA, 1994, p. 90; b) J. Tsuji, *Palladium Reagents and Catalysis*, John Wiley & Sons, Chichester, 1995; c) J. Tsuji, *Organic Synthesis with Palladium Compounds*, Springer, Berlin, 1990; d) R. F. Heck, *Palladium Reagents in Organic Synthesis*, Academic Press, London, 1985.

7. R. F. Heck, *Acc. Chem. Res.* 1979, **12**, 146.

8. J. K. Stille, *Angew. Chem. Int. Ed. Engl.*, 1986, **25**, 508.

9. a) A. Suzuki, *Acc. Chem. Res.*, 1982, **15**, 178; b) N. Miyaura and A. Suzuki, *Chem. Rev.*, 1995, **95**, 2457.

10. E.-I. Negishi, *Acc. Chem. Res.*, 1982, **15**, 340.

11. a) J. K. Stille and J. H. Simpson, *J. Am. Chem. Soc.*, 1987, **109**, 2138; b) D. E. Rudisill, L. A. Castonguay and J. K. Stille, *Tetrahedron Lett.*, 1988, **29**, 1509.

12. a) F. Tellier, R. Sauvetre and J. F. Normant, *Tetrahedron Lett.*, 1986, **27**, 3147; b) N. Yoneda, S. Matsuoka, N. Miyaura, T. Fukahara and A. Suzuki, *Bull. Chem. Soc. Jpn.*, 1990, **63**, 2124.

13. M. I. Al-Hassan, *J. Organomet. Chem.*, 1990, **395**, 227.

14. R. Rossi, A. Capita and A. Lezzi, *Tetrahedron*, 1984, **40**, 2773.

15. a) J. A. Soderquist, K. Matos, A. Rane and J. Ramos, *Tetrahedron Lett.*, 1995, **36**, 2401; b) A. Furstner and G. Siedel, *Tetrahedron*, 1995, **41**, 11165.

16. L. Cassar, *J. Organomet. Chem.*, 1975, **93**, 253.

17. H. A. Dieck and R. F. Heck, *J. Organomet. Chem.*, 1975, **93**, 259.

18. K. Sonogashira, Y. Toda and N. Hagihara, *Tetrahedron Lett.*, 1975, 4467.

19. A. S. Hay, *J. Org. Chem.*, 1962, **27**, 3320.

20. a) P. Nguyen, Z. Yuan, L. Agocs, G. Lesley and T. B. Marder, *Inorg. Chim. Acta*, 1994, **220**, 289; b) S. Mukhopadahyay, G. Rothenberg, D. Gitsi and Y. Sasson, *Org. Lett.*, 2000, **2**, 211.

21. Q.-Y. Chen and Z.-Y. Yang, *Tetrahedron Lett.* 1986, **27**, 1171.

22. a) R. Singh and G. Just, *J. Org. Chem.*, 1989, **54**, 4453; b) H. Yamanaka, T. Sakamoto, M. Shiraiwa and Y. Kondo, *Synthesis*, 1983, 312.

23. a) I. B. Campbell, in *Organocopper Reagents: A Practical Approach*, ed. R. J. K. Taylor, Oxford University Press, Oxford, 1994, p. 224; b) R. Rossi, A. Carpita and F. Bellina, *Org. Prep. Proced. Int.*, 1995, **27**, 127; c) K. Sonogashira, in *Metal Catalyzed Cross-Coupling Reactions*, ed. F. Diederich and P. J. Stang, Wiley-VCH, Weinheim, Germany, 1998, p. 203; d) L. Brandsma, S. F. Vasilevsky and H. D. Verruijsse, in *Application of Transition Metal Catalysts in Organic Synthesis*, Springer, Berlin, 1988. p. 179.

24. a) R. F. Heck, *Palladium Reagents in Organic Synthesis*, Academic Press, London, 1985, p. 18; b) L. Brandma, S. F. Vasilevsky and H. D. Verruijsse, *Application of Transition Metal Catalysts in Organic Synthesis*, Springer-Verlag, 1988, p. 4.

25. A. Kasahara, T. Izumi and M. Maemura, *Bull. Chem. Soc. Jpn.*, 1977, **50**, 1021.

26. a) W. B. Austin, N. Bilow, W. J. Kellegan and K. S. Y. Lau, *J. Org. Chem.*, 1981, 2280; b) G. Menchi, A. Scrivanti and U. Matteoli, *J. Mol. Catal. A.*, 2000, **152**, 77.

27. E. T. Sabourin and A. Onopchenko, *J. Org. Chem.*, 1993, **48**, 5135.

28. V. P. W. Bohm and W. A. Herrman, *Eur. J. Org. Chem.*, 2000, 3679.

29. T. Hundertmark, A. F. Littke, S. L. Buchwald and G. C. Fu, *Org. Lett.*, 2000, **2**, 1729.

30. W. A. Hermann, C.-P. Reisinger, K. Ofele, C. Brossmer, M. Beller and H. Fischer, *J. Mol. Catal. A*, 1996, **108**, 51.

31. W. A. Hermann, C.-P. Reisinger and M. Spiegler, *J. Organomet. Chem.*, 1998, **557**, 93.

32. a) M. A. de la Rosa, E. Verlarde and A. Guzman, *Synth. Commun.*, 1990, **20**, 2064; b) J. Li, A. M.-H. Mau and C. R. Strauss, *Chem. Commun.*, 1997, 1275.

33. N. A. Bumagin, A. B. Ponomarev and I. P. Beletskaya, *Bull. Acad. Sci. USSR*, 1985, **33**, 1433.

34. a) G. T. Crisp, P.D. Turner and K. A. Stevens, *J. Organomet. Chem.*, 1998, **570**, 219; b) M. Beller, A. Zapf, *Synlett.*, 1998, **7**, 792.

35. M. Alami, F. Ferri and G. Linstrumelle, *Tetrahedron*, 1993, **34**, 6403.

36. S. Thorand and N. Krause, *J. Org. Chem.*, 1998, **63**, 8551.

37.   a) A. L. Casalnuovo and J. C. Calabrese, *J. Am. Chem. Soc.*, 1990, **112**, 4324; b) J. P. Genet, E. Blart and M. Savignac, *Syn. Lett.*, 1992, 715.

38.   a) N. A. Bumagin, L. I. Sukhomlina, E. V. Luzihova, T. P Tolstaya and I. P. Beletskaya, *Russ. J. Org. Chem.*, 1996, **32**, 996; b) N. A. Bumagin, L. I. Sukhomlima, E. V. Luzihova, T. P. Tolstaya and I. P. Beletskaya, *Tetrahedron Lett.*, 1996, **37**, 897.

39.   M. A. Carroll and A. B. Holmes, *Chem. Commun.*, 1998, 1395.

40.   a) G. W. Kabalka, L. Wang, V. Namboodiri and R. M. Pagni, *Tetrahedron Lett.*, 2000, **51**, 5151; b) G. W. Kalbalka, L. Wang and R. M. Pagni, *Tetrahedron*, 2001, **57**, 8017.

41.   J. F. Fauvarque and A. Jutand, *Bull. Soc. Chim. Fr.* 1976, 765.

42.   E.-I. Negishi, A. O. King and N. Okukado, *J. Org. Chem.*, 1977, **42**, 1821.

43.   a) J. K. Stille, in *The Chemistry of the Metal-Carbon σ-Bond, Vol. 2*, ed. R. F. Hartley and S. Patai, John Wiley & Sons, New York, 1985, p. 625; b) J. K. Stille and K. S. Y. Lau, *Acc. Chem. Res.*, 1977, **10**, 434; c) J. K. Stille and W. R. Roper, *Adv. Organomet. Chem.*, 1968, **7**, 53.

44.   M. Hidai, T. Kashiwagi, T. Ikeuchi and Y. Uchida, *J. Organomet. Chem.*, 1971, **30**, 279.

45.   P. Fitton and E. A. Rick, *J. Organomet. Chem.*, 1971, **28**, 287.

46. a) J. F. Fauvearque, F. Pfluger and F. Troupel, *J. Organomet. Chem.*, 1981, **208**, 419; b) C. Amatore, and F. Pfuger, *Organometallics*, 1990, **9**, 2276; c) J. F. Hartwig and F. Paul, *J. Am. Chem. Soc.*, 1995, **117**, 5373.

47. A. L. Cassado and P. Espinet, *Organometallics*, 1998, **17**, 954.

48. E.-I. Negishi, *Organometallics in Organic Synthesis*, Wiley, New York, 1980.

49. K. Osakada, R. Sakata and T. Yamamoto, *Organometallics*, 1997, **16**, 5354.

50. a) A. Gillie and J. K. Stille, *J. Am. Chem. Soc.* 1980, **102**, 4933; b) F. Ozawa, T. Ito, Y. Nakamura and A. Yamamoto, *Bull. Chem. Soc. Jpn.*, 1981, **54**, 1868.

51. a) E.-I. Negishi, T. Takahashi and K. Akiyoshi, *J. Organomet. Chem.*, 1987, **334**, 181; b) J. M. Brown and P. J. Guery, *Inorg. Chim. Acta*, 1994, **220**, 249.

52. R. Singh and G. Just, *J. Org. Chem.*, 1989, **54**, 4453.

53. Z. Yuan, Ph.D. Thesis, University of Waterloo, Ontario, Canada, 1992, p. 179.

54. R. Benhaddou, S. Czernecki, G. Ville and A. Zegar, *Organometallics*, 1988, **7**, 2435.

55. C. Amatore, M. Azzabi and A. Jutand, *J. Organomet. Chem.*, 1989, **363**, C41.

56. E.-I. Negishi, T. Takahashi and K. Akiyoshi, *J. Chem. Soc., Chem. Commun.*, 1986, 1338.

57. a) C. Amatore, M. Azzabi and A. Jutand, *J. Am. Chem. Soc.*, 1991, **113**, 8375; b) C. Amatore, E. Carre, A. Jutand, H. Tanaka, Q. Ren and S. Torri, *Chem. Eur. J.*, 1996, **2**, 957.

58. C. Amatore and A. Jutand, *J. Organomet. Chem.*, 1999, **576**, 254.

59. C. Amatore and A. Jutand, *Acc. Chem. Res.*, 2000, **33**, 314.

Chapter Four

An Introduction to the Arene-Perfluoroarene Interaction

4.1 Introduction to Arene-Arene Interactions

Although much of chemistry is primarily concerned with covalent interactions between atoms, namely chemical bonds, non-covalent interactions, typically those that occur between molecules, are also very important in many areas of chemistry, biology and materials science.[1] Non-covalent interactions are responsible for many of the physical properties of organic materials, such as phase transitions, solid-state structure, viscosity, etc. Aside from ionic effects, the strongest non-covalent interaction is the hydrogen bond, which plays a very important role in many chemical and biological systems, and is now well-understood.[2] However, there are several weaker interactions, which are also important, particularly in the absence of any hydrogen bonds, and about which less is known. They are grouped into three categories. Electrostatic interactions are those occurring between permanent charges or charge distributions on the molecules. They are dominated by the lowest order molecular multipole moment, and have a large dependence on orientation. Inductive interactions occur when a permanent molecular moment causes a polarisation of the electrons on another molecule. These interactions are always attractive. Finally there are dispersive forces, which are caused by the

random fluctuations of electrons, which perturb those of the neighbouring species, leading to a net attraction. Dispersive forces are typically the weakest non-covalent interaction, but occur in all species, including the noble gases, and follow the Leonard-Jones 6-12 potential.

Intermolecular interactions between aromatic molecules first came to light when it was observed that certain binary combinations of aromatic molecules, usually involving a good electron donor, and a good electron acceptor, form intensely coloured solutions when mixed in non-polar solvents. These solutions showed characteristic bands in their UV-visible absorption spectra, which were not present in the spectra of the two individual components. It was postulated that binary complexes were being formed as a result of charge transfer (CT) from the donor to the acceptor.[3] A structure was proposed in which the molecules were aligned face-to-face to one another, so as to facilitate charge transfer, which was later confirmed by X-ray diffraction studies. However, recent evidence has found that the term 'charge transfer' is often misleading, as in many complexes, significant charge transfer only occurs in the excited state. Instead, it has been suggested that these complexes are primarily stabilised by electrostatic and dispersive forces, with CT arising as a consequence of the favourable alignment.[4] Elegant studies have been carried out on naphthalenes substituted by phenyl rings at the peri-positions,[5] in which the barrier to ring rotation was observed to increase with increasing electron-withdrawing power of the substituent on one of the rings. This was taken as evidence of there being a large dependence on electrostatic forces.

Arene-arene interactions are widespread in biological systems. A particularly good example is the double helical conformation of DNA, which is thought to be in part due to the stacking of the aromatic bases.[6] Several aromatic species have been shown to be able to intercalate themselves between the

bases of oligonucleotides, which in turn alters their helical conformations. Such species have been found to reduce tumour growth.[7] However, this intercalation has also been postulated as the cause of the high carcinogenity of many polyaromatic compounds.[8] Aromatic interactions are also believed to be involved in the organisation of certain peptides and proteins.[9] Other examples are in catalysis. It has been reported that aromatic interactions may be responsible for the activity of certain metallocene catalysts.[10] Arene-arene interactions have also been found to be of potential use in molecular recognition of aromatic molecules by cyclophanes.[11]

4.2 Introduction to Arene-Perfluoroarene Interactions

4.2.1 Thermodynamic and Phase Studies

A specific type of arene-arene interaction, which is becoming the focus of much interest, is the one which occurs between arenes and perfluoroarenes. The arene-perfluoroarene interaction has been known for 40 years, during which time it has become the subject of a good deal of interest, both experimental and theoretical. Arene-perfluoroarene interactions were first discovered when it was found that an equimolar mixture of benzene and hexafluorobenzene (HFB) at room temperature formed a solid with a melting point of 24 °C, about 20° higher than those of the individual components themselves.[12] A phase diagram was later constructed of the melting points against the composition, which clearly showed a maximum at the equimolar composition, as shown in Figure **5.1**. This was taken as evidence of a congruently melting 1:1 complex being formed in the system.
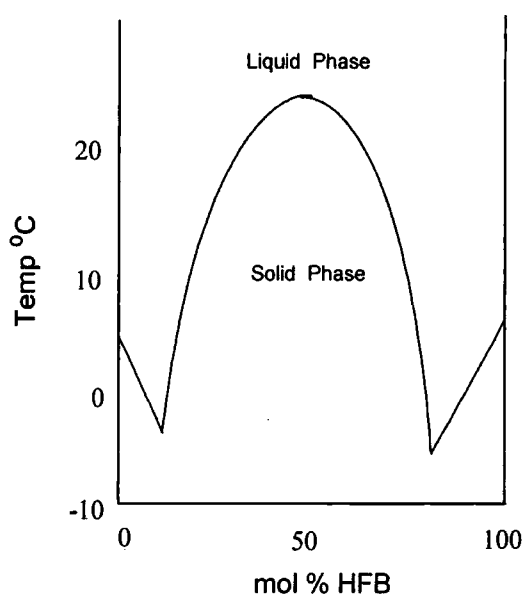
Figure **4.1** Phase diagram for the HFB-benzene system

The phenomenon was immediately shown not to be restricted to this particular mixture, as at around the same time, a similar white solid was also observed in 1:1 mixtures of HFB and aniline.[13] In the years that followed a comprehensive program of work was undertaken by a number of groups in order to gain a better understanding of the nature of mixtures and complexes of HFB with benzene and other aromatics, and the interactions that lie behind them. This work was comprehensively reviewed in 1974,[14] but will be outlined below. Phase diagrams were constructed for binary mixtures of HFB with a variety of methyl-substituted benzene derivatives.[15] The majority of these revealed the formation of congruently melting complexes, at equimolar composition. Phase diagrams were also obtained for mixtures in which the HFB component was substituted for pentafluorobenzene (PFB).[16] Although formation of a congruently melting complex did not occur in the mixture of PFB with benzene, such complexes were shown to be present in mixtures of PFB with several methyl-substituted benzenes.

Measurement of the various thermodynamic excess functions upon mixing of the components in the liquid state can reveal much about the nature of the interactions between them. Large negative values of the excess enthalpy, entropy, volume and Gibbs free energy are associated with attractive interactions between the components upon mixing. Calorimetry has been used to determine the molar excess enthalpies of HFB / benzene mixtures of various compositions, and also with HFB and a number of methyl-substituted benzenes.[17] These were all negative at equimolar composition. Similar results were found for the complexes with pentafluorobenzene,[18] although in every the case, the excess enthalpy was less negative for the PFB complex than the corresponding HFB one. The enthalpies of mixing of many binary combinations of partially fluorinated benzene derivatives have been obtained over a range of compositions.[19] There was shown to be a large variation in the

values at the equimolar composition, with both negative and positive values being found. In several systems, the enthalpies of mixing alternated from positive to negative over the course of composition. It was also noted that systems composed of molecules with opposite arrangements of fluorine atoms had markedly low enthalpies of mixing, which led the investigators to suggest a 'lock and key' effect, which was predicated to reach a maximum for the unstudied 1,3,5-trifluorobenzene system.

In addition, the excess Gibbs free energies have also been determined from analysis of the total vapour pressure at different compositions.[20] Graphs of the free energy of mixing against composition have been plotted, showing large deviations from ideal behaviour in all cases. This behaviour was rationalised by considering the free energy to be a superposition of two components: an asymmetric positive one due to the non-specific physical interactions between the components which occur upon mixing, and a symmetric negative one arising from the formation of a specific complex between the components. The specific part is called the free energy of complexation and can be found by subtracting the free energy of mixing of a system in which there is no specific interaction between the components, such as that of HFB and cyclohexane. A graph of the free energy of complexation against composition is shown in Figure **5.2**. It was found to be symmetrical about the equimolar composition, with a minimum of -0.6 kJ mol^{-1}. The equimolar values were used to determine the equilibrium constants of complex formation using the theory of associated solutions for the formation of the 1:1 complexes.
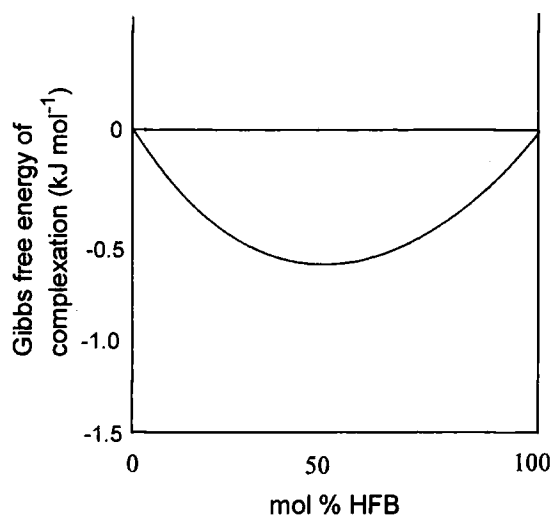
Figure **4.2**   Plot of the Gibbs free energy of complexation for the HFB-benzene system

The phase behaviour of the solid HFB·benzene complex was studied using the technique of differential scanning calorimetery (DSC).[21] There were several sharp peaks present in this thermogram, in addition to the one occurring at the melting point of the complex. These were attributed to phase transitions in the solid state, which was taken as evidence of the existence of four solid-state phases. The enthalpy of fusion was determined from the area under the melting peak. The enthalpy of formation of the solid complex at 273 K, from the components in their solid states, was calculated to be +1 kJ mol^{-1} from a thermodynamic cycle involving this enthalpy of fusion. This would strongly confirm that the complex is stabilized by entropic effects.

It was suggested that the phase transitions come about as the result of excessive molecular motion in the complex. The molecular motion in the lowest temperature phase has been be studied by analysis of static wide-line solid-state ^{1}H and ^{19}F NMR spectra, at low temperature.[22] As the temperature increased, the line-widths and second moments also increased. Rapid re-

orientations of six-fold symmetry about the molecular axis were postulated as being the most probable cause. The line-widths were correlated with theory to obtain values for the activation energies and correlation time for the re-orientations. Similar results were obtained from analysis of the relaxation times.[21(b)] Analysis of the solid-state fluorine spectra lineshapes, displayed a gradual loss of fine structure as the temperature increased. This was taken to be indicative of relatively slow rotation of the HFB molecules in the lowest temperature phase. Later, solid-state cross polarisation ^{13}C NMR spectroscopy employing magic-angle spinning was used to show that the molecules are also wobbling on their axes.[23]

The molecular dynamics of the higher temperature phases and phase changes of this complex have been studied by quasi-elastic neutron scattering at a range of temperatures.[24] Low energy neutrons are scattered inelastically as a result of interaction with moving molecules. The energy of the scattered neutrons disperses with increasing molecular motion, and the dispersion can be fitted to theoretical models, to enable values of activation energies and diffusion constants for molecular processes to be ascertained. In agreement with the NMR results, it was found that the motion in the lowest temperature phase was due to the six-fold molecular re-orientations. However, in the higher temperature phases, translational diffusion came into play, which was assumed to be responsible for some of the phase transitions. Neither pure benzene nor HFB undergo any of these first-order solid-state phase transitions, a fact which was attributed to a packing arrangement that does not enable the molecules to diffuse in the solid state.

The HFB·benzene complex has also been studied by Raman spectroscopy, and its spectrum compared to those of the individual components.[25] The high frequency region of the complex spectra corresponds to the intramolecular vibrations, and hardly differs from the superposition of the spectra of the

components, indicating that there is little change in the molecular structure of the components, which would not be the case if it were a charge-transfer complex. The low frequency region corresponds to excitation of the quantitized lattice vibrations or phonons. This spectrum differs appreciably from the summation of those of the components, which was attributed to the different structure of the complex. The spectrum of the deuterated complex, shows significant high frequency shifts for approximately half of the peaks. These are believed to be optical phonons in which the majority of motion is located on the benzene, whereas the remainder are acoustic ones where most of the motion is on the HFB molecules, and are therefore unaffected upon deuteration.

4.2.2 Crystallographic Studies

The greatest insight into the nature of the complex came several years later when the crystal structure of the highest temperature phase of the HFB·d_6-benzene was determined by X-ray diffraction.[26] Although the structure of the highest-temperature phase contained much disorder, reflecting the degree of molecular motion found by the neutron scattering experiments, it did show the constituent molecules to be arranged in infinite columns of stacked HFB/benzene pairs. Structures of the lower temperature phases could not be obtained by single-crystal X-ray diffraction because the samples shattered into powder form upon cooling through the phase transition. This problem was overcome several years later using the technique of neutron powder diffraction for the first time on an organic material, to determine fully the structure of the lowest-temperature phase and to obtain cell parameters and space groups for the remaining ones.[27] The structure of the lowest-

temperature phase was found to be composed of infinite stacks of equally spaced, near parallel alternating HFB and benzene molecules. The alternating molecules adopt neither a staggered nor eclipsed conformation in their columns. A view taken perpendicular to the mean of the stacking axis, reveals that there is considerable offset between the two molecules, which are neither in an eclipsed or staggered conformation. This arrangement is in dramatic contrast to the structures of the HFB and benzene components, which display herringbone packing in the solid-state.[28] Three views of the crystal structure of the lowest temperature phase are given in Figure **4.3**.
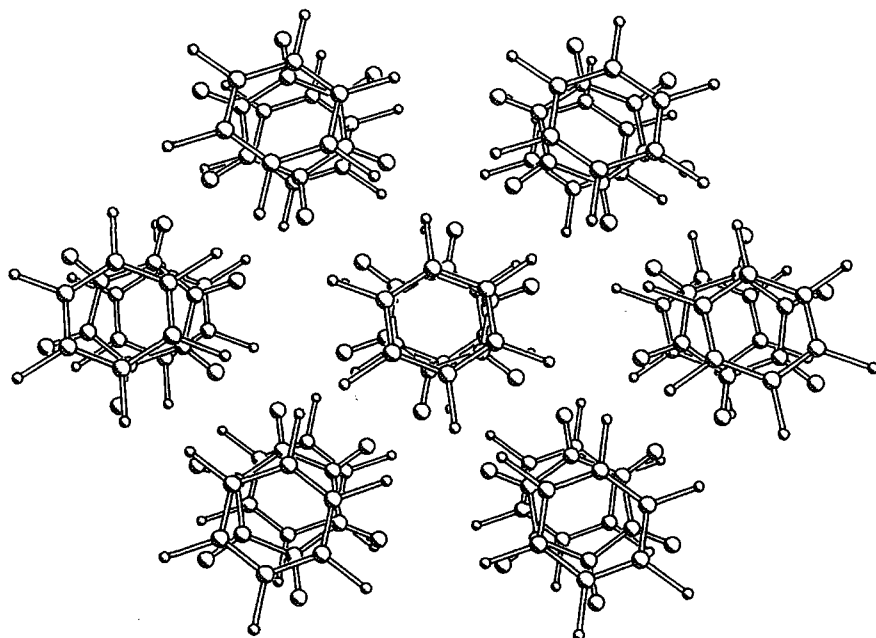
Figure **4.3(a)**   The molecular packing of the HFB·d_6-benzene complex viewed perpendicular to molecular planes of the HFB molecules

Figure **4.3**(b) The arrangment of the HFB and benzene molecules in a stack
showing the offset
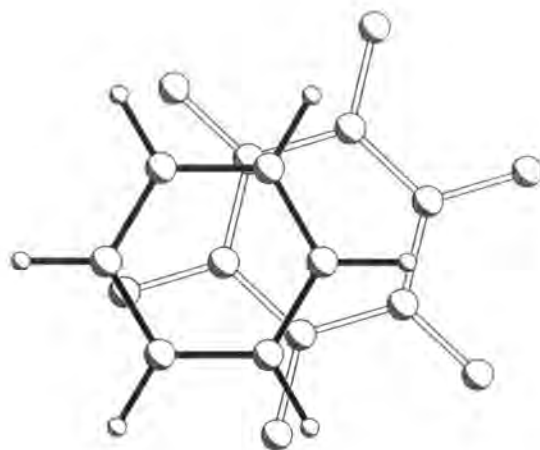
Figure **4.3**(c) Overlap diagram of adjacent HFB and benzene molecules in a
stack

An ambitious program of work was undertaken by Dahl to solve the crystal
structures of the complexes of HFB with several methyl-substituted benzene[29]
and aniline derivatives.[30] Most of these crystal structure determinations were

carried out at room temperature or slightly below, in order to avoid the deleterious effects such as crystal shattering or twinning which occur upon cooling. Several problems were encountered with disorder and twinning, which affected the reliability of some of the structures. The results of these experiments were later collated in a review.[31] All of the structures obtained clearly show the HFB and aromatic molecules to be stacked alternately in infinite columns. There were considerable differences in the overlap and orientation between the individual component molecules when projected onto their average plane. It was noted that there was a trend towards a more parallel orientation as the number of methyl groups increased, from an angle of 30° in the complexes with para-xylene and mesitylene, to approximately 0° for the complex with hexamethylbenzene (HMB). The mean interplanar distances of the complexes of HFB with the methyl-substituted benzenes were compared with each other, revealing a general trend of decreasing interplanar distance, with increasing methyl group substitution. They were all, however, noted to be somewhat larger than those in the crystal structures of typical CT complexes, such as those of analogous complexes with fluoranil.[32]

This stacking is not merely restricted to benzene derivatives. The structure of the 1:1 complex of biphenyl and perfluorobiphenyl,[33] has a packing that is very similar to that of 1,2,3,4,5-pentafluorobiphenyl, in which the molecules are arranged in a head-to-tail arrangement.[34] None of these molecules are planar, with dihedral angles in the range 36.4 – 52.9°. A similar complex has been obtained with trans-stilbene and trans-decafluoroazobenzene.[35] Similar 1:1 complexes have been formed between selectively fluorinated (phenylethynyl)benzene derivates, namely 1,4-bis(phenylethynyl)-tetrafluoro-benzene·1,4-bis(pentafluorophenylethynyl)benzene[36] and 1,3,5-tris(phenyl-ethynyl)benzene · 1,3,5,-tris(pentafluorophenylethynyl)benzene.[37] Various crystal structures of 1:1 complexes of fluorinated 1,4-distyrylbenzenes have

been solved by single-crystal and powder diffraction technique, and shown to exhibit the arene-perfluorarene interaction.[38]

4.2.3   The Nature of the Arene-Perfluoroarene Interaction

The arene-perfluoroarene complexes were initially thought to arise because of charge transfer between a donor and acceptor. However, the complexes between HFB and methyl-substituted benzenes failed to show any characteristic absorption bands in the UV region, and, as a result, the charge-transfer theory was abandoned. In contrast, the complexes of HFB with aromatic amines did show charge transfer bands in UV absorption spectra, which were assumed to result from charge transfer to the HFB molecule from the non-bonding orbitals of the amines.[39] Recently, charge transfer bands were also found in a complex between HFB and bis(benzene)chromium.[40] However, it was recognised that HFB and benzene molecules have a specific tendency to align parallel to each other, which is not merely a result of lattice energy minimisation, as was evidenced by molecular beam studies, which showed the molecules to form face-to-face dimers in the gas phase.[41]

It was first proposed in the 1970s that it is electrostatic forces which are the dominant attractive interactions between the benzene and HFB molecules.[42] The electrostatic forces between two molecules are dominated by the first non-vanishing electrical moment, which in the case of both HFB and benzene is the quadrupole moment. The quadrupoles can be envisaged as a torus of some charge surrounding a central tube of opposite charge. Values of these quadrupole moments have been determined using vapour-phase electric field

gradient induced birefringence, to be -29×10^{-40} C m^{-2} for benzene, and 31.7 $\times 10^{-40}$ C m^{-2} for HFB,[43] which are approximately equal in magnitude and opposite in sense. Quadrupole moments have also been calculated for HFB and benzene using *ab initio* methods and found to be in good agreement with the experimental values.[44] The cause of the opposite senses is the difference in electro-negativity of the fluorine and hydrogen atoms. Calculations of the quadrupole-quadrupole interaction energy between benzene and HFB molecules, separated by a distance comparable to their van der Waals surfaces, showed that this energy was minimized when the molecules adopt a parallel face-to-face orientation as observed in the crystal structures.[45] This is in contrast to the molecules of benzene and HFB in their pure states, in which the potential minima are found when the respective molecules are arranged perpendicular to each other. This is shown in Figure **4.4**. However, both of these minima in the pure components are surpassed considerably by the minimum of the HFB·benzene complex, which led to this quadrupole-quadrupole interaction being postulated as the cause of the extra stability of the complex in the solid-state.[46]
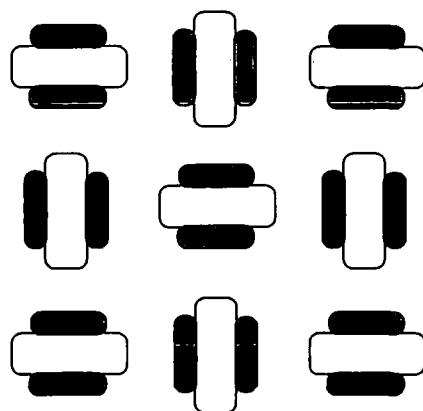
Figure **4.4**(a) Schematic of the arrangement of identical quadrupole moments corresponding to a minimum energy
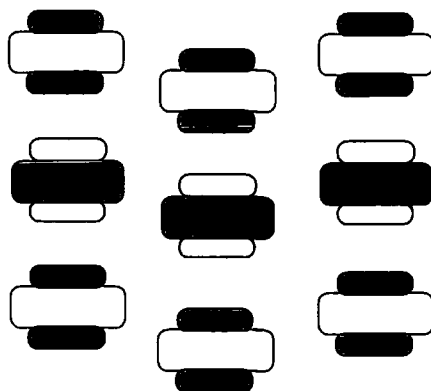
Figure **4.4(b)** Schematic of the arrangement of opposite quadrupole moments
corresponding to a minimum energy

Experimental evidence to support this postulate came from dynamic NMR studies of *peri*-substituted naphthalenes with both perfluorinated and non-fluorinated substituents. This revealed that the energetic barrier to rotation is increased with increasing electron donating power of the substituent on the non-fluorinated ring, which is consistent with an electrostatic interaction.[47] Theoretical studies have also been carried out upon a metal complex,[48] and on a cyclohexane derivative substituted with a para-phenyl and a perfluorophenyl at the *cis*-1,3-positions,[49] as shown in Figure **4.5**, which confirmed that the complex interaction was mainly electrostatic in origin.
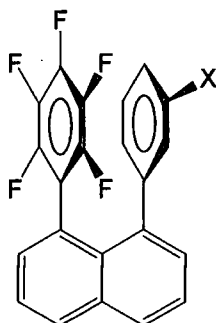
Figure **4.5** A substituted naphthalene with a pentafluorophenyl group

Molecular packing analyses have been performed on several of the HFB·methyl-subsitituted benzene complexes, and the results compared to the experimentally obtained crystal structures.[50] Minimum lattice energies and structures for each complex were calculated using atom-to-atom potentials. In these calculations the lattice energy was assumed to be the sum of attractive dispersive, repulsive and electrostatic components between partially charged atoms separated by any distance of up to 9 Å. Fairly close agreement was obtained between the calculated and experimental structures, particularly with regard to their orientation, which would indicate that the complexes are held together largely by a combination of van der Waals forces and electrostatic interactions. However, there was a tendency for the experimental structures to have more of an offset, and the decrease in inter-planar distance with increasing methyl substitution was not observed in the minimum energy structures. These may be indicative of the presence of additional interactions or an incomplete parameter set. Most of the cell parameters are considerably lower in the calculated structures than in the experimental ones, which is to be expected, as the structures were not obtained at low temperature. However, in several complexes, some of the calculated cell parameters are comparable or even larger. This indicates a particularly strong interaction in that direction. In the HFB·hexamethylbenzene complex this occurs for the stacking axis, which can be interpreted as an indication of a strong stacking interaction. In several other cases, it occurs for the axes perpendicular to the stack axis, which suggests there are interactions between the stacks, probably based on intermolecular H···F interactions.

In order to gain a much better understanding of the system, quantum mechanical calculations have been carried out upon the HFB·benzene complex as various levels of theory. Self-consistent field MP2 pseudopotential *ab initio* calculations have been carried out upon HFB·benzene dimers. Several molecular configurations were chosen, namely eclipsed and

staggered perpendicular configurations and eclipsed and staggered co-facial ones. Only the co-facial configurations were found to be attractive, with the eclipsed one having an interaction energy of 4.33 kcal mol^{-1},[51] which was 0.05 kcal mol^{-1} lower in energy than the staggered conformation. The calculated inter-planar separation between the molecules corresponding to the energy minimum is also in excellent agreement with that found in the crystal structure. Further calculations at the MP2/6-31G** level to include correlation effects gave the energy of the interaction of the HFB benzene dimer to be 3.7 kcal mol^{-1}, with an interplanar separation of 3.6 Å.[52] The latest density functional calculations (DFT) involved apportioning partial charges to the atoms of a HFB·d_6-benzene molecular pair, and then calculating the electrostatic and Leonard-Jones 6-12 potentials for the charge distributions. These indicated that the energy of interaction was 4.7 kcal mol^{-1} and that the contribution of the electrostatic component was less than 15% of the total,[53] with the remainder being ascribed to van der Waals forces.

4.2.4 Applications of the Arene-Perfluoroarene Interaction

Several applications have been considered for the arene-perfluoroarene interaction, and some have been demonstrated. One possible application could be in molecular recognition. This has been demonstrated using a di-nuclear palladium macrocycle containing fluorinated aromatic moieties, shown in Figure **4.6**.[54] The association constant of the fluorinated macrocycle with

para-dimethoxybenzene was over 25 times larger than for para-dicyanobenzene. No such specificity was observed for the non-fluorinated macrocycle.
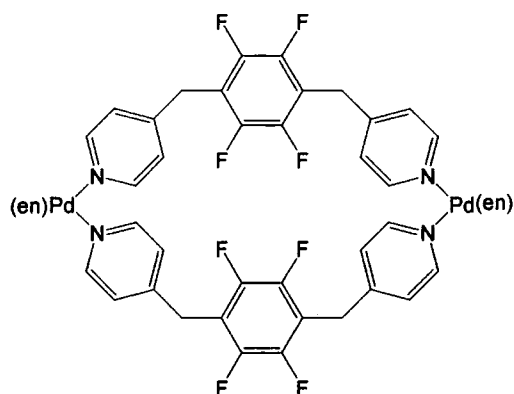
Figure **4.6** A fluorinated palladium macrocycle for recognition of arenes

Recently, the arene-perfluoroarene interaction has been used to align stacked monomers for UV-initiated, topological solid-state dimerisations and polymerisations. It has been used to polymerise phenyl-substituted butadiynes.[55] These normally polymerise to give *trans*-polydiacetylenes; however, the stacked arrangement of monomers should result in *cis*-polydiacetylenes, although the stereochemistry of the resulting polymers was not determined. Selectively fluorinated stilbenes and distyrylbenzenes have also been treated in a similar fashion to give cyclobutanes and polycyclobutanes, as illustrated in Scheme **4.1**.[56] The interaction has also been used in the solution state to align molecules for the synthesis of macrocycles.[57] The yields were found to be higher for the synthesis of partially fluorinated macrocycles compared to the non-fluorinated and completely fluorinated ones, which was attributed to a transition state, stabilised by an arene-perfluoroarene interaction
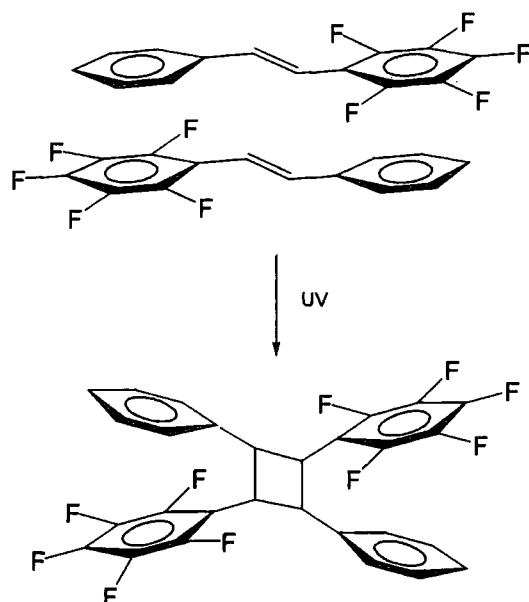
Scheme **4.1** The solid-state UV-initiated regioselective dimerisation of pentafluorostilbene

Recently, arene-perfluoroarene interactions have been implicated in the liquid crystal mesophase behaviour of some of the selectively fluorinated 1,4-bis(phenylethynyl)benzene derivatives.[37] Since many stereo-selective catalysts make use of the repulsive steric interactions between ligand and substrate, there should be scope to use attractive arene-perfluoroarene interactions to favour the binding of substrates in a particular orientation, and thus to increase selectivity, particularly in the synthesis of chiral compounds. However, to date, there have been no reports in this area.

4.3 References

1. a) C. G. Mailand, M. Rigby, E. B. Smith and W. A. Wakeham, *Intermolecular Forces*, Oxford University Press, Oxford, 1981; b) A. J. Stone, *The Theory of Intermolecular Forces*, Oxford University Press, Oxford, 1996.

2. a) J. C. Speakman, *The Hydrogen Bond and Other Intermolecular Forces*, Royal Society of Chemistry, London, 1975; b) G. A. Jeffrey and W. Saenger, *Hydrogen Bonding in Biological Structures*, Springer, Berlin, 1991.

3. R. Foster, *Organic Charge Transfer Complexes*, Academic Press, London, 1969.

4. a) C. A. Hunter, K. R. Lawson, J. Perkins and C. J. Urch, *J. Chem. Soc., Perkin Trans. 2*, 2001, 651; b) C. A. Hunter, *Chem. Soc. Rev.*, 1994, 101; c) C. A. Hunter and J. K. M. Sanders, *J. Am. Chem. Soc.*, 1990, **112**, 5525.

5. a) F. Cozzi, M. Cinquini, R. Annunziata, T. Dwyer and J. S. Siegel, *J. Am. Chem. Soc.*, 1992, **114**, 5729; b) F. Cozzi, M. Cinquini, R. Annunziata, T. Dwyer and J. S. Siegel, *J. Am. Chem. Soc.*, 1993, **115**, 5330.

6. W. Saenger, *Principles of Nucleic Acid Structure*, Springer-Verlag, New York, 1984, p. 132.

7. L. P. G. Wakelin, *Med. Res. Rev.*, 1986, **6**, 275.

8.   L. S. Lerman, *J. Mol. Biol.*, 1961, **3**, 18.

9.   a) S. K. Burley and G. A. Petsko, *Science*, 1985, **229**, 23; b) K. Burley and G. A. Petsko, *Adv. Protein Chem.*, 1988, **39**, 125; c) C. A. Hunter, *J. Mol. Biol.*, 1993, **230**, 1025; d) C. A. Hunter, J. Singh and J. M. Thornton, *J. Mol. Biol.*, 1991, **218**, 837.

10.   M. A. Pietsch and A. K. Rappe, *J. Am. Chem. Soc.*, 1996, **118**, 10908.

11.   a) F. Diederich, *Angew. Chem. Int. Ed. Engl.*, 1988, **27**, 362; b) J. Rebek, *Angew. Chem. Int. Ed. Engl.*, 1990, **29**, 245.

12.   C. R. Patrick and G. S. Prosser, *Nature*, 1960, **271**, 1021.

13.   G. M. Brooke, J. Burdon, M. Stacey and J. C. Tatlow, *J. Chem. Soc.*, 1960, 1768.

14.   F. L. Swinton, in *Molecular Complexes* Vol. 2, ed. R. Foster, Elek Science, London, 1974.

15.   a) W. A. Duncan and F. L. Swinton, *Trans. Faraday Soc.*, 1966, **62**, 1082; b) E. McLaughlin and C. E. Messer, *J. Chem. Soc. A*, 1966, 1106.

16.   T. Kelly and F. L. Swinton, *J. Chem. Thermodynamics*, 1974, **6**, 435.

17.   a) D. A. Armitage and K. W. Morcom, *Trans. Faraday Soc.*, 1968, **64**, 688; b) A. Andrews, K. W. Morcom, W. A. Duncan, F. L. Swinton and J. M. Pollock, *J. Chem. Thermodynamics*, 1970, **2**, 95.

18. P. J. Howell, B. J. Skillerene de Bristowe and D. Stubley, *J. Chem. Thermodynamics*, 1972, **4**, 225.

19. a) D. A. Fenby, I. A. McLure and R. L. Scott, *J. Phys. Chem.*, 1966, **70**, 602; b) D. A. Fenby and R. L. Scott, *J. Phys. Chem.*, 1967, **71**, 4103.

20. W. J. Gaw and F. L. Swinton, *Trans. Faraday Soc.*, 1968, **64**, 2023.

21. a) J. S. Brennan, N. M. D. Brown and F. L. Swinton, *Trans. Faraday Soc.*, 1974, **70**, 1965; b) J. A. Ripmeester, D. A. Wright, C. A. Fyfe and R. K. Boyd, *J. Chem. Soc. Faraday Trans. 2*, 1978, **74**, 1164.

22. D. F. R. Gilson and C. A. McDowell, *Can. J. Chem.*, 1966, **44**, 945.

23. M. J. Duer, *J. Chem. Soc., Faraday Trans.*, 1993, **89**, 823.

24. a) J. H. Williams, *Mol. Phys.*, 1991, **73**, 99; b) J. H. Williams, *Chem. Phys.*, 1992, **167**, 215; c) J. H. Williams and B. Frick, *Chem. Phys.*, 1992, **166**, 425; d) J. H. Williams, *Chem. Phys.*, 1993, **172**, 171; e) J. H. Williams and R. P. White, *J. Chim. Phys.*, 1992, **89**, 1755.

25. J. D. Laposa, M. J. McGlinchey and C. Montgomery, *Spectrochim. Acta A*, 1983, **39**, 863.

26. J. S. W. Overell and G. S. Pawley, *Acta Crystallogr. Sect. B*, 1982, **38**, 1966.

27. J. H. Williams, J. K. Cockcroft and A. N. Fitch, *Angew. Chem. Int. Ed. Engl.*, 1992, **31**, 1655.

28. a) B. E. G. Cox, D. W. J. Cruikshank and J. A. S. Smith, *Proc. R. Soc. London A*, 1958, **247**, 1; b) N. Boden, P. P. Davis, C. H. Stam and G. A. Wesselink, *Mol. Phys.*, 1973, **25**, 81.

29. a) T. Dahl, *Acta Chem. Scand.*, 1971, **25**,1031; b) T. Dahl, *Acta Chem. Scand.*, 1972, **26**, 1569; c) T. Dahl, *Acta Chem. Scand.*, 1973, **27**, 1031; d) T. Dahl, *Acta Chem. Scand. Sect. A.*, 1975, **29**, 170; e) T. Dahl, *Acta Chem. Scand. Sect. A.*, 1975, **29**, 699.

30. a) T. Dahl, *Acta Crystallogr. Sect B.*, 1977, **33**, 3021; b) T. Dahl, *Acta Chem. Scand. Sect. A*, 1979, **33**, 665; c) T. Dahl, *Acta Crystallogr. Sect. B*, 1981, **37**, 98; d) T. Dahl, *Acta Crystallogr. Sect. C*, 1989, **41**, 931.

31. T. Dahl, *Acta Chem. Scand. Sect. A*, 1988, **42**, 1.

32. a) T. Dahl, *Acta Chem. Scand. Sect. A*, 1981, **35**, 701; b) T. Dahl, *Acta Chem. Scand. Sect. B*, 1985, **39**, 423; c) T. Dahl, *Acta Chem. Scand.*, 1990, **44**, 56.

33. D. G. Naae, *Acta Crystallogr. Sect. B*, 1979, **35**, 2765.

34. C. P. Brock, D. G. Naae, N. Goodhand and T. A. Hamor, *Acta Crystallogr., Sect. B*, 1978, **34**, 3691.

35. M. I. Bruce, M. R. Snow and E. R. T. Tiekink, *Acta Crystallogr., Sect C*, 1987, **43**, 1640.

36.   C. Dai, P. Nguyen, T. B. Marder, A. J. Scott, W. Clegg and C. Viney, *Chem. Commun.*, 1999, 2493.

37.   F. Ponzini, R. Zagha, K. Hardcastle and J. S. Siegel, *Angew. Chem. Int. Ed. Engl.*, 2000, **39**, 2323.

38.   G. P. Bartholomew, X. Bu and G. C.Bazan, *Chem. Mater.*, 2000, **12**, 2311.

39.   a) T. G. Beaumont and K. C. M. Davies, *J. Chem. Soc. B*, 1967, 1131; b) T. G. Beaumont and K. C. M. Davies, *Nature*, 1968, **218**, 865; c) D. A. Armitage, T. G. Beaumont, K. C. M. Davies, D. J. Hall and K. W. Morcom, *Trans. Faraday Soc.*, 1971, **67**, 2548.

40.   C. J. Aspley, C. Boxwell, M. L. Buil, C. L. Higgitt, C. Long and R. N. Perutz, *Chem. Commun.*, 1999, 1027.

41.   J. M. Steed, T. A. Dixon and W. Klemperer, *J. Chem. Phys.*, 1979, **70**, 4940.

42.   N. M. D. Brown and F. L. Swinton, *J. Chem. Soc., Chem. Commun.*, 1974, 770.

43.   a) M. R. Battaglia, A. D. Buckingham and J. H. Williams, *Chem. Phys. Lett.*, 1981, **78**, 421; b) J. Vrbancich and G. L. D. Ritchie, *J. Chem. Soc., Faraday Trans. 2.*, 1980, **76**, 648.

44.   a) K. E. Laidig, *Chem. Phys. Lett.*, 1991, **185**, 483; b) J. Hernandez-Trujillo and A. Vela, *J. Phys. Chem.*, 1996, **100**, 6524.

45. J. Hernandez-Trujillo, M. Costas and A. Vela, *J. Chem. Soc., Faraday Trans.*, 1993, **89**, 2441.

46. J. H. Williams, *Acc. Chem. Res.*, 1993, **26**, 593.

47. a) F. Cozzi, F. Ponzini, R. Annunziata, M. Cinquini and J. S. Siegal, *Angew. Chem. Int. Ed. Engl.*, 1995, **34**, 1019; b) R. Annunziata, F. Ponzini and L. Raimondi, *Magn. Reson. Chem.*, 1995, **33**, 347.

48. C. A. Hunter, X.-J. Lu, G. M. Kapteijn and G. van Koten, *J. Chem. Soc., Faraday Trans.*, 1995, **9**, 2009.

49. V. E .Williams, R. P. Lemieux and G. R. J. Thatcher, *J. Org. Chem.*, 1996, **61**, 1927.

50. T. Dahl, *Acta Crystallogr. Sect. B*, 1990, **46**, 283.

51. J. Hernandez-Trujillo, F. Colmenares, G. Cuevas and M. Costas, *Chem. Phys. Lett.*, 1997, **265**, 503.

52. A. P. West, Jr., S. Mecozzi and D. A. Dougherty, *J. Phys. Org. Chem.*, 1997, **10**, 347.

53. S. Lorenzo, G. R. Lewis and I. Dance, *New. J. Chem.*, 2000, **24**, 295.

54. a) M. Fugita, S. Nagao, M. Iida, K. Ogata and K. Ogura, *J. Am. Chem. Soc.* 1993, **115**, 1574; b) M. Fugita, F. Ibukuro, F. Hagihara and K. Ogura, *Nature*, 1994, **367**, 720.

55.   G. W. Coates, A. R. Dunn, L. M. Henling, D. A. Dougherty and R. H. Grubbs, *Angew. Chem. Int. Ed. Engl.*, 1997, **36**, 248.

56.   G. W. Coates, A. R. Dunn, L. M. Henling, J. W. Ziller, E. B. Lobkovsky and R. H. Grubbbs, *J. Am. Chem. Soc.*, 1998, **120**, 3641.

57.   M. J. Marsella, Z.-Q. Wang, R. J. Reid and K. Yoon, *Org. Lett.*, 2001, 885.

Chapter Five

The Synthesis and Crystal Structures of Selectively Halogenated Tolans of Formulae C_6F_5-$C \equiv C$-C_6H_4X and XC_6F_4-$C \equiv C$-C_6H_5

5.1 Introduction

Over the past few years, there has been, within our group, a systematic programme on the synthesis and investigation of the properties of simple conjugated phenylene-ethynylene based rigid-rod molecules.[1] We have largely concentrated on simple derivatives of diphenylethyne (also known as tolan), 1,4-bis(phenylethynyl)benzene (BPEB) and 1,4-bis(phenylethynyl)-anthracene (BPEA), substituted, both symmetrically and asymmetrically, with various functional groups at the terminal para- positions, as shown in Figure **5.1**. In particular, we have been interested in obtaining information on the luminescence, solid-state packing, liquid crystalline behaviour and non-linear optical properties of such molecules, both with a view to gaining more understanding of their fundamental properties, as well as looking for some potential applications.

Tolan

BPEB

R_1 / R_2 = NO_2, CN, CF_3, Me, OMe, SMe, NH_2, NMe_2
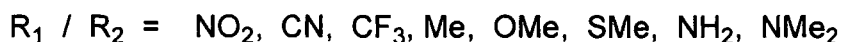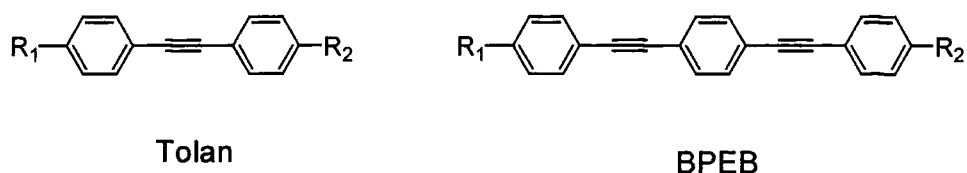
Figure **5.1**. The structures of tolan and BPEB derivatives synthesized within the group

The crystal structures of tolans are of considerable interest. Their molecular structures are of particular importance, especially in respect to their planarity. The dihedral angles between the mean planes of the phenyl rings is determined mainly by the rotation about the carbon-carbon single bonds. This in turn depends on the degree of conjugation between the two phenyl rings through the carbon-carbon triple bond. The barrier to rotation about the carbon-carbon triple bond of a tolan in the gas phase has been calculated to be very small.[2] Although tolan itself is planar in the solid state, the structures of tolans reveal a variety of dihedral angles in the solid state, which is thought to be due to the effect of crystal packing forces. However, the molecular packing is also important, in particular, whether the molecules pack in a non-centrosymetric space group. If this is the case, the material may be suitable for second-harmonic generation. This has been shown for several tolans derivatives.[3]

Despite the number of tolan derivatives to have been synthesized, there remains a dearth of structural information on these types of molecules. This was evidenced by a 1988 Cambridge Crystallographic Database search for the tolan structure which revealed only 14 hits (excluding organometallics).[4] The survey was made with the intention of finding molecules which crystallise

in non-centrosymmetric space groups for potential use in second harmonic generation. One particularly interesting compound in this regard is 4-methoxy-4'-nitrotolan. This is polymorphic, exhibiting at least three phases depending on the solvent from which it is grown. Although at least two of these polymorphs are centrosymmetric, one polymorph is non-centrosymmetric and is therefore potentially suitable for SHG.[5] This polymorphism should single out tolans as worthy of further structural study. Recently, non-centrosymmetric crystal structures have been discovered for tolans containing a terminal alkyne group, and these have been shown to have large SHG activities.[6] Although the structures of several tolans have been added to the database since 1988, there still remains a significant lack of structural information on tolans. In recent years, the group of Prof. T. B. Marder has been actively engaged in a program of ameliorating this situation, and, although most of their structures have yet to be published and added to the Cambridge Crystallographic Database, several have been reported in thesis form.[7]

Recently, the group has obtained the crystal structures of several selectively fluorinated tolans.[8] It succeeded in crystallising a 1:1 complex of tolan with decafluorotolan, and subsequently determined its crystal structure from X-ray diffraction data. The packing of the molecules was shown to comprise infinite stacks made up of alternating parallel tolan and decafluorotolan molecules, much like other arene-perfluoroarene complexes (see Chaper 4). It has also recently determined the crystal structure of (phenylethynyl)pentafluoro-benzene. This is almost isostructural with that of the tolan·decafluorotolan complex, consisting of stacks of parallel molecules in a head-to-tail arrangement. It has also obtained the crystal structures of several derivatives of (phenylethynyl)tetrafluorobenzene, substituted with alkoxy groups, which were synthesized with a view to establishing liquid crystal properties.[9] Although many of these displayed arene-perfluoroarene stacking, this was not true in all cases.

However, almost no crystal structures of partially fluorinated molecules are known which contain halogen atoms other than fluorine. Therefore, it is not known what effect, if any, the presence of other halogens has on the arene-perluoroarene interaction. This chapter is an attempt to establish this, as it is devoted to the synthesis and crystal structures of a series of selectively fluorinated tolans containing one other halogen atom.

5.2 Results and Discussion

5.2.1 Synthesis

There are eight members of the series of molecules with the general formulae p-X-C$_6$H$_4$-C≡C-C$_6$F$_5$ and p-X-C$_6$F$_4$-C≡C-C$_6$H$_5$ (where X represents a halogen atom). These are 1-iodo-4-(pentafluorophenylethynyl)benzene (**1**), 1-bromo-4-(pentafluorophenylethynyl)benzene (**2**), 1-chloro-4-(pentafluorophenyl-ethynyl)benzene (**3**), 1-fluoro-4-(pentafluorophenylethynyl)benzene (**4**), 1-iodo-4-(phenylethynyl)tetrafluorobenzene (**5**), 1-bromo-4-(phenylethynyl)-tetrafluorobenzene (**6**), 1-chloro-4-(phenylethynyl)tetrafluorobenzene (**7**), shown schematically in Figure **5.2**. (Phenylethynyl)pentafluorobenzene has been previously synthesized within the group. They can all potentially be synthesized by using Sonogashira reactions involving the palladium-catalysed cross-coupling of an aryl halide with a phenylacetylene. All of these potential precursors needed are available commercially with the exception of pentafluorophenylacetylene. However, this can be obtained in respectable yields from the base-induced hydrodesilation of its trimethylsilylated precursor, obtained from the Sonogashira cross-coupling of trimethylsilylacetylene (TMSA) to iodopentafluorobenzene.[10]
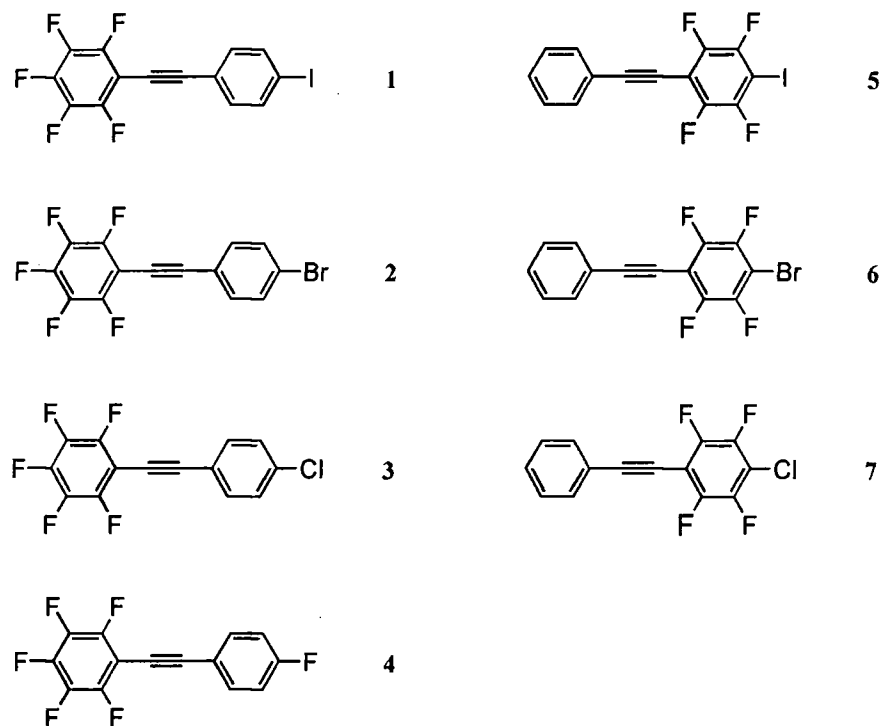
Figure **5.2** The structures of compounds **1-7**

All of the cross-coupling reactions were carried out under standard conditions, using a catalyst system composed of bis(triphenylphosphine)palladium(II) dichloride and copper iodide, each in 1% molar ratio compared to the aryl halide. A slight excess (1.2 equivalents) of the terminal alkyne was employed in order to compensate for that used in the initiation step. Most of the reactions took place at room temperature, although several needed some additional heating to proceed to completion. All of the reactions were performed in dried amine solvents, with triethylamine being used in preference to diisopropylamine for all reactions involving reagents with a pentafluorophenyl group, in order to avoid possible nucleophilic substitution at the para position by a secondary amine.[11] The progress of the reactions was monitored by GC-MS, which could also detect the formation of any side-

products. In most cases trace amounts of butadiynes were observed, consistent with them bring formed only in the initiation step.

The 1-halogeno-4-(pentafluorophenylethynyl)benzenes (**1-4**) were prepared by coupling pentafluorophenylacetylene with the appropriate aryl halide, as shown in Scheme **5.1**. The synthesis of **1** required a threefold excess of 1,4-diiodobenzene was used relative to pentafluorophenylacetylene, with a view to minimizing the quantity of 1,4-bis(pentafluorophenylethynyl)benzene side-product, arising from coupling at both of the iodo postions. A similar strategy has been employed previously in the synthesis of 1-iodo-4-(phenylethynyl)benzene.[12] When the reaction was complete, the product was obtained as a mixture with the remaining unreacted 1,4-diiodobenzene and 1,4-bis(pentafluorophenylethynyl)benzene. The product was isolated, and much of the diiodobenzene also recovered, by column chromatography and re-crystallisation, although the yield of product was very low. This can probably be accounted for by the fact that the pentafluorophenylethynyl group is electron-withdrawing, and therefore serves as an activating group, which makes the product more susceptible to further coupling, resulting in an increased amount of 1,4-bis(pentafluorophenylethynyl)benzene, and decreased yield of product. The synthesis of compounds **2-4** was more straightforward, as the bromo-, chloro-, and fluoro- groups present did not undergo coupling to pentafluorophenylacetylene under the reaction conditions. Therefore, no excess of the aryl halide starting material was required, no significant amounts of side products were generated, and purification involved only recrystallisation in order to obtain analytically pure samples.
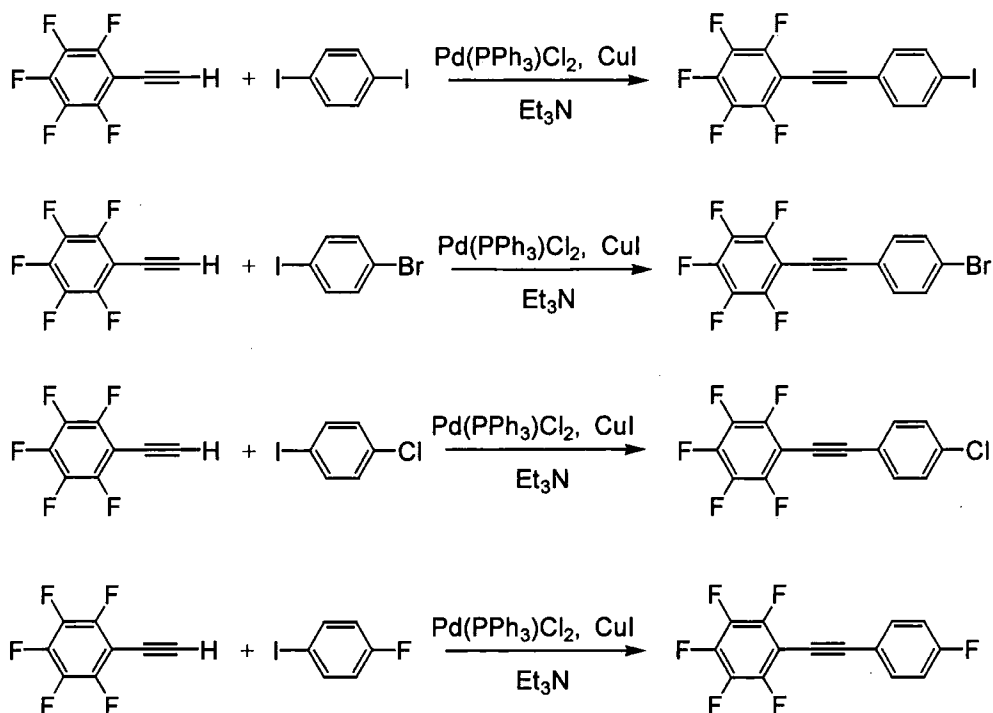
Scheme **5.1** Synthesis of 1-halogeno-4-(pentafluorophenylethynyl)benzenes

The synthesis of the 1-halogeno-4-(phenylethynyl)tetrafluorobenzenes **5** and **6** was achieved by the coupling of 1,4-diiodotetrafluorobenzene and 1,4-dibromotetrafluorobenzene to phenylacetylene respectively. This is shown in Scheme **5.2**. Here, as in the synthesis of **1**, a large excess of the dihalogenotetrafluorobenzene was used for similar reasons to those outlined above, and the products were separated from the remaining starting materials by column chromotography. However, these reactions gave respectable yields of product and only small amounts of 1,4-(phenylethynyl)-tetrafluorobenzene, which is probably due to the products being less reactive towards further coupling, than the dihalogenobenzenes because of the electron-donating properties of the phenylethynyl group.
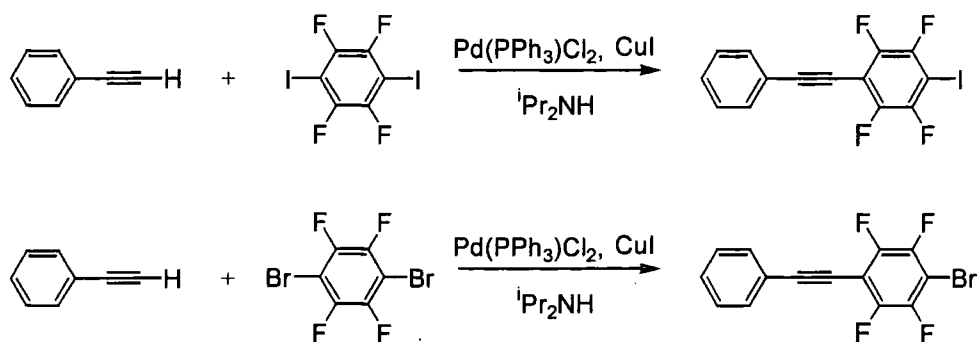
Scheme **5.2** The synthesis of 1-halogeno-4-(phenylethynyl)-
tetrafluorobenzenes (**5-6**)

It was initially decided to attempt the synthesis of compound **7** by
Sonogashira cross-coupling of phenylacetylene to 1-bromo-4-
chlorotetrafluorobenzene. However, the resulting reaction was shown by GC-
MS to produce a mixture of **7**, and 1-phenylethynyl-2,3,5,6-
tetrafluorobenzene, arising from hydrodehalogenation of the chloro- group.
Hydrodehalogenation has been observed previously in these cross couplings,
and seems to be particularly prevalent for highly fluorinated aryl halides.[13] As
the side-product could not be separated from the product by either column
chromotography or recrystallisation, an alternative route to the synthesis of **7**
was sought. It has been shown that highly fluorinated arenes are susceptible
to nucleophilic substitution reactions, often at the para position relative to any
substituents. Several fluorinated phenylene ethynylenes have been
synthesized by nucleophilic substitution of fluoroarenes using lithium
acetylides.[14] Compound **7** was reported to have been synthesized previously
by adding chloropentafluorobenzene to a solution of lithium phenylacetylide at
low temperature as shown in Scheme **5.3**, although no experimental details
were given, and the product was not fully characterized.[15] Athough the yield
was found to be low, some pure compound was obtained.

113
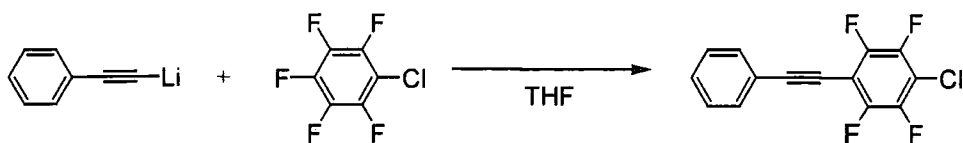
Scheme **5.3**   The synthesis of 1-chloro-4-(phenylethynyl)tetrafluorobenzene

5.2.2 Crystal Growth and Crystallographic Data

Diffraction quality crystals of compounds 1-iodo-(pentafluorophenylethynyl)benzene **1**, 1-bromo-4-(pentafluorophenylethynyl)-benzene **2**, 1-chloro-4-(pentafluorophenylethynyl)benzene **3**, and 1-iodo-4-(phenylethynyl)tetrafluorobenzene **5**, were obtained by re-crystallisation from n-hexane or by slow evaporation of dichloromethane (DCM) solutions. The crystal structures of all of these compounds were solved from from single-crystal X-ray diffraction data at 100-110 K by Jacquie Burke at the University of Durham. The crystallographic data and structure refinement parameters for the compounds are summarised in Table **5.1**. The crystal structures of compounds **1** and **2** are very closely related. Both molecules crystallise in the monoclinic space group $P2_1/c$, with Z = 4, with one molecule comprising the asymmetric unit which contains no elements of crystallographic symmetry. Compound **3** crystallises in triclinic space group $P\bar{1}$ with Z = 2, with the molecules being related to each other through inversion centres. Compound **5** crystallises in space group $P2_1/n$ with Z = 4. Again, a single molecule comprises the asymmetric unit.

Table **5.1** Crystal data and structure refinement parameters

Compound	1	2	3	5
Formula	$C_{14}H_4F_5I$	$C_{14}H_4F_5Br$	$C_{14}H_4F_5Cl$	$C_{14}H_5F_4I$
Formula weight	394.07	347.08	302.62	376.08
T (K)	105(2)	100(2)	110(2)	100(2)
Crystal system	Monoclinic	Monoclinic	Triclinic	Monoclinic
Space group	$P2_1/c$	$P2_1/c$	$P\bar{1}$	$P2_1/n$
a (Å)	21.417(7)	20.517(1)	6.076(1)	12.668(2)
b (Å)	4.9672(16)	5.181(1)	7.488(1)	5.074(1)
c (Å)	11.692(4)	11.254(1)	13.168(1)	18.833(3)
α (°)	90	90	85.343(1)	90
β (°)	92.288(5)	96.922(1)	86.054(1)	93.703(4)
γ (°)	90	90	83.332(1)	90
V (Å^3)	1242.9(7)	1187.6(1)	592.1(1)	1208.1(3)
Z	4	4	2	4
ρ_{calcd} (g cm^{-3})	2.106	1.941	1.698	2.068
μ (mm^{-1})	2.623	3.510	0.371	2.682
Trans. range	0.58	0.62	0.18	0.16
θ Range (°)	0.95-27.48	2.00-27.00	1.55-27.49	1.88-27.49
Total reflections	11360	10137	6110	11022
Unique refls.	2850	2697	2698	2769
Parameters	181	197	181	172
R_{int}	0.0524	0.0389	0.0158	0.0387
R (F, I>2σ(I))	0.053	0.030	0.030	0.027
wR (F^2, all data)	0.143	0.082	0.088	0.057

5.2.3 Molecular Structures and Intramolecular Parameters

Although the compounds are very similar in molecular structure, they differ slightly in terms of their intramolecular parameters such as bond lengths and bond angles. The molecular structures of the compounds **1**, **2**, **3** and **5** are shown in Figure **5.3**. Each molecule is viewed perpendicular to the fluorinated phenyl group. In all cases, the thermal ellipsoids are plotted at 50% probability.
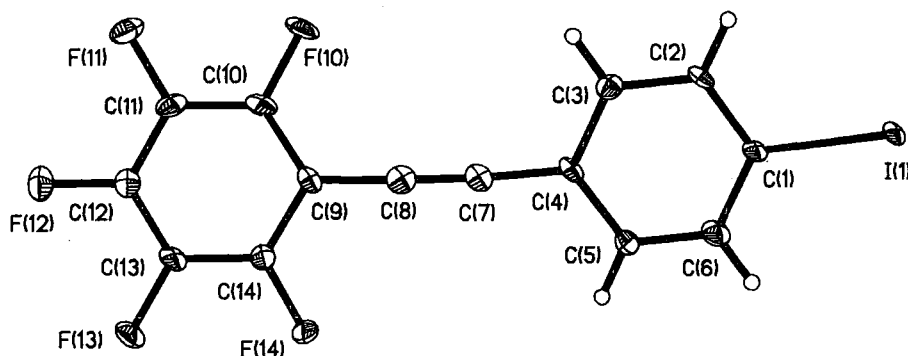
Figure **5.3**(a) Molecular structure of **1**
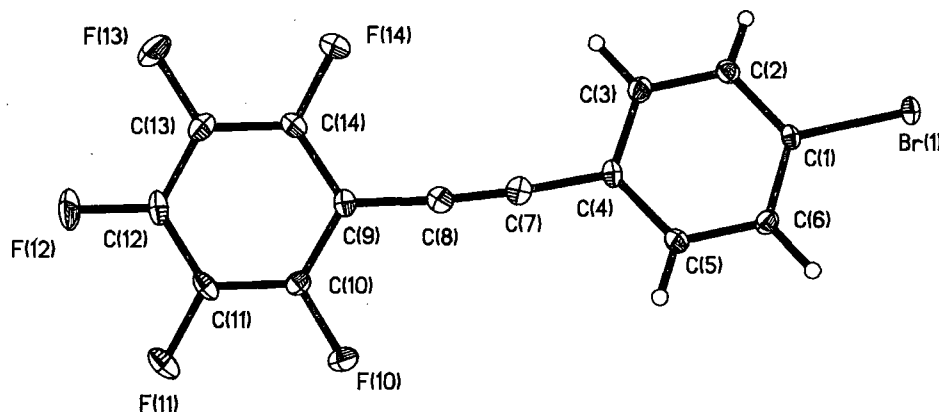
Figure **5.3**(b) Molecular structure of **2**
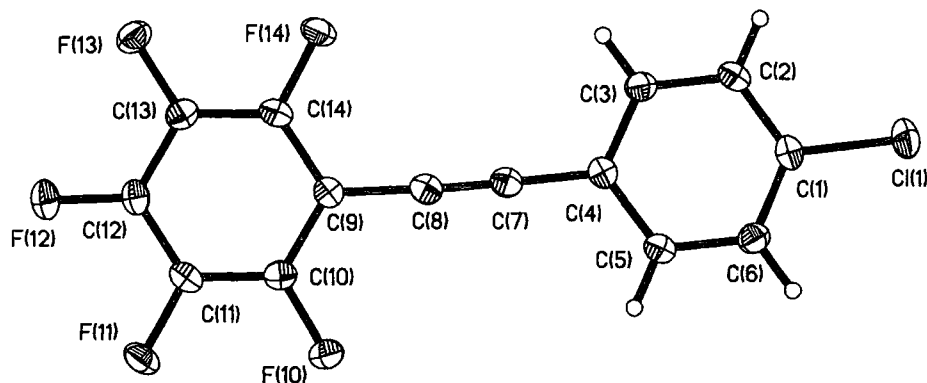
Figure **5.3**(c) Molecular structure of **3**
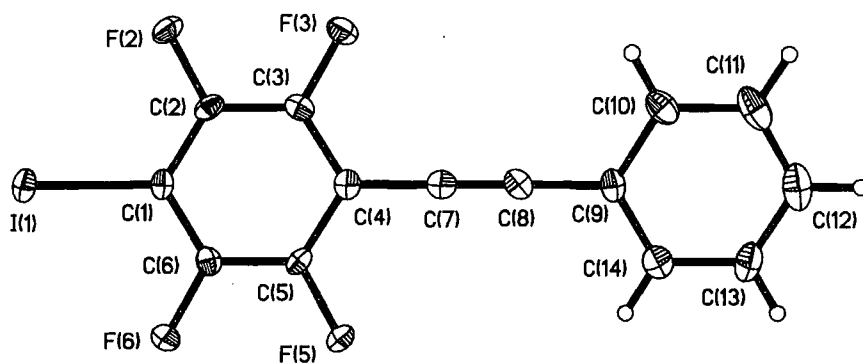
Figure **5.3**(d) Molecular structure of **5**

The C≡C bond lengths of **1** and **2** are 1.205(9) Å and 1.203(4) Å respectively, identical within experimental error. The mean $C(sp)$-$C(sp^2)$ bond lengths are 1.420(8) Å and 1.432(3) Å respectively. The C≡C bond length of **3** is 1.1950(19) Å, and the mean $C(sp)$-$C(sp^2)$ bond length is 1.4225(17) Å. The

C≡C bond length of **5** is 1.175(4) Å, and the mean C(sp)-C(sp^2) bond length is 1.438(4) Å. All of the molecules are significantly distorted from linearity. The degree of distortion can be quantified by a distortion angle, which is defined as the complement of the angle formed by the two centroids of the phenyl rings, and the centre of the triple bond. In **1** it is 4.7° whereas in **2** it is 7.1°. The distortion angle of **3** is 3.5°, whereas in **5** it is much less at 1.1°. The phenyl rings of each molecule are not parallel, which can be quantified by the dihedral angle between the mean planes of the phenyl rings, called the phenyl-phenyl interplanar angle. In compounds **1** and **2,** these are 9.4° and 15.7° respectively. Molecules of **3** are more planar than the ones above, with an angle of only 3.4° The phenyl-phenyl interplanar angle of **5** is 13.1°. The intramolecular parameters are summarised in Table **5.2**.

Table **5.2**   Intramolecular Parameters

Compound	C≡C Bond Length (Å)	Mean C(sp)- C(sp^2) Bond Length (Å)	Phenyl-Phenyl Interplanar Angle (°)	Linear Distortion Angle (°)
1	1.205(9)	1.425(8)	9.4	4.7
2	1.203(4)	1.435(3)	15.7	7.3
3	1.195(2)	1.428(2)	3.4	3.1
5	1.175(4)	1.428(4)	13.1	1.1

5.2.4 Molecular Packing and Intermolecular Parameters

The molecular packing arrangement of all the compounds consists of infinite stacks of parallel molecules running along the b–axes. However, there are several differences in their molecular arrangements. These can be described by use of intermolecular parameters, which are given in Table **5.3** and are defined here. The distance between the mean planes of adjacent molecules within a stack is known as the intrastack interplanar separation. The intrastack interplanar separations of **1** and **2** are 3.371 Å and 3.459 Å respectively. In **3,** this separation is 3.375 Å, and for **5**, it is 3.478 Å. The mean planes of the molecules are not perpendicular to the stacking axes, but are inclined at an angle to them. The angle between the stacking axis and the normal to the mean molecular planes is defined as the intrastack offset angle, as it is a measure of the degree of offset between adjacent molecules in a stack. If this angle is 0° the molecules are stacked directly on top of each other and there is no offset. These parameters are similar to the ones defined in Figure **5.6**. The intrastack offset angles of **1** and **2** are 47.2° and 48.1° respectively. The intrastack offset angle of the stack is **3** is 25.4°, whereas in **5**, it is 46.7°. Although the stack axes are all parallel, and the molecules within a given stack are parallel, the molecules within adjacent stacks are typically arranged in layers a herringbone fashion. The dihedral angle between the mean planes of molecules in adjacent layers is termed the inter-layer interplanar angle. The interlayer interplanar angle of **1** and **2** is 88.5° and 83.8° respectively. The interlayer interplanar angle of **5** is 87.2°. However, in structure **3**, the mean planes of all the molecules in all layers are parallel, which means that the interlayer interplanar angle is 0°.

Table **5.3**. Intermolecular Parameters

Compound	Intrastack Inter-planar Separation (Å)	Intra-stack Offset Angle (°)	Inter-layer Inter-planar Angle (°)
1	3.371	47.26	88.5
2	3.459	48.12	83.8
3	3.375	25.40	0
5	3.478	46.73	87.2

Although the structures all consist of stacks of parallel molecules, the orientations of the molecules within a stack do vary. In structures **1** and **2**, they are oriented in the same sense, i.e. in a head-to-head arrangement. The phenyl rings lie approximately over the triple bonds in both cases, thus, there is no arene-perfluoroarene stacking motif. However, in contrast, adjacent molecules within the same stack of **3** are arranged in an opposite sense, i.e. in a head-to-tail arrangement. This arrangement clearly displays an arene-perfluoroarene stacking motif. The structure is almost isostructural to that of (phenylethynyl)pentafluorobenzene. In **5,** the stacked molecules are oriented in the same sense, i.e. in a head-to-head arrangement. The respective head-to-head and head-to-tail arrangements can be seen in the overlap diagrams in Figure **5.4** which show two adjacent molecules within a stack, viewed perpendicular to the mean molecular planes.
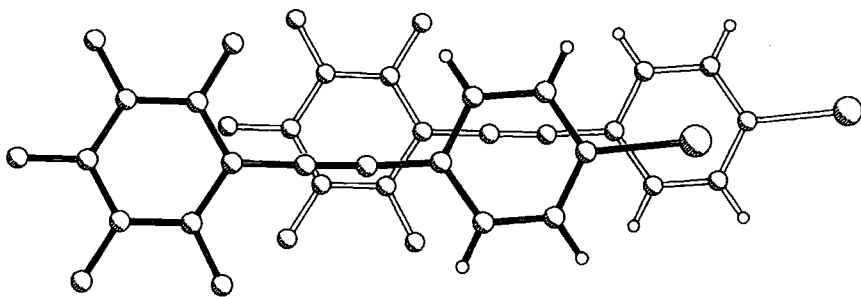
Figure **5.4**(a) Overlap diagram for **1**
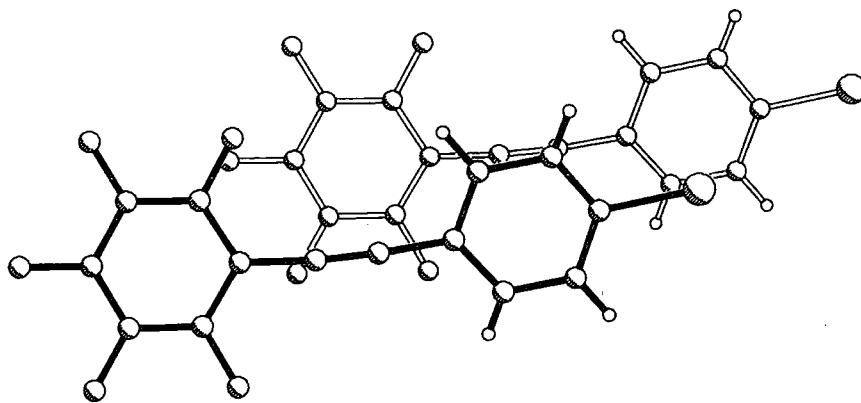
Figure **5.4**(b) Overlap diagram for **2**
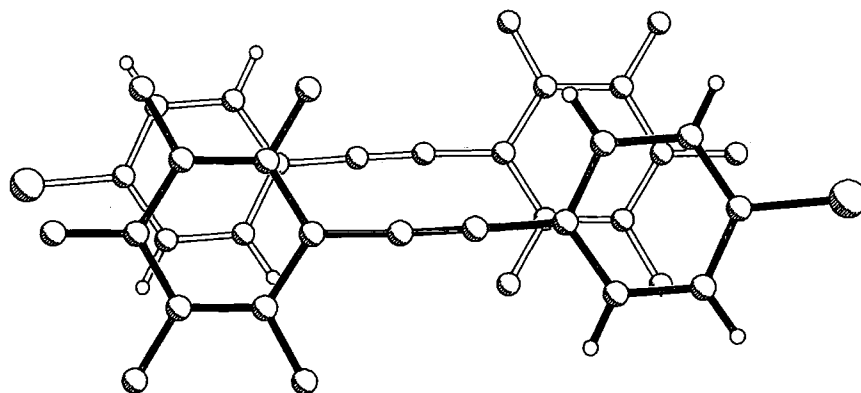
Figure **5.4**(c) Overlap diagram for **3**
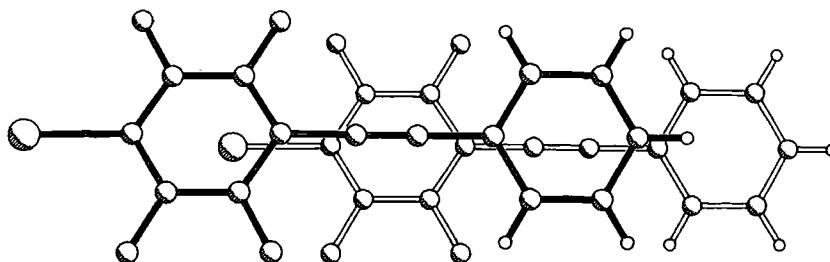
Figure **5.4(d)** Overlap diagram for **5**

5.2.5 Intermolecular Close Contacts and Interactions

Intermolecular interactions between specific atoms or groups may have a role to play in the stablization of the particular packing arrangement. A close intermolecular contact between two atoms is defined as one which is below the sum of their two van der Waals radii, the van der Waals radius being a measure of the effective size of an atom. Several years ago, values of van der Waals radii were tabulated by Bondi for several atoms, based on X-ray diffraction data, gas phase kinetic collision cross-sections and critical densities.[16] Recently, however, some of these values have been revised based on results obtained from statistical analysis of the intermolecular distances between the atoms in a large number of crystal structures.[17] Close intermolecular contacts often occur because of specific attractive interactions between the atoms concerned, although they can arise merely as a

consequence of crystal packing forces, involving other atoms or groups in the structure.

Close intermolecular contacts between halogen atoms have been classified into two types.[18] Type I contacts are centro-symmetric, which implies that C–X⋯X angles (where X represents a halogen atom) for both halogen atoms are approximately or exactly equal, so these contacts usually occur between molecules related by a centre of inversion. These contacts have been shown to arise purely as a consequence of the close approach of the molecules, and play no role in directing the packing. By contrast, type II contacts are characterised by two C–X⋯X angles of approximately 90° and 180°. These contacts are believed to arise from a strong polarisation interaction between the halogens, and can play a significant role in stabilising the crystal structures of many compounds. They have even been postulated to be quasi-covalent for some of the larger halogens.[19] Previous studies seem to indicate that type II interactions occur much less frequently for fluorine atoms. This is probably a consequence of fluorine being much less polarisable than the larger halogens, and indeed C–F⋯F–C interactions may well be repulsive in nature.[20] A schematic of these contacts are shown in Figure **5.5**.

Type I $\theta_1 \approx \theta_2$ Type II $\theta_1 \approx 180°$

                                                                $\theta_2 \approx 90°$

Figure **5.5**   Schematic of the two types of intermolecular C–F⋯F–C contacts

The structures of **1** and **2** contain close intermolecular contacts between the iodine and bromine atoms of molecules in adjacent layers. The closest intermolecular $I \cdots I$ and $Br \cdots Br$ distances are 3.744 Å and 3.557 Å respectively. Both of these values are less than the sum of the van der Waals radii of the two iodine and bromine atoms, which are 4.00 Å and 3.70 Å respectively.[17] The $C-I \cdots I$ angles are 167.4° and 95.6° for structure **1**, and the $C-Br \cdots Br$ angles 163.6° are 85.5° in structure **2**. This is consistent with both of these contacts being of type II, and therefore being due to definite interactions between the atoms. The closest intermolecular $Cl \cdots Cl$ contact is 3.927 Å in structure **3**. This is greater than the sum of the van der Waals radii which is 3.48 Å; therefore, it is not deemed to be a close contact. There are also no intermolecular close contacts between the iodine atoms in **5**. The close interlayer halogen-halogen contacts are shown as dotted lines in the packing diagrams in Figure **5.6**.
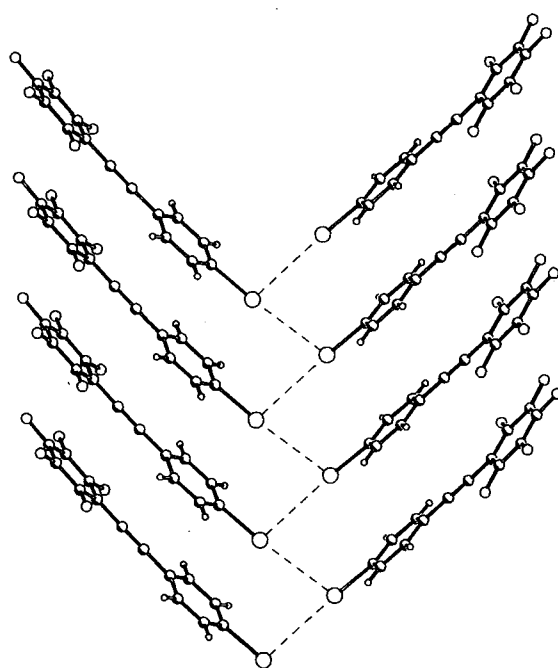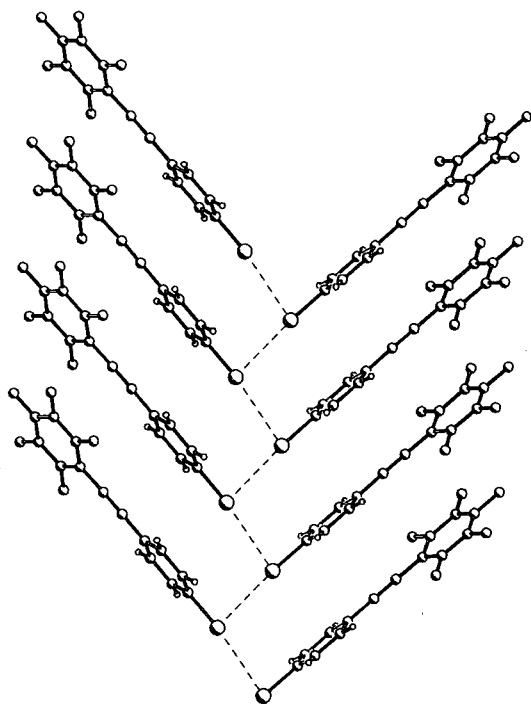

Figure **5.6**(a) Packing diagram of **1**
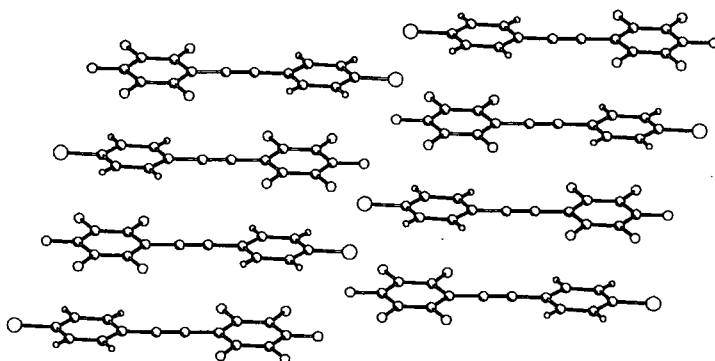
Figure **5.6**(b) Packing diagram of **2**

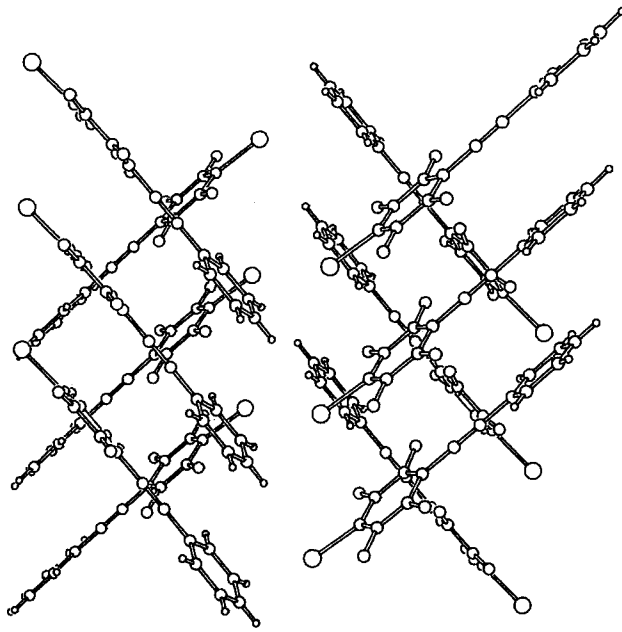Figure **5.6**(c) Packing diagram of **3**

Figure **5.6**(d) Packing diagram of **5**

5.3 Conclusions

A number of fluorinated tolans of the series 1-halogeno-4-(pentafluorophenyl-ethynyl)benzene and 1-halogeno-4-(phenylethynyl)tetrafluorobenzene have been synthesized. In all but one case this was achieved by homogeneous palladium-catalyzed Sonogashira cross-coupling. In the case of 1-chloro-4-(pentafluorophenylethynyl)benzene, nucleophilic attack on chloropentafluoro-benzene by lithium phenylacetylide was used. All of the compounds have been fully characterised.

The crystal structures of 1-iodo-4-(pentafluorophenylethynyl)benzene, 1-bromo-4-(pentafluorophenylethynyl)benzene, 1-chloro-4-(pentafluorophenyl-ethynyl)benzene and 1-iodo-4-(phenylethynyl)tetrafluorobenzene have been solved from single-crystal X-ray diffraction data. The structures reveal a variety of molecular packing arrangements. The compounds 1-iodo-4-(pentafluorophenylethynyl)benzene and 1-bromo-4-(pentafluorophenyl-ethynyl)benzene pack in a very similar manner, consisting of stacks of parallel molecules arranged in layers in a pseudo-herringbone motif. No arene-perfluoroarene stacking motifs are observed in these structures, however, close intermolecular halogen-halogen contacts of type II are present. Thus, it can be assumed that these halogen-halogen interactions, rather than arene-perfluoroarene interactions are the dominant stabilising force governing the packing of these molecules. This packing arrangement can be contrasted with that of 1-chloro-4-(pentafluorophenylethynyl)benzene, which also consists of stacks of parallel molecules but in a laminar arrangement. Adjacent molecules within a stack are arranged in a head-to-tail arrangement, which displays an arene-perfluoroarene stacking motif. No intermolecular close contacts between the chlorine atoms are observed. This is the first crystal structure of

a compound that contains a halogen atom other than fluorine, in which arene-perfluoroarene interactions are present.

In this group of compounds, arene-perfluoroarene interactions occur only in where there are no other apparently stronger intermolecular interactions present to prevent it. Thus, in crystals of 1-iodo-4-(pentafluoro-phenylethynyl)benzene and 1-bromo-4-(pentafluorophenylethynyl)benzene strong iodo-iodo and bromo-bromo interactions occur at the expense of arene-perfluoroarene interactions. However, in that of 1-chloro-4-(pentafluoro-phenylethynyl)benzene, arene-perfluoroarene interactions occur at the expense of the weaker chloro-chloro interactions. By this reasoning, it can be reasonably expected that the crystal structure of the hitherto unobtained 1-fluoro-4-(pentafluorophenylethynyl)benzene, will also show an arene-perfluoroarene stacking motif.

However, this simple argument is complicated by the crystal structure of 1-iodo-4-(phenylethynyl)tetrafluorobenzene. Although it also consists of stacks of parallel molecules arranged in layers in a herringbone motif, it contains neither arene-perfluoroarene stacking motifs nor close iodo-iodo contacts. This is suprising in view of the fact that iodo-iodo interactions are expected to be the strongest of any halogen. It is clear that structures of 1-bromo-4-(phenylethynyl)tetrafluorobenzene and 1-chloro-4-(phenylethynyl)tetrafluoro-benzene need to be obtained in order to ascertain whether this packing is a general. Work is currently in progress to attempt to grow crystals of these remaining tolans.

5.4 Experimental

5.4.1 Synthesis and Characterisation

All reactions were carried out under a dry nitrogen atmosphere using standard Schlenk techniques, although once the reactions were complete, further procedures were carried out without any precautions against air. Triethylamine and diisopropylamine were distilled from calcium hydride under nitrogen and THF was distilled over sodium metal under nitrogen, prior to use. All other solvents were GPR grade and used without further purification or drying. Pentafluorophenylacetylene was prepared using a modified literature procedure.[21] All other reagents were obtained from Aldrich and used without further purification. The bis(triphenylphosphine) palladium(II) dichloride complex was made via the literature procedure.[22]

Proton and ^{19}F NMR experiments were performed on a Varian Mercury spectrometer at 200 MHz and 188 MHz respectively. The chemical shifts are reported in ppm and referenced to the internal standards tetramethylsilane and trichlorofluoromethane respectively. Carbon-13 NMR experiments were performed on a Varian Spectrometer at 125 MHz. with chemical shifts referenced to tetramethylsilane. All spectra were recorded in dry $CDCl_3$. MS analyses were performed on a Hewlett-Packard 5890 Series II gas chromatograph with a 5971A MSD mass selective ion detector and a 12 m fused silica (5% cross-linked phenylmethylsilicone) capillary column, under the following operating conditions: injector temperature 250 °C, detector temperature 270 °C, the oven temperature was ramped from 70 °C to 270 °C at the rate 20 °C / min. UHP helium was used as the carrier gas. Elemental analyses were performed using an Exeter Analytical CE-440 analyzer at the

University of Durham by Ms. J. Dostal. Melting points were obtained using a Laboratory Devices Mel-Temp II equipped with a Fluke 51 digital thermometer, and are uncorrected.

1-Iodo-4-(pentafluorophenylethynyl)benzene (1)
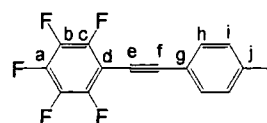
To a 500 ml Schlenk flask were added 1,4-diiodobenzene (9.90 g, 30 mmol), Pd(PPh$_3$)$_2$Cl$_2$ (0.07 g, 0.1 mmol) and CuI (0.02 g, 0.1 mmol) and the flask was evacuated and purged with dry nitrogen three times. Ca. 300 ml of triethylamine was added via cannula under nitrogen, and then pentafluorophenylacetylene (2.30 g, 12 mmol) was added dropwise by pipette under a nitrogen purge. The reaction mixture was stirred for 4 h at 60°C, filtered through a coarse sinter, and then evaporated to dryness *in vacuo*. The crude residue was extracted with hexane, filtered through a 3 cm thick silica pad, and the filtrate evaporated under reduced pressure. The residue was purified via column chromotography on silica with cyclohexane as the eluent, to obtain 5.50 g of recovered 1,4-diodobenzene, and the product, which was re-crystallised from hexane to give colourless plates. Yield: 0.72 g (18%)

m.p. 95-96 °C.

^{1}H NMR (200 MHz): δ 7.74 (m, 2H, H$_i$), 7.29 (m, 2H, H$_h$).

^{19}F NMR (188 MHz): δ -136.2 (m, 2F, F$_b$), -152.5 (m, 1F$_a$), -162.0 (m, 2F, F$_c$).

^{13}C {^{1}H} NMR (125 MHz): δ 147.1 (d, C$_b$, J$_{CF}$ = 250 Hz), 141.5 (d, C$_a$, J$_{CF}$ = 255 Hz), 137.8 (d, C$_c$, J$_{CF}$ = 250 Hz), 137.7 (s, C$_h$), 133.2 (s, C$_i$), 120.9 (s, C$_d$), 100.5 (s, C$_e$), 100.0 (s, C$_f$), 96.0 (s, C$_j$), 74.4 (s, C$_g$).

MS (EI) m/z (rel): 394 (m$^+$, 100), 266 (10), 248 (10), 217 (10).

Anal. Calcd. for C$_{14}$H$_4$F$_5$I: C 42.67, H 1.02; Found: C 42.45, H 0.98.

1-Bromo-4-(pentafluorophenylethynyl)benzene (2)
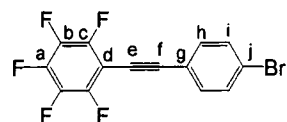
To a 250 ml Schlenk flask were added 1-bromo-4-iodobenzene (2.82 g, 10 mmol), Pd(PPh$_3$)$_2$Cl$_2$ (0.07 g, 0.1 mmol) and CuI (0.02 g, 0.1 mmol) and the flask was evacuated and purged with dry nitrogen three times. Ca. 150 ml of triethylamine was added via cannula under nitrogen, and then pentafluorophenylacetylene (2.30 g, 12 mmol) was added dropwise by pipette under nitrogen purge. The reaction mixture was stirred for 4 h at room temperature, then filtered through a coarse sinter, and was evaporated to dryness *in vacuo*. The crude residue was extracted with hexane, filtered through a 3 cm thick silica pad, and the filtrate evaporated under reduced pressure. The residue was re-crystallised from hexane to give the pure product as colourless cubes. Yield: 2.80 g (85%)

m.p. 103-104 °C.

^{1}H NMR (200 MHz): δ 7.53 (m, 2H, H$_i$), 7.44 (m, 2H$_h$)

^{19}F NMR (188 MHz): δ -136.2 (m, 2F, F$_b$) -152.5 (m, 1F, F$_a$) -162.0 (m, 2F, F$_c$).

^{13}C {^{1}H} NMR (125 MHz): δ 147.1 (d, C$_b$ J$_{CF}$ = 252 Hz), 141.5 (d, C$_a$, J$_{CF}$ = 254 Hz), 137.7 (d, C$_c$, J$_{CF}$ = 250 Hz), 133.2 (s, C$_h$), 131.9 (s, C$_i$), 124.2 (s, C$_j$), 120.9 (s, C$_d$), 100.3 (s, C$_e$), 100.0 (s, C$_f$), 74.2 (s, C$_g$).

MS (EI) m/z (rel): 348 (m+, 94), 346 (100), 266 (74), 248 (82), 247 (39), 241 (22), 240 (30), 217 (79), 216 (36), 173 (26).

Anal. Calcd. for C$_{14}$H$_4$F$_5$Br: C 48.45, H 1.16; Found: C 48.48, H 1.14.

1-Chloro- 4-(pentafluorophenylethynyl)benzene (3)
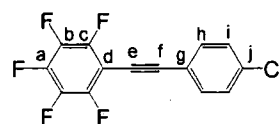
To a 100 ml Schlenk flask were added 1-chloro-4-iodobenzene (0.48 g, 2 mmol), Pd(PPh₃)₂Cl₂ (0.0014 g, 0.02 mmol) and CuI (0.001 g, 0.02 mmol) and the flask was evacuated and purged with dry nitrogen three times. Ca. 50 ml of triethylamine was added via cannula under nitrogen, and then pentafluorophenylacetylene (0.46 g, 2.4 mmol) was added by pipette to the mixture under a nitrogen purge. The reaction mixture was allowed to stir for 3 h at room temperature, and then heated at 60°C for 1 h. It was subsequently filtered through a coarse sinter, and then evaporated under reduced *in vacuo*. The crude residue was extracted with hexane, filtered through a 3 cm thick silica pad, and the filtrate evaporated under reduced pressure. The residue was re-crystallised from hexane to give the product as colourless needles. Yield: 0.46 g (85%)

m.p. 99-100 °C.

^{1}H NMR (200 MHz): δ 7.51 (m, 2H, H$_i$), 7.37 (m, 2H, H$_h$).

^{19}F NMR (188 MHz): δ -136.3 (m, 2F, F$_b$), -152.6 (m, 1F, F$_a$), -162.0 (m, 2F, F$_c$).

^{13}C {^{1}H} NMR (125 MHz): δ 147.3 (d, C$_b$, J$_{CF}$ = 253 Hz), 141.8 (d, C$_a$, J$_{CF}$ = 254 Hz), 137.9 (d, C$_c$, J$_{CF}$ = 250 Hz), 136.1 (s, C$_j$), 133.3 (s, C$_h$), 129.2 (s, C$_i$), 120.2 (s, C$_d$), 100.5 (s, C$_e$), 100.2 (s, C$_f$), 74.2 (s, C$_g$).

MS (EI) m/z (rel): 304 (m+, 31), 302 (100), 266 (15), 248 (21), 217 (19), 216 (12).

Anal. Calcd. for C₁₄H₄F₅Cl: C 55.54, H 1.32, Found: C 55.56, H 1.24.

1-Fluoro-4-(pentafluorophenylethynyl)benzene (4)
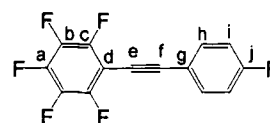
To a 100 ml Schlenk flask were added 1-fluoro-4-iodobenzene (0.44 g, 2 mmol), Pd(PPh$_3$)$_2$Cl$_2$ (0.0014 g, 0.02 mmol) and CuI (0.001 g, 0.02 mmol) which was evacuated and purged with dry nitrogen three times. Ca. 50 ml of triethylamine was added via cannula under nitrogen, and then pentafluorophenylacetylene (0.46 g, 2.4 mmol) was added by pipette under nitrogen purge. The reaction mixture was stirred for 3 h at room temperature, and then heated at reflux for 2 h. It was then filtered through a coarse sinter, and the evaporated to dryness *in vacuo*. The crude residue was extracted with hexane, filtered through a 3 cm thick silica pad, and the filtrate evaporated under reduced pressure. The residue was re-crystallised from hexane to give the product as colourless crystals. Yield: 0.45 g (79%)

m.p. 82-83 °C.

^{1}H NMR (200 MHz): δ 7.57 (m, 2H, H$_h$), 7.09 (m, 2H, H$_i$).

^{19}F NMR (188 MHz): δ -108.8 (m, 1F, F$_j$), -136.5 (m, 2F, F$_b$), -153.0 (m, 1F, F$_a$), -162.1 (m, 2F, F$_c$).

^{13}C {^{1}H} NMR (125 MHz): δ 163.3 (d, C$_j$, J$_{CF}$ = 255 Hz), 147.1 (d, C$_b$, J$_{CF}$ = 255 Hz), 141.5 (d, C$_a$, J$_{CF}$ = 250 Hz), 137.6 (d, C$_c$, J$_{CF}$ = 250 Hz), 134.0 (s, C$_h$), 117.6 (s, C$_d$), 116.0 (s, C$_i$), 100.4 (s, C$_e$), 100.1 (s, C$_f$), 72.8 (s, C$_g$).

MS (EI), m/z (rel): 286 (m+ 100), 266 (7), 255 (11), 235 (9), 217 (8), 216 (8).

Anal. Calcd. for C$_{14}$H$_4$F$_6$: C 58.74, H 1.40; Found: C 58.87, H 1.42.

1-Iodo-4-(phenylethynyl)tetrafluorobenzene (5)
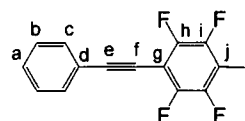
To a 500 ml Schlenk flask were added 1,4-diiodotetrafluorobenzene (12.06 g, 30 mmol), $Pd(PPh_3)_2Cl_2$ (0.07 g, 0.1 mmol) and CuI (0.02 g, 0.1 mmol) and the flask was evacuated and purged with dry nitrogen three times. Ca. 300 ml of diisopropylamine was added via cannula under nitrogen, and then phenylacetylene (1.22 g, 12 mmol) was added dropwise by pipette under a nitrogen purge. The reaction mixture was allowed to stir for 4 h. The reaction mixture was filtered through a coarse sinter, and was then evaporated to dryness *in vacuo*. The crude residue was extracted with hexane and filtered through a 3 cm silica thick silica pad, and the filtrate evaporated under reduced pressure. The residue was purified via column chromotography using hexane as the eluent, to obtain 6.40 g of recovered 1,4-diiodotetrafluorobenzene, and the product, which was re-crystallised from hexane to give colourless needles. Yield: 2.70 g (72%)

m.p. 123-124 °C.

^{1}H NMR (200 MHz): δ 7.60 (m, 2H, H_c), 7.40 (m, 3H, H_{ab}).

^{19}F NMR (188 MHz): δ -137.5 (m, 2F, F_h) -159.3 (m, 2F, F_i).

^{13}C {^{1}H} NMR (125 MHz): δ 148.3 (d, C_h, J_{CF} = 253 Hz) 145.8 (d, C_i, J_{CF} = J_{CF} = 256 Hz), 132.2 (s, C_b), 130.0 (s, C_a), 128.8 (s, C_c), 121.8 (s, C_d), 102.8 (s, C_e), 100.3 (s, C_f), 74.7 (s, C_g), 73.1 (m, C_j)

MS (EI), m/z (rel): 377 (26), 376 (m+, 100), 248 (11).

Anal. Calcd. for $C_{14}H_5F_4I$: C 44.71, H 1.34; Found: C 44.51, H 1.30.

1-Bromo-4-(phenylethynyl)tetrafluorobenzene (6)
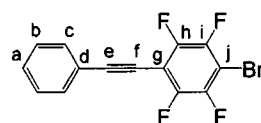
To a 500 ml Schlenk flask were added 1,4-dibromotetrafluorobenzene (9.24 g, 30 mmol), Pd(PPh₃)₂Cl₂ (0.07 g, 0.1 mmol) and CuI (0.02 g, 0.1 mmol) and the flask was evacuated and purged with dry nitrogen three times. Ca. 300 ml of diisopropylamine was added via cannula under nitrogen, and then phenylacetylene (1.22 g, 12 mmol) was added dropwise by pipette under a nitrogen purge. The reaction mixture was allowed to stir for 4 h. The reaction mixture was filtered through a coarse sinter, and the filtrate evaporated to dryness *in vacuo*. The crude residue was extracted with hexane, filtered through a 3 cm think silica pad, and the filtrate evaporated under reduced pressure. The residue was purified via column chromotography using hexane as the eluent, to obtain 4.30 g of recovered 1,4-dibromotetrafluorobenzene, and the product, which was re-crystallised from hexane to give colourless needles. Yield: 2.12 g (65%)

m.p. 100-101 °C.

^{1}H NMR (200 MHz): δ 7.60 (m, 2H, H$_c$), 7.40 (m, 3H, H$_{ab}$).

^{19}F NMR (188 MHz): δ -134.2 (m, 2F, F$_i$), -136.3 (m, 2F, F$_h$).

^{13}C {^{1}H} NMR (125 MHz): δ 148.1 (d, C$_h$ J$_{CF}$ = 254 Hz), 145.6 (d, C$_i$, J$_{CF}$ = 250 Hz), 131.9 (m, C$_b$), 129.7 (s, C$_a$), 128.5 (s, C$_c$), 121.5 (s, C$_d$), 102.9 (s, C$_e$), 100.3 (s, C$_f$), 74.0 (s, C$_g$).

MS (EI), m/z (rel): 330 (31), 328 (m+, 100), 248 (57), 230 (36), 229 (21), 199 (29).

Anal. Calcd. for C$_{14}$H$_5$F$_4$Br: C 51.17, H 1.52; Found: C 51.32, H 1.54.

1-(Phenylethynyl)-4-chlorotetrafluorobenzene (7)
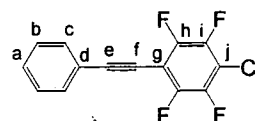
A three-necked 250 ml flask was equipped with a dropping funnel and evacuated and purged with dry nitrogen three times. Ca. 50 ml of dry THF was added via cannula under nitrogen. Phenylacetylene (1.02 g, 10 mmol) was added via pipette to the flask under nitrogen purge. A 6.5 ml aliquot of a 1.6 M solution of n-butyl lithium in hexanes was added via cannula to the dropping funnel under nitrogen. The butyl lithium solution was then added dropwise to the reaction mixture at -78 °C under nitrogen, and the reaction left to stir for 1 h. Chloropentafluorobenzene (2.02 g, 10 mmol) was added. The mixture was stirred at -78 °C, and it was observed to progressively darken. After 24 h,. the reaction mixture was filtered through a 3 cm silica pad with diethyl ether, and the filtrate was evaporated under reduced pressure to leave a dark residue. The residue was extracted with hexane and filtered through a 3 cm thick silca pad. The filtrate was evaporated under reduced pressure to leave a white residue, which was re-crystallised from hexane to give the product as a white powder. Yield: 1.04 g (37%)

m.p. 95-96 °C.

^{1}H NMR (200 MHz): δ 7.59 (m, 2H, H_c), 7.38 (m, 3H, H_{ab}).

^{19}F NMR (188 MHz): δ -136.3 (m, 2F, F_h), -141.7 (m, 2F, F_i).

^{13}C {^{1}H} NMR (125 MHz): δ 132.0 (m, C_b), 129.7 (s, C_a), 128.5 (s, C_c), 121.4 (s, C_d), 102.3 (s, C_e).

MS (EI) m/z (rel): 286 (m+, 33), 285 (16) 284 (100), 248 (10).

Anal. Calcd. for $C_{14}H_5F_4Cl$: C 58.93, H 1.91; Found: C 58.76, H 1.56.

5.4.2 Crystallography

The crystallographic data collection and structure solutions for all the compounds was performed by Ms. Jacquie Burke. All X-ray diffraction experiments were carried out on a Siemens SMART three-circle diffractomer equipped with a 1K CCD area detector, using graphite-monochromated Mo-K$_\alpha$ radiation. The structures were solved by direct methods, and refined by full-matrix least squares on F^2 of all the data, using SHELXTL software.[26] All C, F, I, Br and Cl atoms were refined in anisotropic approximation.

5.5 References

1.	a) P. Nguyen, G. Lesley, C. Dai, N. J. Taylor, T. B. Marder, V. Chu, C. Viney, I. Ledoux and J. Zyss, in *Applications of Organometallic Chemistry in the Preparation and Processing of Advanced Materials*, ed. J. F. Harrod and R. M. Laine, Kluwer Academic, Dordrecht, 1995, p. 333; b) P. Nguyen, Z. Yuan, L. Agocs, G. Lesley and T. B. Marder, *Inorg. Chim. Acta*, 1994, **220**, 289; c) P. Nguyen, G. Lesley, T. B. Marder, I. Ledoux, J. Zyss, *Chem. Mater.*, 1997, **9**, 406.

2.	a) A. V. Abramenkov, A. Almenningen, B. N. Cyvin, S. J. Cyvin, T. Jonvik, L L. S. Khaikin, C. Romming and L. V. Vilkonv, *Acta Chim. Scand.*, 1988, **A42**, 674; b) K. Inoue, H. Takeuchi and S. Konaka, *J. Chem. Phys.*, 2001, **A105**, 6711.

3.	a) A. E. Stiegman, E. Graham, K. J. Perry, L. R. Khundkar, L.-T. Cheng and J. W. Perry, *J. Am. Chem. Soc.*, 1991, **113**, 7658; b) C. Dehu, F. Meyers and J.-L. Bredas, *J. Am. Chem. Soc.*, 1993, **115**, 6198.

4.	G. R. Desiraju and T. S. R. Krishna, *J. Chem. Soc., Chem. Commun.*, 1988, 192.

5.	a) T. Kurihara, H. Tabei and T. Kaino, *J. Chem. Soc., Chem. Commun.*, 1987, 959; b) H. Tabei, T. Kurihara and T. Kaino, *Appl. Phys. Lett.*, 1987, **59**, 1855; c) C. Wang, J. Feng and C. Yu, *J. Beijing Inst. Tech.*, 1996, **5**, 27; d) C. Dai, A. J. Scott, W. Clegg, G. Cross and T. B. Marder, *unpublished results*.

6.   M. Ohkita, T. Suzuki, K. Nakatani and T. Tsuji, *Chem. Commun.*, 2001, 1454.

7.   A. J. Scott, Ph.D. Thesis, University of Newcastle, Newcastle, UK, 1998.

8.   C. Dai, Ph.D. Thesis, University of Waterloo, Ontario, Canada, 1998.

9.   C. M. Smith, C. Dai, R. L. Thomas, P. Smith, A. S. Batsanov, J. A. K. Howard, A. J. Scott, W. Clegg, T. B. Marder, submitted to *J. Mater. Chem.*

10.   Y. Zhang and J. Wen, *Synthesis*, 1990, 727.

11.   P. Tarrant, in *Fluorine Chemistry Reviews*, ed. P. Tarrant, Marcel Dekker, New York, vol. 7, 1974.

12.   a) J. Kajanus, S. B. van Berlekom, B. Albinsson and J. Martensson, *Synthesis*, 1999, 1155; b) H. Li, D. R. Powell, T. K. Firman and R. West, *Macromolecules*, 1998, **31**, 1093.

14.   P. L. Coe, J. C. Tatlow and R.C. Terrell, *J. Chem. Soc. C.*, 1967, 2626.

15.   M. R. Wiles and A. G. Massey, *Tetrahedron Lett.*, 1967, 5137.

16.   A. Bondi, *J. Phys. Chem.*, 1964, **68**, 441.

17.   R. S. Rowland and R. Taylor, *J. Phys. Chem.*, 1996, **100**, 7384.

18.   N. Ramasubbu, R. Parthasarathy and P. Murray-Rust, *J. Am. Chem. Soc.*, 1986, **108**, 4308.

19.   V. R. Pedireddi, D. S. Reddy, S. Goud, D. C. Craig, A. D. Rae and G. R. Desiraju, *J. Chem. Soc., Perkin Trans. 2*, 1994, 2353.

20.   a) G. R. Desiraju and R. Parthasarathy, *J. Am. Chem. Soc.*, 1989, **111**, 8725; b) V. R. Thalladi, H.-C.Weiss, R. Boese, A. Nangia and G. R. Desiraju, *Acta Crystallogr. Sect. B*, 1999, **55**, 1005.

21.   C. Dai, Ph.D. Thesis, University of Waterloo, Ontario, Canada, 1998, p. 73.

22.   L. Brandsma, S. F. Vasilevsky and H. D. Verruijsse, in *Application of Transition Metal Catalysts in Organic Synthesis*, Springer, Berlin, 1988. p. 179.

23.   *SHELXTL, An integrated system for solving refining and displaying crystal structures from diffraction data, ver. 5.10*, Bruker Analytical X-ray Systems, Madison, Wisconsin, USA, 1997.

Chapter Six

The Arene-Perfluoroarene Interaction in Mismatched Systems: The Structures of Complexes of Polyaromatic Molecules with Hexafluorobenzene and Octafluoronaphthalene

6.1 Introduction

Most studies of the arene-perflouroarene interaction have been restricted to complexes of HFB and benzene derivatives or to molecules with either phenyl or perfluorophenyl groups. Much less is known about arene-perfluoroarene complexes involving larger fused-ring polyaromatic compounds. This is surprising in view of the fact that the discoverers of the HFB·benzene complex also reported that a complex formed between HFB and 2-methylnaphthalene in their original paper.[1] Later, a phase diagram was obtained for the binary mixture of HFB with naphthalene, which clearly showed the formation of a congruently melting complex at equimolar composition.[2] More recently, phase diagrams were obtained of mixtures of octafluoronaphthalene (OFN) and various polyaromatic hydrocarbons.[3] These showed congruent melting points at equimolar composition in the majority of cases. The ground state stabilisation energy of the complex between OFN and anthracene in solution has been determined to be 1.48 kcal mol^{-1} by comparing its fluoresence with that of pure anthracene.[4] This complex was later found to be magnetically sensitive.[5]

There have been few crystallographic studies performed on arene-perfluoroarene complexes with polyaromatic compounds. A rare example is the 1:1 complex between naphthalene and OFN.[6] The crystal structure, obtained from X-ray diffraction, showed the molecules to be stacked alternately in infinite columns with a slight offset, which was very similar to the crystal structures of such complexes with HFB. This complex has also been studied by solid state Raman spectroscopy.[7] A comparison of the resulting spectra with those of the two individual components led the authors to suggest that, although the complex is primarily van der Waals in character, electrostatic multipole-multipole interactions do occur. However, electrostatic interactions were not necessary to account for the Raman spectra of complexes of OFN with 1,4-dihalonaphthalenes.[8] These findings were supported by luminescence studies.[9] Several years later, the structure of the 1:1 complex between triphenylene and perfluorotriphenylene was obtained, and shown to be similar to the others.[10] It was also demonstrated that the addition of perfluorotriphenylene induces crystallinity in a polymer containing triphenylene pendant groups. The molecular structures of the OFN·naphthalene and perfluorotriphenylene·triphenylene complexes are shown in Figure **6.1**.
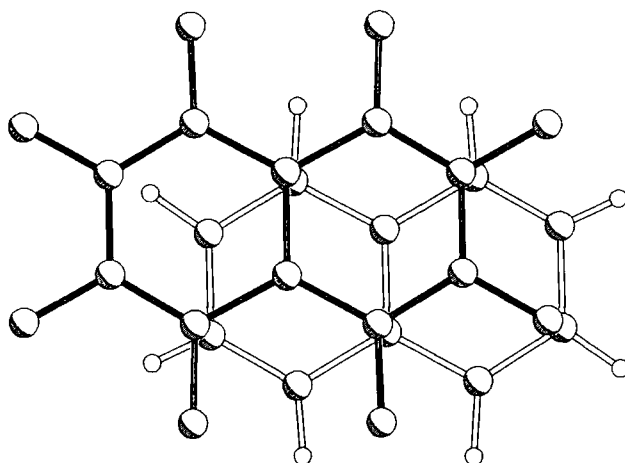
Figure **6.1**(a) Molecular structure of the OFN·naphthalene complex viewed perpendicular to the mean plane of OFN
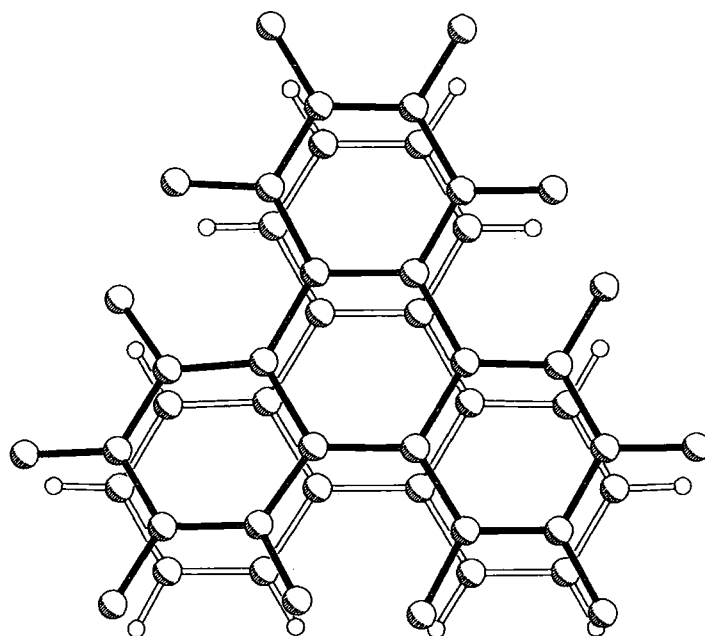

Figure **6.1**(b) Molecular structure of perfluorotriphenylene·triphenylene complex viewed perpendicular to the mean plane of perfluorotriphenylene

However, arene-perfluoroarene complexes may not necessarily to be restricted to polyaromatic hydrocarbons and their perfluorinated analogues. This was conclusively demonstrated when the crystal structure of the 1:1 complex of naphthalene with decafluorobiphenyl was obtained.[11] X-ray diffraction reveal the crystal structure to be composed of ribbons of alternating naphthalene and decafluorobiphenyl molecules, the decafluorobiphenyl being non-planar. The scope of these interactions was increased further when the crystal structure of a 1:1 complex of HFB with a dehydroannulene was obtained.[12] It is unusual in that the HFB is located over the annulene ring and not the phenylene groups, which is shown in Figure **6.2**. The crystal structures of the 1:1 complexes of perfluorophenanthrene with ferrocene and decamethylferrocene have also been obtained.[13] In the former, two ferrocene molecules are stacked between two phenanthrene molecules, whereas in the latter, an orthodox structure consisting of stacks of alternating phenanthrene and decamethylferrocene molecules is observed. See Figure **6.3** All of these structures clearly demonstrate that arene-perfluoroarene complexes can occur between molecules with substantial differences in size and shape.

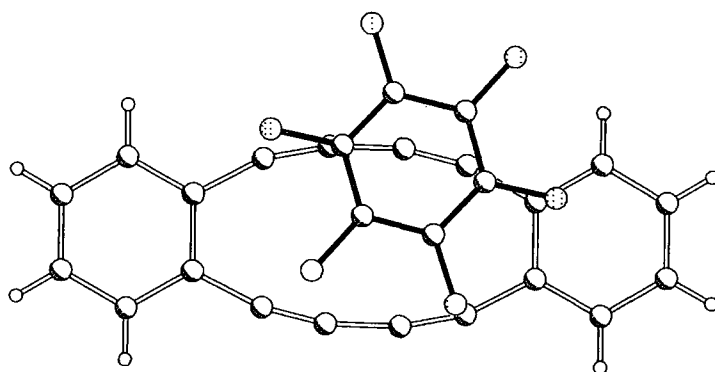Figure **6.2** Molecular structure of the HFB·dehydroannulene complex viewed perpendicular to mean plane of the HFB molecule
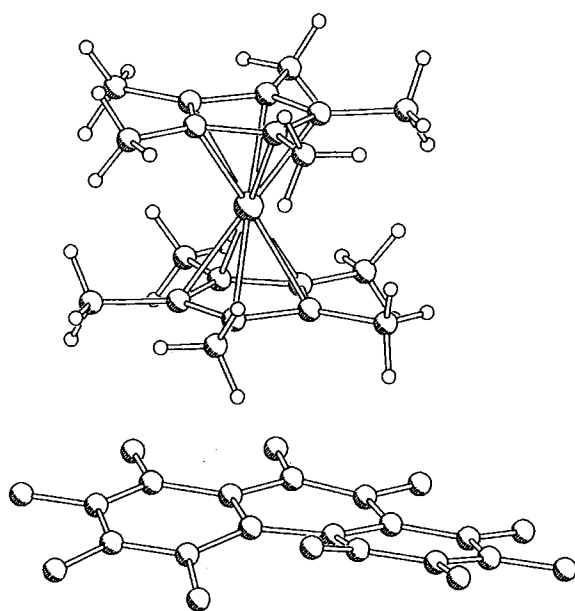
Figure **6.3**(a) Structure of perfluorophenanthrene·decamethylferrocene complex
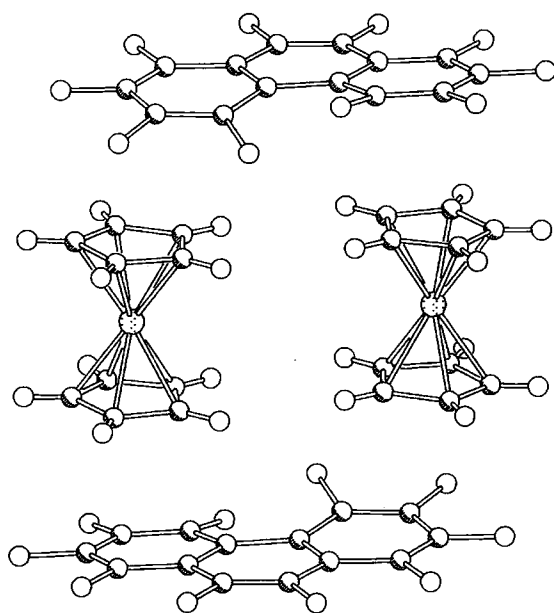
Figure **6.3**(b) Structure of perfluorophenanthrene.ferrocene·complex

146

However, until now the structures outlined above have been the only examples of such arene-perfluoroarene complexes between mismatched arenes. It is clear that the crystal structures of many more mismatched arene-perfluoroarene complexes need to be obtained. What would be particularly useful would be to grow co-crystals (if possible) and obtain the crystal structures of a series of complexes between simple perfluoroarenes, such as HFB and OFN etc., and representative polyaromatic hydrocarbons, for example anthracene and pyrene. This would give a much broader view of the arene-perfluoroarene interaction, especially in terms of its scope and limitations. This chapter is devoted to the formation and crystal structure solution of such a series of binary complexes of HFB and OFN with several simple and commercially available polyaromatic hydrocarbons, namely naphthalene, anthracene, phenanthrene, pyrene and triphenylene.

6.2 Results and Discussion

6.2.1 Crystal Growth and Crystallographic Data

Diffraction quality crystals of the following complexes HFB·naphthalene (**1**), HFB·anthracene (**2**), HFB·phenanthrene (**3**), HFB·pyrene (**4**), HFB·triphenylene (**5**) were grown from the slow evaporation of HFB solutions of the relevant polyaromatic (the crystals of **2** were grown by Dr Edward Robins and the crystals of **4** by Karl Roscoe). The isolated crystals are prone to losing HFB by evaporation at room temperature. They can be preserved for a long time in HFB solution, or in the presence of HFB vapour, but otherwise decompose within seconds, leaving blocks of opaque polycrystalline powder, which, although retaining the form of the original crystal, are composed only of the polyaromatic compound. Diffraction-quality crystals the complexes OFN·anthracene (**6**), OFN·phenanthrene (**7**), OFN·pyrene (**8**) and OFN·triphenylene (**9**) were grown from the slow evaporation of 1:1 molar solutions of OFN and the polyaromatic in dichloromethane.

The crystal structures of all the complexes were solved from single-crystal X-ray diffraction data by Dr. Andrei Batsanov (except for the complex of HFB with pyrene, which was collected and solved by Lorna Stimson) at the University of Durham. Rudimentary X-ray diffraction experiments have been previously carried out on crystals of complexes **2** and **4** at room temperature in sealed capillaries.[14] All X-ray diffraction experiments were performed at low temperature, in order to prevent loss of HFB and/or reduce errors caused by random thermal motion. Complex **1** undergoes a phase transition at ca. 175 K upon cooling. As the low-temperature phase was polycrystalline, only the high-temperature phase was studied at 180 K. The experiment for complex **4** was performed at 200 K, as at lower temperatures the crystals deteriorated,

possibly due to a phase transition. Complex **7** also undergoes a phase transition at ca. 250 K upon cooling. The lower temperature phase is denoted by α, and the higher temperature phase by β in accordance with convention. Crystallographic data were collected for the β-phase at 295 K, but no solution could be found to model the data, either by direct methods, or by inference from the α-phase structure. Relevant crystallographic data and structural refinement parameters for the HFB complexes are given in the Table **6.1**, and for the OFN complexes in Table **6.2**.

The crystal structures of complexes **1** and **2** complexes are very similar, and they crystallise in the same monoclinic space group *C2/c* with Z = 4. In both structures, the polyaromatic molecules lie on crystallographic centres of inversion; however, the HFB molecules lie on crystallographic two-fold axes. Complex **3** crystallises in the triclinic space group $P\overline{1}$. Both the HFB and phenanthrene molecules occupy general positions. The phenanthrene molecules are disordered between two co-planar and partially overlapping positions, with occupancies of 87.3(2) and 12.7(2)% respectively. It is possible that this incomplete disorder may result from an incomplete phase transition that occurred on the rapid cooling of the crystal to 150 K. However, this could not be verified due to the instability of the crystals at room temperature. Complexes **4** and **5** both crystallise in the space group $P2_1/c$, but with Z = 2 and Z = 4 respectively. Whilst both the HFB and polyaromatic molecules lie at crystallographic centres of inversion in complex **4**, in **5** they have no crystallographic symmetry. It is noteworthy that the cell parameters and space groups of **2** and **4** obtained in this study are neither similarly or rationally related to the *C*-centred monoclinic cell parameters observed in the earlier investigation.[14] It is possible that given the instability these complexes, the room temperature crystals may have been of a different composition.

Complex **6** crystallises is space group $P2_1/c$ with both components lying on inversion centres. The low temperature phase of complex **7** also crystallises in the $P2_1/c$ space group, with very similar cell parameters to those of complex **6**. This is probably a consequence of the similar size and shape of the anthracene and phenanthrene molecules. The complexes of these polyaromatics with tetracyanobenzene are also isomorphous.[15] The OFN centroid is located on a centre of inversion; however, the phenanthrene molecules are statistically disordered over two positions related by another centre of inversion, with equal occupancy of each positions. A similar type of disorder is found in the high temperature phase of phenanthrene itself, although the occupancies are only approximately equal.[16] Complex **8** crystallises in the space group $P\bar{1}$, with both molecules located on inversion centres. Complex **9** also crystallises in $P\bar{1}$; however, neither of the components is located on an inversion centre, but instead at arbitrary positions in the unit cell.

Table **6.1**. Crystallographic data and structure refinement parameters for the HFB complexes.

Complex	1	2	3	4	5
CCDC dep. no.	175695	175696	175697	175698	175699
Formula	$C_6F_6 \cdot C_{10}H_8$	$C_6F_6 \cdot C_{14}H_{10}$	$C_6F_6 \cdot C_{14}H_{10}$	$C_6F_6 \cdot C_{16}H_{10}$	$C_6F_6 \cdot C_{18}H_{12}$
Formula weight	314.22	364.28	364.28	388.30	414.34
T (K)	180	150	120	200	120
Crystal system	Monoclinic	Monoclinic	Triclinic	Monoclinic	Monoclinic
Space group	$C2/c$	$C2/c$	$P\bar{1}$	$P2_1/c$	$P2_1/c$
a (Å)	11.806(1)	16.122(3)	6.929(2)	6.946(2)	13.935(2)
b (Å)	13.508(1)	12.086(2)	7.308(1)	13.331(3)	7.211(2)
c (Å)	8.426(2)	8.955(3)	15.991(3)	9.301(2)	17.370(8)
α (°)	90	90	91.51(1)	90	90
β (°)	97.15(1)	118.39(3)	102.16(1)	106.67(3)	92.55(1)
γ (°)	90	90	100.16(1)	90	90
V (Å^3)	1333.3(4)	1535.0(5)	777.5(3)	825.2(3)	1743.7(10)
Z	4	4	2	2	4
ρ_{calcd} (g cm^{-3})	1.565	1.576	1.556	1.563	1.578
$\bar{\lambda}$ (Å)	0.71073	1.54178	0.71073	0.71073	0.71073
μ (mm^{-1})	0.15	12.49	0.14	0.14	0.14
Total reflections	4725	1608	9769	5231	10590
Unique refls.	1530	1279	4080	1882	3075
R_{int}	0.050	0.045	0.034	0.033	0.144
Refls. ($I > 2\sigma(I)$)	1083	1133	3056	1287	1722
R (F, $I > 2\sigma(I)$)	0.050	0.050	0.043	0.043	0.102
wR (F^2, all data)	0.121	0.155	0.132	0.122	0.285

Table 6.2 Crystallographic data and structural refinement parameters for the OFN complexes

Complex	6	α-7	β-7	8	9
CCDC dep. no.	157246	157247	157248	157249	157250
Formula	$C_{10}F_8 \cdot C_{14}H_{10}$	$C_{10}F_8 \cdot C_{14}H_{10}$	$C_{10}F_8 \cdot C_{14}H_{10}$	$C_{10}F_8 \cdot C_{16}H_{10}$	$C_{10}F_8 \cdot C_{18}H_{12}$
Formula weight	450.32	450.32	450.32	474.34	500.38
T (K)	120(2)	120(2)	296(2)	120(2)	120(2)
Crystal system	Monoclinic	Monoclinic	Monoclinic	Triclinic	Triclinic
Space group	$P2_1/n$	$P2_1/n$	I-centred	$P\bar{1}$	$P\bar{1}$
a (Å)	6.810(1)	6.776(2)	6.923(2)	6.725(1)	6.732(1)
b (Å)	18.326(1)	18.180(6)	17.925(3)	8.864(1)	9.365(2)
c (Å)	7.390(1)	7.666(3)	8.080(3)	9.488(1)	16.550(4)
α (°)	90	90	90	107.51(1)	86.44(1)
β (°)	100.35(1)	102.45(1)	104.39(1)	105.23(1)	87.30(1)
γ (°)	90	90	90	106.82(1)	77.30(1)
V (Å^3)	907.3(2)	922.1(5)	971.3(4)	476.9(1)	1015.3(4)
Z	2	2	2	1	2
ρ_{calcd} (g cm^{-3})	1.648	1.622		1.652	1.637
μ (mm^{-1})	0.15	0.15		0.15	0.15
Trans. range	0.93-0.99	0.92-0.99		0.92-0.99	0.92-0.99
θ Range (°)	2.2-27.5	2.2-25.0		2.4-25.0	1.2-27.5
Total reflections	6480	4586		2866	8936
Unique refls.	2083	1621		1661	4599
Parameters	165	138		174	374
R_{int}	0.061	0.051		0.047	0.042
Refls. ($I > 2\sigma(I)$)	1205	942		1106	2704
R (F, $I > 2\sigma(I)$)	0.04	0.049		0.044	0.042
wR (F^2, all data)	0.086	0.13		0.115	0.118

6.2.2 Molecular Structures

The molecules of all the components are all planar within experimental error. In all of the complexes, there was no significant discrepancy between the intramolecular bond lengths and angles of the molecules in the complex and those of the molecules in the structures of the individual components, which were obtained at similar temperatures.[17,18] This is further evidence of the lack of charge transfer in these complexes. The molecular structures of the two adjacent components viewed perpendicular to the mean plane of the HFB or OFN component are shown in Figure **6.4**, with thermal ellipsoids plotted at 50% probability.
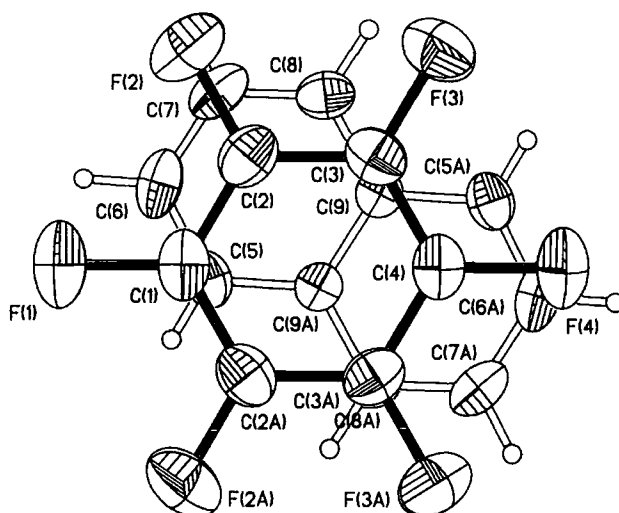
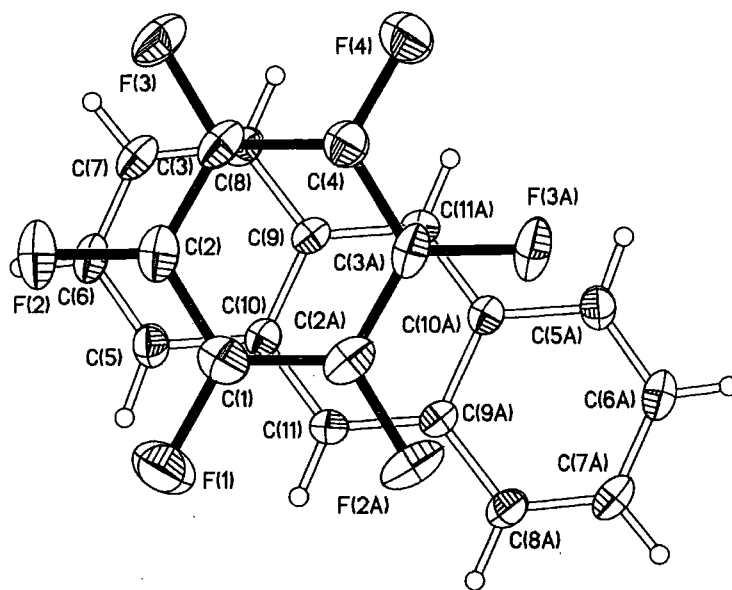Figure **6.4(a)** Molecular structure of HFB·naphthalene (**1**)

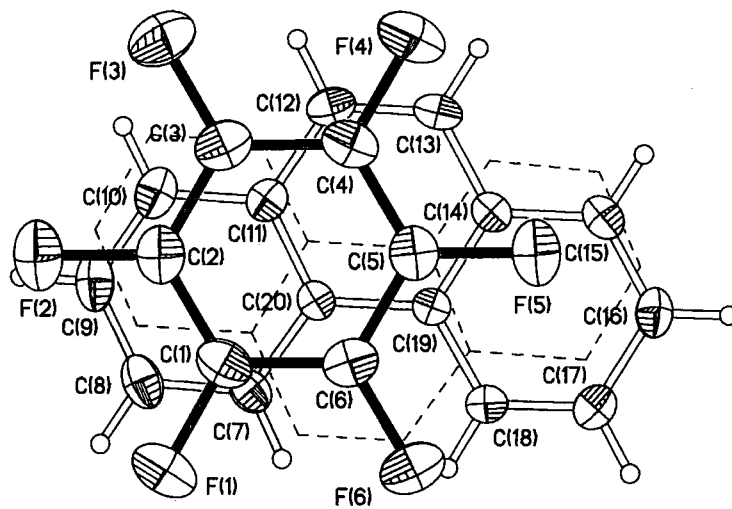Figure **6.4**(b)   Molecular structure of HFB·anthracene (**2**)

Figure **6.4**(c)   Molecular structure of HFB·phenanthrene (**3**) (carbon-carbon
bonds of one orientation of phenanthrene represented by dashed lines)

154

Figure **6.4(d)** Molecular structure of HFB·pyrene (**4**)

Figure **6.4(e)** Molecular structure of HFB·triphenylene (**5**)

Figure **6.4**(f)   Molecular structure of OFN·anthracene (**6**)

Figure **6.4**(g)   Molecular structure of OFN·phenanthrene (**7**) (carbon-carbon
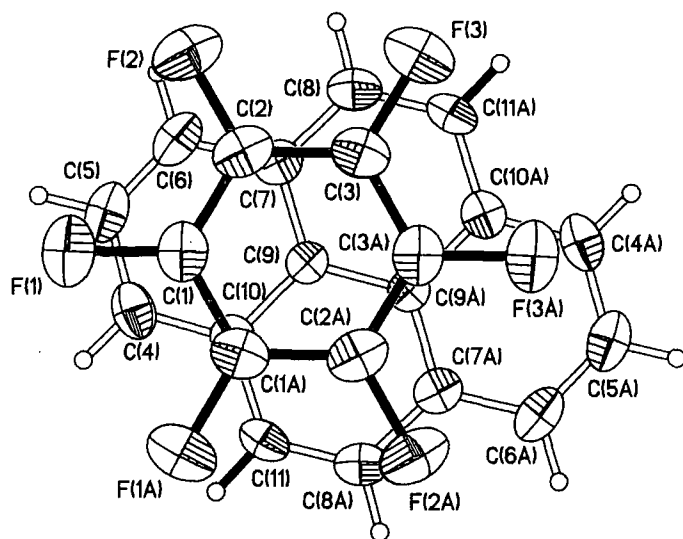bonds of one orientation of phenanthrene represented by dashed lines)
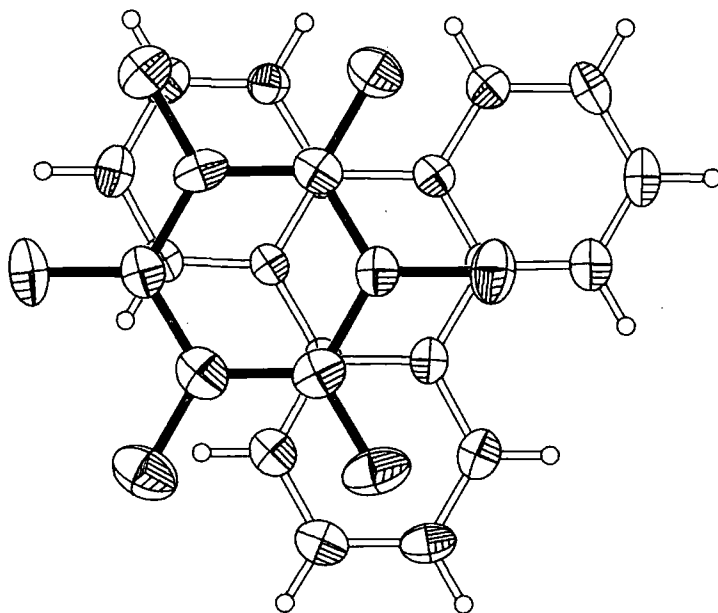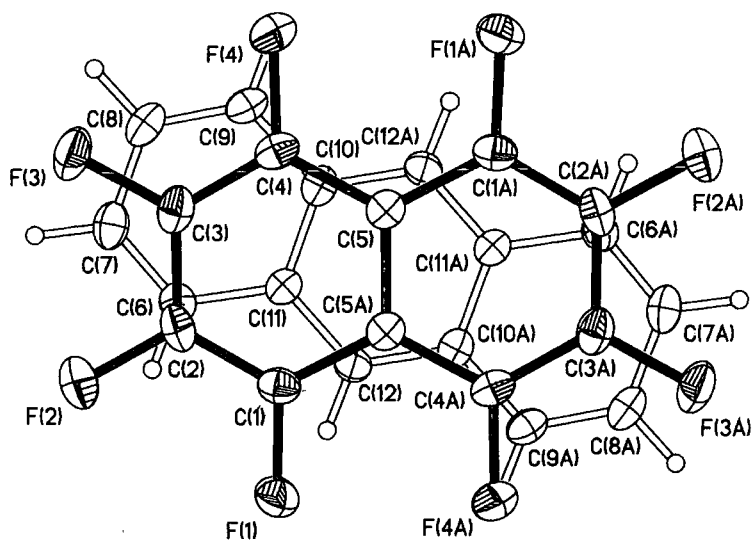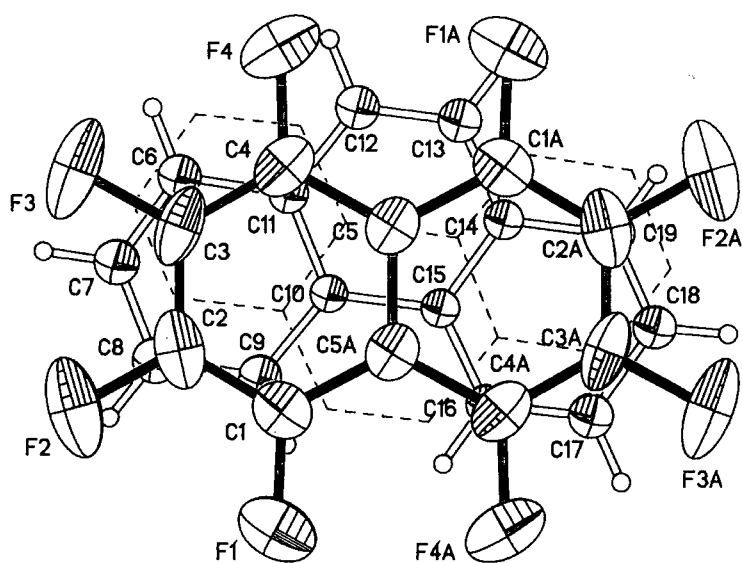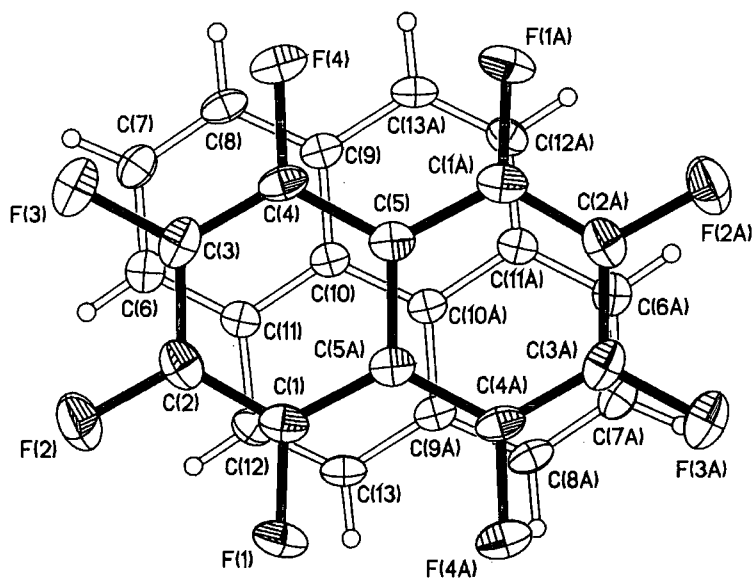
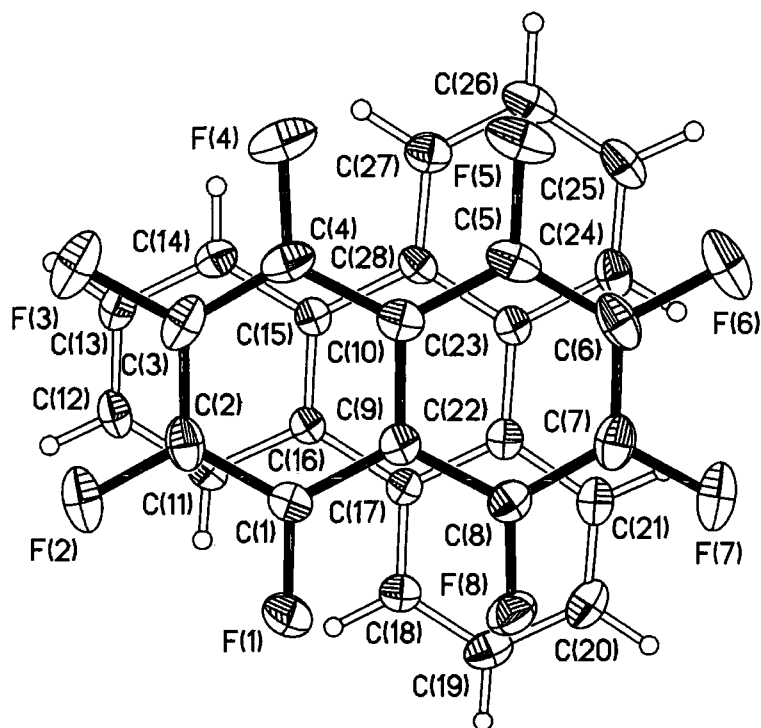Figure **6.4**(h) Molecular structure of OFN·pyrene (**8**)

Figure **6.4**(i) Molecular structure of OFN·triphenylene (**9**)

157

6.2.3 The Packing of the Complexes and their Pure Components

The crystal structures of all of the complexes revealed the component molecules to be arranged in infinite stacks of alternating arene and perfluoroarene molecules, usually running parallel to one of the cell axes. The molecules within a stack are nearly parallel, which would appear to indicate the presence of arene-perfluoroarene interactions in all of the complexes. Such packing arrangements are v~~ry closely related to those of other previously obtained arene-perfluoroarene complexes, and in stark contrast to those of the individual components themselves. Polyaromatic hydrocarbon molecules have been observed to pack in one of four different motifs, which have been classified by Desiraju: namely herringbone, herringbone of sandwiches, flattened herringbone (also known as γ-type), and pseudo-graphitic type (β-type).[19] Schematics of these packing modes are shown in Figure **6.5**. Naphthalene, anthracene, phenanthrene and triphenylene all belong to the herringbone motif, whereas pyrene crystallises as a herringbone of sandwiches. Octafluoronaphthalene, which has recently had the structure of its low-temperature phase unambiguously solved after many attempts, also crystallises in a herringbone motif.[18]
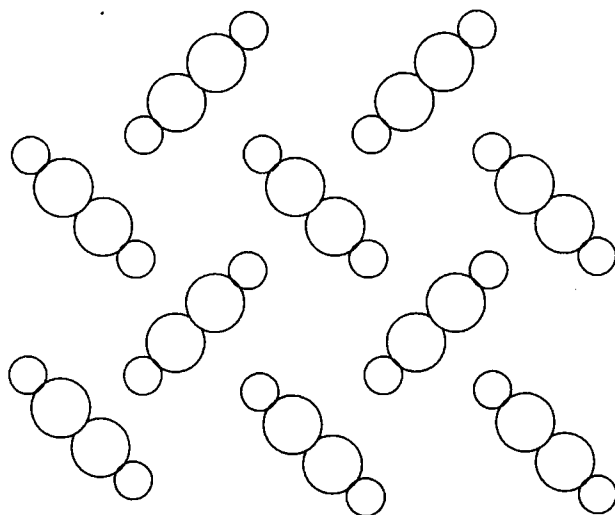
Figure **6.5**(a) Schematic of the herringbone packing arrangement.
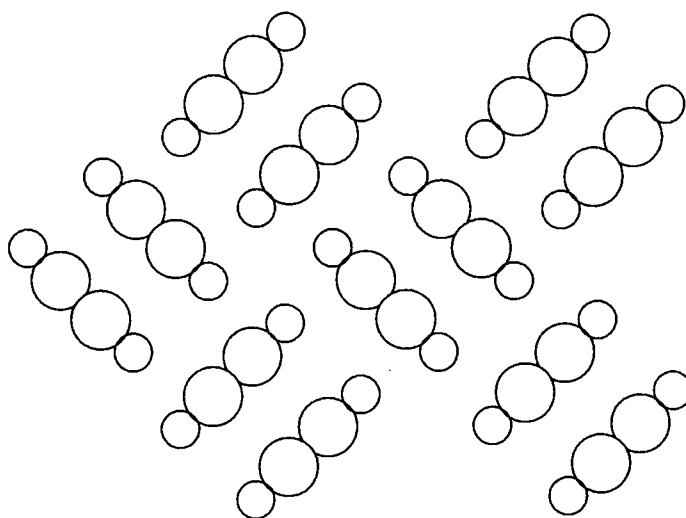

Figure **6.5**(b) Schematic of the herringbone of sandwiches packing arrangement.
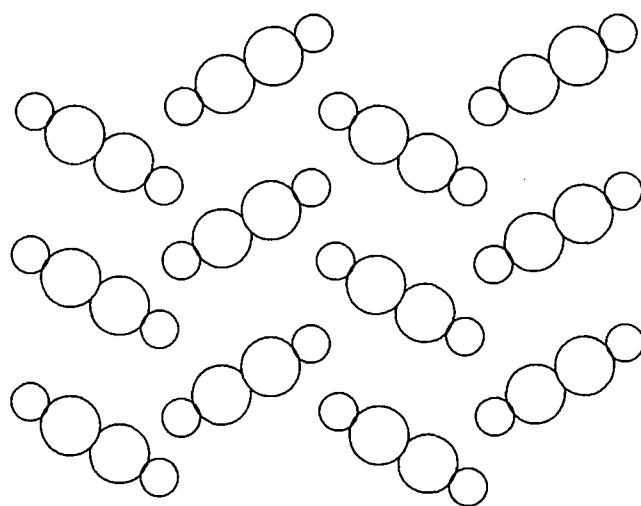
Figure **6.5**(c) Schematic of the flattened herringbone (γ-type) packing arrangement.
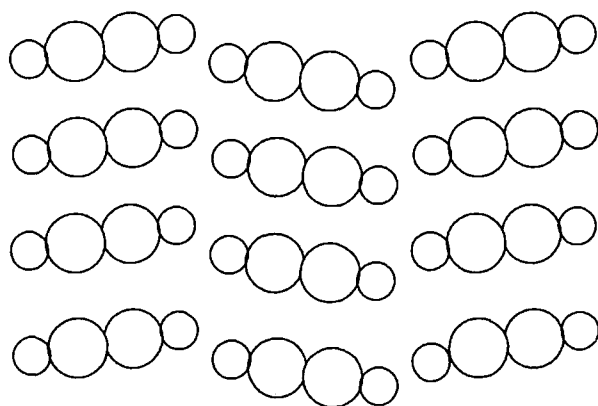

Figure **6.5**(d) Schematic of the graphitic (β-type) packing arrangement.

Although the packing of these complexes are observed to be generally very similar, namely consisting of infinite stacks of alternating component molecules, there are several subtle differences between them. These can be described, and then compared and contrasted, through the use of several intermolecular parameters, which will be defined here, and are illustrated schematically in Figure **6.6**. An important parameter is the distance between adjacent molecules in a given stack. This can be defined as the distance between their two molecular centroids, which is usually equal to (or a sub-division of) the cell parameter in the direction along which stacking occurs. A more meaningful definition of this distance is the interplanar spacing. However, although molecules of the same component are usually parallel within a stack, molecules of the different components usually are not exactly parallel, which leads to complications in the definition of this parameter. The extent of this aparallelism can be defined as the dihedral angle between the two components, which is termed the inter-component interplanar angle. An intercomponent interplanar separation can be defined as the mean distance between the plane of one molecule and the centroid of the adjacent one, and vice-versa. When both molecular centroids lie on crystallographic centres of inversion, it follows that all of these interplanar separations are identical. However, in those structures for which this is not the case, there will be two or more independent values of this parameter.

As with other such complexes, the mean molecular planes are usually not orthogonal to the stacking axis. This means that the molecules are not stacked directly on top of one another, instead they have a slight offset, which means that the interplanar distance will be less than the inter-centroid distance. Such an offset can be quantified by means of an offset angle, which is defined as the angle between the stacking axis and the normal to the mean molecular plane for each of the components; the larger the angle, the greater

the offset. If the components of a stack are not parallel, there will be two slip angles, one for each component, which can be averaged to give a mean.

Although all molecules of each component are usually parallel within a given stack, this parallelism does not necessarily extend to the molecules in different stacks. For some arene-perfluoroarene complexes, the crystallographic symmetry dictates that all the molecules of the same component in every stack are strictly parallel, and the structure is said to have a laminar motif. However, often, the stacks are arranged in alternating layers of parallel molecules, in a pseudo-herringbone motif. The degree of parallelism can be quantified by the angles between the mean planes of components in adjacent layers. Within laminar motifs, the relative positions of similar molecules in adjacent stacks can be defined by a shift distance, which is the inter-planar distance between the two parallel components in adjacent stacks.
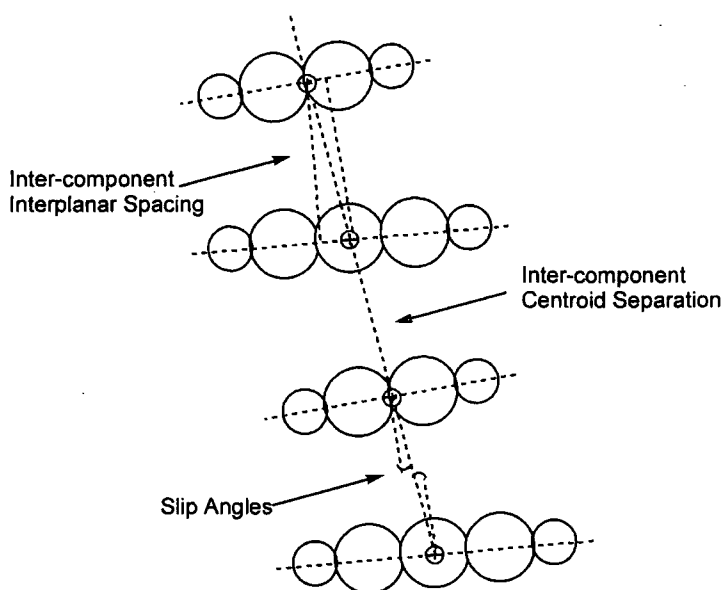

Figure 6.6. Schematic of a stack of alternating arene and perfluoroarene components showing the definition of some intermolecular parameters

For the HFB complexes, within a given stack all molecules of each component are parallel, except for complexes **1** and **2**. Although, in these, all the HFB molecules within a stack are rigorously parallel, this does not apply to the polyaromatic molecules which are arranged alternately within each stack. The dihedral angle between the average molecular planes of these polyaromatic molecules, within the stack is $3.6°$ for the naphthalenes in **1** and $2.5°$ for the anthracenes in **2**. The intermolecular parameters for the HFB complexes are listed in Table **6.3**. For the HFB complexes, the inter-planar angles between adjacent components in the stacks vary in the range $0.6 - 2.5°$. The offset angles range from $3.6° - 23.4°$, and tend to increase with increasing size of the polyaromatic molecules. The inter-component inter-planar distances are in the range $3.31 - 3.44$ Å, and comparable to the van der Waals thickness of the polyaromatic molecules (3.4 Å).

The intermolecular parameters for all the OFN complexes are given in Table **6.4**. The centroid-centroid distances are all in the range $3.35 - 3.45$ Å, with no clear trend. The inter-component inter-planar distances are all very similar ranging from $3.34 - 3.40$ Å. These are towards the lower region of the scale of inter-planar separation in arene-perfluorarene complexes. The offset angles are in the range $1.2 - 6.4°$ for the polyaromatic molecules, and $1.5 - 9.1°$ for the OFN molecules. There is a general trend that as the polyaromatic molecule increases in size both the dihedral and offset angles decrease, which means that there is less offset between the components and the stacks become more columnar.

Table **6.3** Intermolecular parameters for the HFB complexes

Complex	1	2	3[a]	4	5
Inter-component Interplanar Angle (°)	2.5	1.5	1.0 (1.2)	0.6	1.5
HFB Offset Angle (°)	4.8	20.7	14.6	12.1	22.7
Polyaromatic Offset Angle (°)	3.6	20.1	13.4 (13.6)	12.7	23.4
Intercomponent Centroid-Centroid Distance(s) (Å)	3.43	3.57	3.44 (3.36) 3.50 (3.57)	3.47	3.61 3.71
Mean Interplanar Spacing(s) (Å)	3.40	3.34	3.36 (3.28) 3.35 (3.44)	3.39	3.32 3.31

[a] Quantities in parentheses correspond to those of minor disordered position of phenanthrene.

Table **6.4**. Intermolecular parameters for the OFN complexes

Complex	6	α-7	8	9
Inter-component Interplanar Angle (°)	2.7	1.4	0.4	1.0
OFN Offset Angle (°)	9.0	4.6	2.7	1.5
Polyaromatic Offset Angle (°)	6.4	3.1	2.8	1.2
OFN Offset (Å)	1.07	0.59	0.32	0.18
Polyaromatic Offset (Å)	0.76	0.38	0.33	0.14
Intercomponent Centroid-Centroid Distance(s) (Å)	3.41	3.39	3.36	3.45 3.42
Mean Inter-component Interplanar Separation(s) (Å)	3.37	3.38	3.36	3.40 3.34

In complexes **1** and **2,** the stacks run parallel to the crystallographic [101] direction, whereas in **3** they are parallel to the *a*-axis. The stacks run parallel to the *a*-axis in complex **4** and parallel to the *b*-axis in **5**. The structures of all the HFB complexes with the exception of **5** are based on a laminar motif, where all equivalent molecules in every stack are parallel. The structure of complex **5** consists of alternating layers of stacks of parallel molecules, arranged in a pseudo-herringbone motif. The dihedral angles between equivalent molecules in adjacent layers are 44.7° for HFB and 46.8° for triphenylene. These angles are twice those of their respective offset angles. In all of the OFN complexes the molecules are stacked along the *a*-axis. In the structures of complexes **8** and **9**, all molecules of the same type are strictly parallel in every stack, so they have a laminar motif. However, this is not the case in the complexes **6** and α-**7**, in which the stacks are arranged in alternating layers made up of stacks with parallel axes, with the molecules in adjacent layers being inclined to one another in a pseudo-herringbone motif. In **6** the angle between the OFN molecules in adjacent layers is 7.8°, and that between analogous anthracene ones is 7.0°. In α-**7** the angles between adjacent OFN and phenanthrene molecules are 1.5° and 1.7° respectively. These angles are much smaller than those of the previously obtained structure of the OFN·naphthalene complex,[6] in which they are 34.5° for the OFN molecules and 31.5° for the naphthalenes. The laminar and herringbone motifs are clearly illustrated in the packing diagrams of all the complexes shown in the Figure **6.7**.
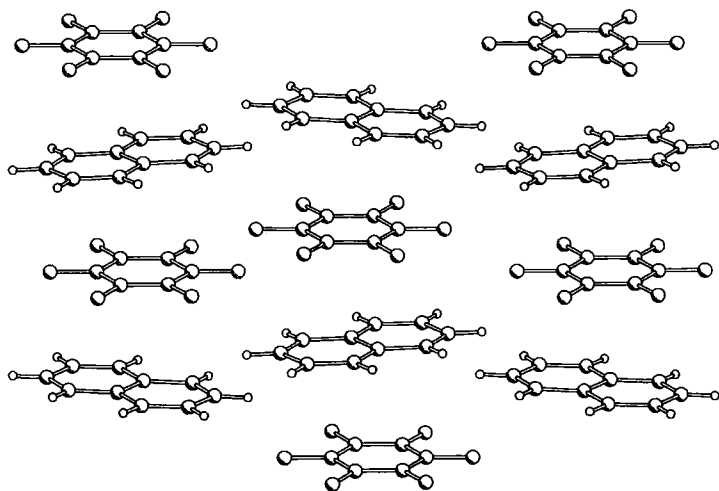
Figure **6.7**(a)   Packing diagram of HFB·naphthalene (**1**)
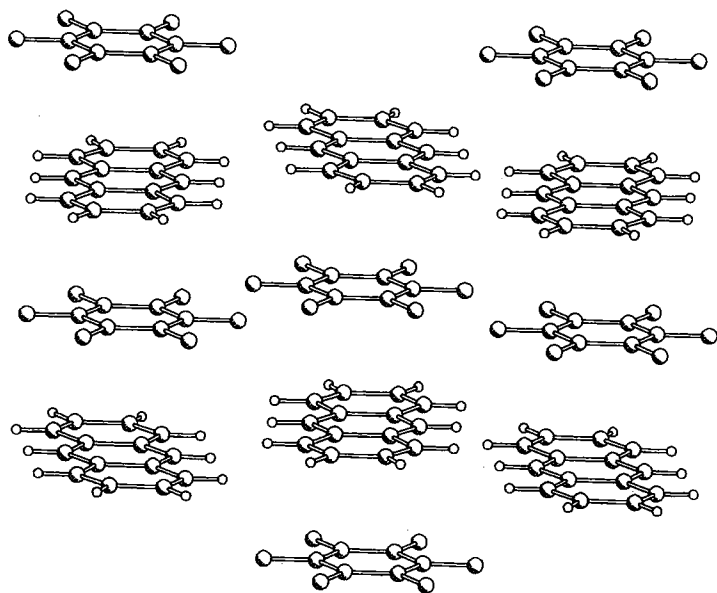
Figure **6.7**(b)   Packing diagram of HFB·anthracene (**2**)
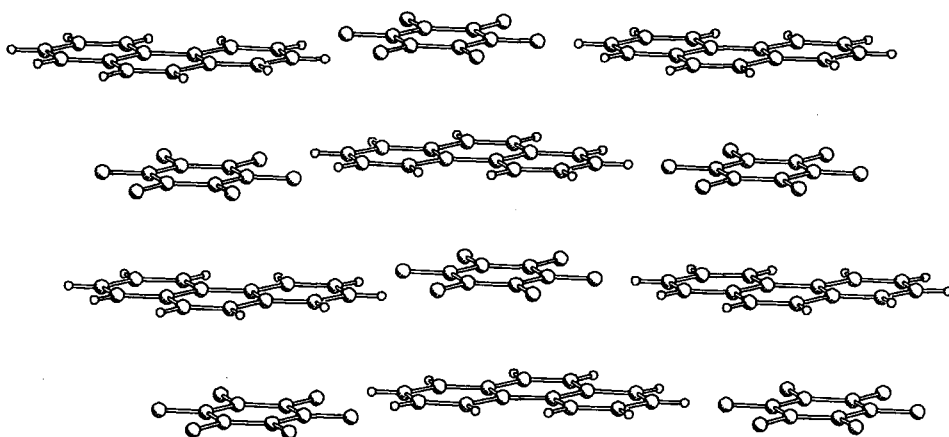
Figure **6.7**(c) Packing diagram of HFB·phenanthrene (**3**) (only one
orientation of disordered phenanthrene shown)
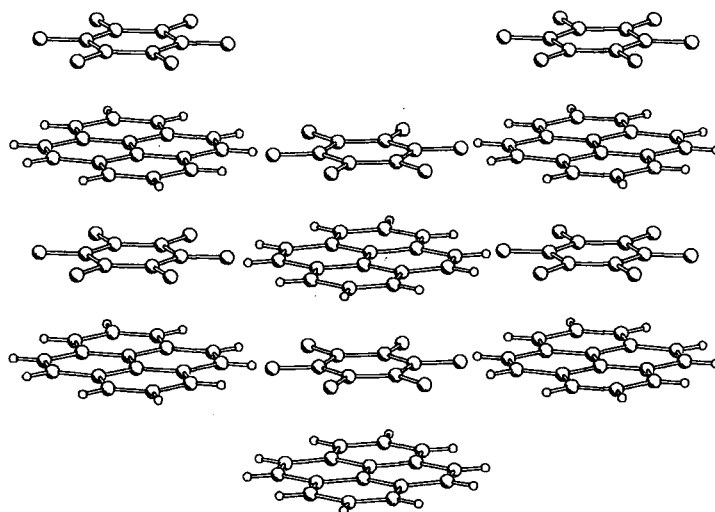
Figure **6.7**(d)   Packing diagram of HFB·pyrene (**4**)
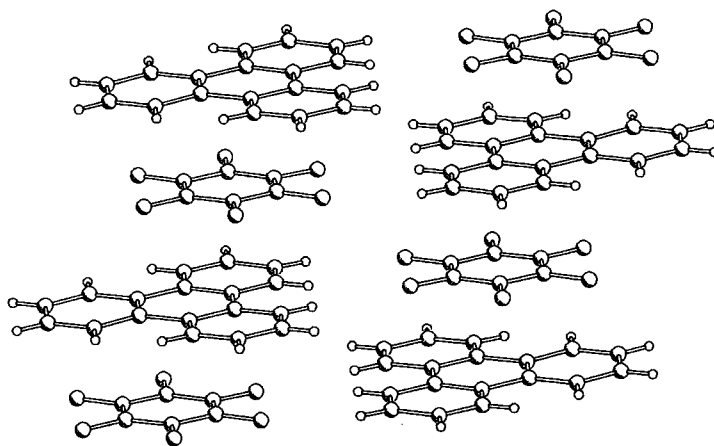
Figure **6.7**(e) Packing diagram of HFB·triphenylene (**5**)
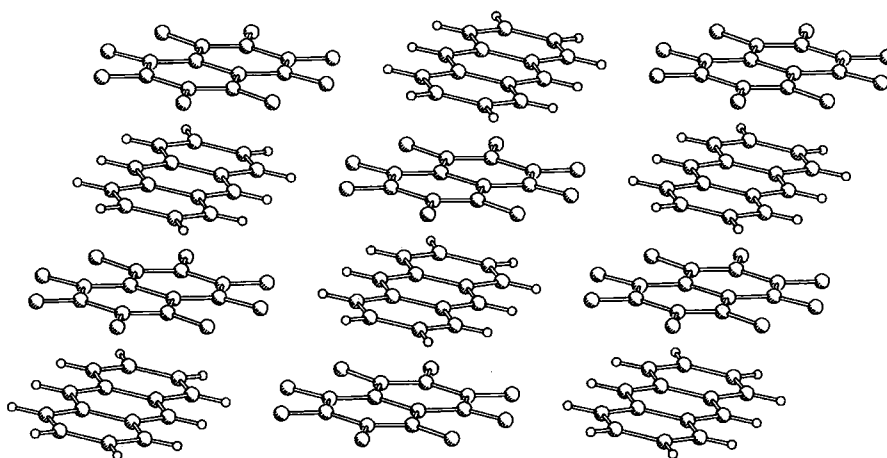
Figure **6.7**(f) Packing diagram of OFN·anthracene (**6**)
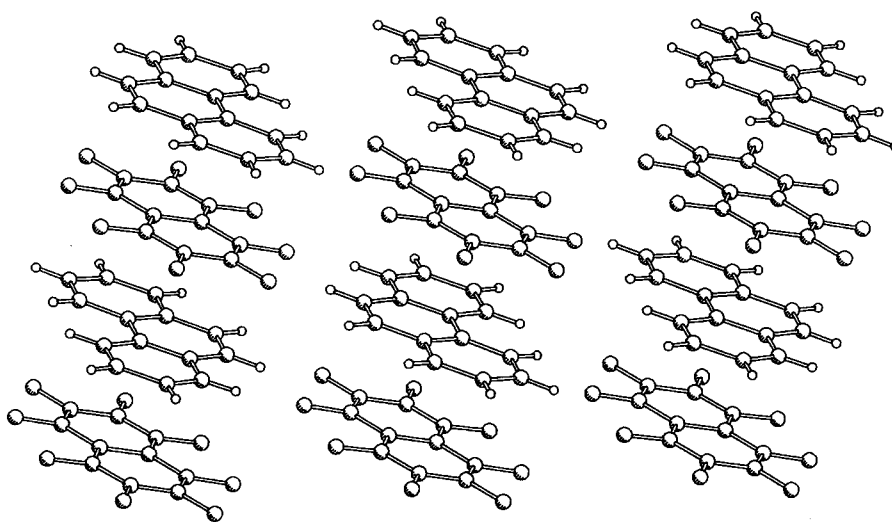
Figure **6.7**(g) Packing diagram of OFN·phenanthrene (**7**) (only one orientation
of phenanthrene is shown)
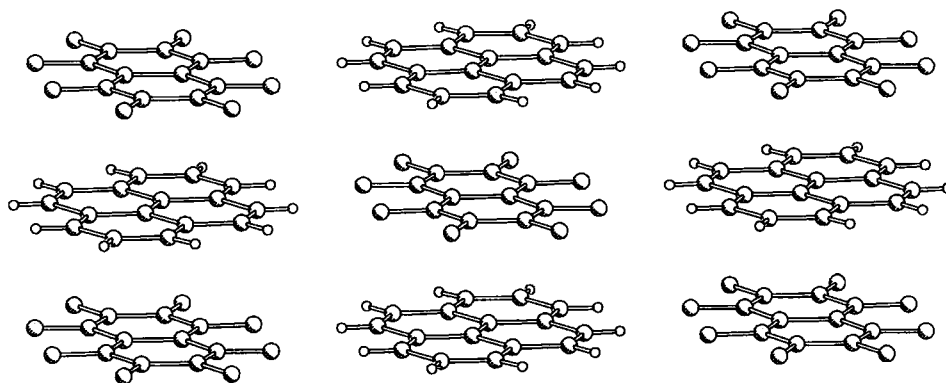
Figure **6.7**(h)   Packing diagram of OFN·pyrene (**8**)
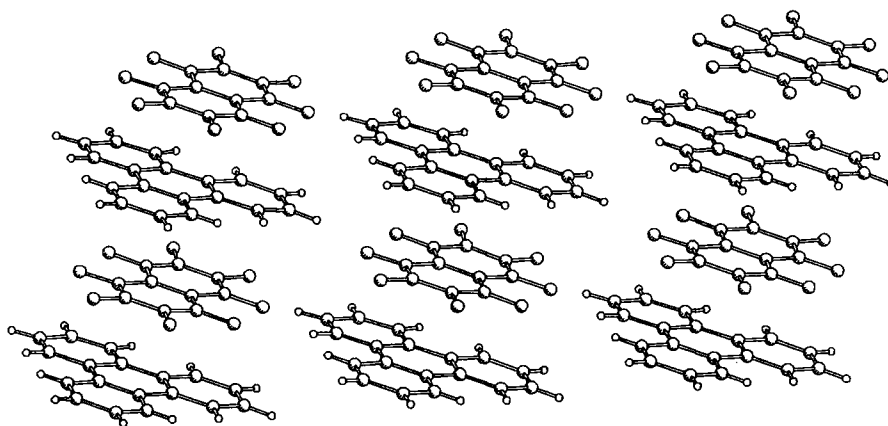
Figure **6.7**(i) Packing diagram of OFN·triphenylene **(9)**

6.2.4 Intermolecular Interactions

It is possible that arene-perfluoroarene face-to-face interactions may not be the only stabilizing force on the molecules. Intermolecular interactions between fluorine atoms and hydrogen atoms may have a role to play, and have been subject to much recent attention.[20] Such interactions were not judged to be hydrogen bonds, as their calculated energies were similar to those of van der Waals interactions.[21] However, a C–H bond may be more likely to form hydrogen bonds if it is more acidic in nature due to it being sp or sp^2 hybridised. A recent study of the packing of several fluorinated benzene derivatives, in which no other fluorinated molecules were present, concluded that the interaction was largely responsible for the packing of these molecules.[22]

All of the structures obtained contain some intermolecular C–H···F–C contacts which are closer than the sum of the van der Waals radii of the hydrogen and fluorine atoms (2.55 Å).[23] In all cases, the aromatic sp^2 C–H bond lengths have been corrected to the mean of those obtained from neutron diffraction data (1.08 Å).[24] Those intermolecular separations that are below the van der Waals radii are plotted graphically with their corresponding C–H···F angle in Figure **6.8**. The data points are very scattered and there appears to be no strong linear correlation of separation distance with angle. This is consistent with most of the close H···F contacts arising largely as a consequence of the electrostatic arene-perfluoroarene interactions.
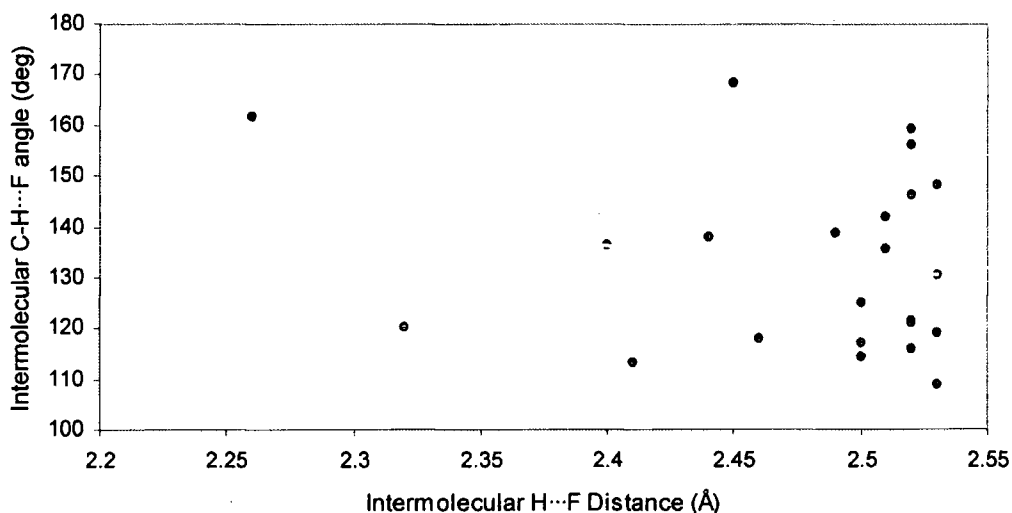
Figure **6.8**   Graph of Intermolecular C-H···F distances against C-H···F angles

6.2.5 The Stability of the Complexes

There are several indicators as to the stability of the complexes. The simplest of these are their melting points. Of the HFB complexes, only the melting point of complex **1** could be obtained, as the others were prone to loss of HFB from the crystal. Its melting point was 94-95 °C, which was slightly higher than that of naphthalene itself. The melting points of the OFN complexes, were found to be larger than those of each of the individual components, with the exception of complex **6**, which was found to be intermediate between the two. Complex **8** has an exceptionally high melting point. Another indication is the change in crystal density of the complex compared to the components. Generally speaking, there should be an increase in density upon complexation. However, this is not true for any of the OFN complexes. The melting points and changes in density of the OFN complexes are given in Table **6.5**.

The stability of binary molecular complexes has been linked to the degree of geometrical similarity between the component molecules. It has been suggested that a close congruity of molecular shapes is both the necessary and sufficient condition for the formation of binary complexes, at least in the absence of hydrogen bonding and large molecular dipoles.[25] A co-efficient of molecular similarity has been defined as ε:

$$\varepsilon \approx 1 - \frac{V_A - V_B}{V_{AB}}$$

where V_A is the calculated molecular volume of one component V_B is the volume of the other and V_{AB} is the combined volumes. It has been stated that formation of a complex is likely when this is greater than $\varepsilon = 0.85$ and impossible when less than $\varepsilon = 0.80$. Values of the co-efficient have been calculated for all the complexes, and are listed in Table **6.5**. Although most of

these values fall into the category for the formation of mixed crystals, complex **9** does not, having $\varepsilon = 0.75$.

Table **6.5**. Complex Stability Parameters for the OFN Complexes.

Complex [a]	m.p. (°C)	V_B (Å^3)	ε	V_{AB} (Å^3)	Δ
OFN·anthracene **6**	174-175	229 [b]	0.94	453.7	-0.022
OFN·phenanthrene α-**7**	172-174	236 [c]	0.91	461.1	-0.021
OFN·pyrene **8**	248-250	256 [b]	0.95	476.9	-0.014
OFN·triphenylene **9**	205-208	286 [b]	0.84	507.7	-0.016
OFN·naphthalene [d]	132	180.5	0.75	397.4 [d]	0.026

[a] For OFN, V = 215 Å^3 at 120 K, 227 Å^3 at room temperature. [b] Adjusted for 120 K. [c] No experimental data is available below 248 K; extrapolated to 120 K proportionally to anthracene. [d] Room temperature.

6.2.6 Theoretical Calculations

Ab initio calculations for the HFB complexes **1**, **2**, **4** and **5** have been performed by Dr Stuart Clark of the Department of Physics at the University of Durham. These calculations use the time-independent density functional theory (DFT) method in the generalised gradient approximation (GGA), which uses periodic boundary conditions to simulate the infinite lattice, and includes all interactions of the infinite system through the use of Bloch's theorem. The forces on the atoms and stresses on the unit cell were calculated by an *ab*

initio method using the Hellmann-Feynman theorem, which enabled a calculation of the atomic co-ordinates and the unit cell parameters. The unit cell parameters are given in Table **6.6**, and found to be very close to the experimental ones (within 1 %). The fact that this method describes van der Waals interactions poorly, indicates that the good agreement in the present case shows that the cohensive forces are predominantly of electrostatic, rather than van der Waals character.

Integration of the calculated electron charge density over each molecule in the unit cell, shows that both HFB and polyaromatic components are essentially neutral within the accuracy of the calculation, which indicates the absence of charge transfer. Estimates of the total electrostatic cohesion were made based on the charge density distribution for each component, rather than using partial atomic charges or multiple approximations. The resulting values were over 90 % of the total cohension energy. This is in contrast to results obtained for the HFB·benzene complex, which suggested that electrostatic component made up only 15 % of the total interaction energy.[26] However, their calculations were based on the DFT formalism using the doubtful assumption of fitting partial charges to the atoms, and various exchange-correlation potentials within the GGA. It was found that the interaction energy varied with the GGA used, which was attributed to van der Waals contribution. However, it has been found that this need not necessarily be the case, as much of the residual energy could be a manifestation of the functional form and its fitting to quantum Monte Carlo data.[27] Within DFT, the only reliable method of calculating van der Waals interactions is within the time-dependant formalism where the charge fluctuations are correctly calculated. The calculations in reference 26 were performed on isolated pairs of molecules rather than infinite lattices, and were not checked against experimental data.

Table 6.6 Calculated cell parameters and cohesive energies (E_c) of the HFB complexes

Complex	HFB·naphthalene 1	HFB·anthracene 2	HFB·pyrene 4	HFB·triphenylene 5
a (Å)	11.821	16.136	6.970	13.959
b (Å)	13.533	12.128	13.366	7.241
c (Å)	8.451	8.984	9.313	17.393
β (°)	97.94	117.19	105.99	92.66
E_c (eV)	0.287	0.304	0.327	0.341

6.3 Conclusions

It has been shown that both octafluoronaphthalene and hexafluorobenzene are able to form 1:1 complexes with the fused-ring polyaromatic molecules, naphthalene, anthracene, phenanthrene, pyrene and triphenylene, which have substantially different molecular geometries. The crystal structures of these complexes have been solved from X-ray diffraction data. In all cases, the crystal structures of the complexes are completely different to those of the components in their pure states. Specifically, the structures of the complexes comprise infinite stacks of alternating component molecules, in place of the herringbone arrangements, which are observed in the pure components. The cause of these stacking arrangements can be ascribed to arene-perfluoroarene interactions, and these results demonstrate the general applicability of the arene-perfluoroarene interaction in crystal engineering, and show it to be relatively insensitive to the morphology of the particular aromatic molecules concerned. Although several trends in intermolecular parameters have been observed for these complexes, it is clear that further experimental and theoretical studies on these complexes, and related ones, are required in order to understand fully these interactions.

Ab initio DFT calculations have been performed for the HFB complexes with naphthalene, anthracene, pyrene and triphenylene, and have resulted in very close matches to the experimental structures. The fact that these calculations model van der Waals forces means that show the interaction energy between the components must be predominantly electrostatic in nature, which is in contrast to an earlier calculation on the HFB·benzene complex which suggested that the interaction was predominantly van der Waals in nature.

6.4 Experimental

6.4.1 Crystal Growth and Characterisation

The polyaromatic hydrocarbons were obtained from Aldrich. **Caution**: Many polyaromatics are carcinogenic and should be handled accordingly. Octafluoronaphthalene was obtained from Bristol Organics. All components were analyzed by GC-MS and used without further purification. The OFN was found to contain traces of chloroheptafluoronapthalene. Elemental analyses were carried out in the Department using an Exeter Analytical Inc. Analyzer CE-440 Elemental Analyzer. Melting points were obtained using a Laboratory Devices Mel-Temp II equipped with a Fluke 51, digital thermometer, and are uncorrected.

Crystals of HFB·naphthalene (**1**), HFB·anthracene (**2**), HFB·phenanthrene (**3**), HFB·pyrene (**4**) and HFB·triphenylene (**5**) were obtained from the slow evaporation of a solution of the polyaromatic in 1-2 ml HFB over several weeks. The co-crystals of the napthalene, pyrene and triphenylene complexes were obtained as blocky needles, the complex with anthracene formed irregular blocks, whereas the complex with phenanthrene formed large planar blocks. The presence of both components was verified by GC-MS. Unfortunately, a melting point and elemental analysis could only be obtained for the complex **1** (94-95 °C), as in all the other complexes the HFB evaporated during heating. This was also found to occur when the complexes were left open to the atmosphere at room temperature, leaving an opaque polycrystalline residue of the polyaromatic.

Crystals of OFN·anthracene (**6**), OFN·phenanthrene (**7**), OFN·pyrene (**8**) and OFN·triphenylene (**9**) were obtained from the slow evaporation (over 1-3

days) of a 1:1 mole % solution containing of both components in 1-2 ml of dichloromethane. The crystals of complex **6** were obtained as large tetragonal blocks, whereas all of the others were obtained as fine needles. All of the crystals were colourless. The presence of both components in the crystals was verified by GC-MS and elemental analysis. The impurity in OFN did not appear in any of the co-crystals.

OFN·anthracene (**6**): m.p. 174-175 °C, Anal. Calc for $C_{24}H_{10}F_8$: C 64.01, H 2.24, Found: C 64.60, H 2.26.

OFN·phenathrene: (**7**) m.p. 172-174 °C, Anal. calc. for $C_{24}H_{10}F_8$: C 64.01, H 2.24, Found: C 63.88, H 2.17.

OFN·pyrene (**8**): m.p. 248-250 °C, Anal. calc. for $C_{26}H_{10}F_8$: C 65.83, H 2.12, Found: C 65.88, H 2.37.

 OFN·triphenylene (**9**): m.p. 205-208 °C, Anal. calc. for $C_{26}H_{12}F_8$: C 64.61, H 2.42, Found: C 64.21, H 2.37.

6.4.2 X-ray Diffraction and Structure Solution

The X-ray crystallographic data collection and structure solutions for all the complexes was performed by Dr. Andrei S. Batsanov of the Crystallography Service at the University of Durham, except for complex **4**, for which data was collected and the structure solved by Ms. Lorna Stimson. All X-ray diffraction experiments, with the exception of complex **2**, were carried out on Siemens SMART three-circle diffractometer equipped with a 1K CCD area detector, using graphite-monochromated Mo-K_α radiation. The data for **2** was obtained using a Rigaku AFC6S four-circle diffractometer using graphite-monochromated Cu-K_α radiation. The temperature of the crystals was maintained by an Oxford Cryosystems open-flow nitrogen gas cryostat.[28] The

temperature was calibrated on the phase transition of K_2HPO_4 at 122.5 K,[29] the possible error not exceeding ±2 K. For each sample, a hemisphere of reciprocal space was covered by a combination of four (three for **7**) sets of ω-scans, each at different φ and/or 2θ angles. Reflection intensities were integrated using SAINT software.[30] For complex **4**, these intensities were corrected for absorption (mainly by glass) by semi-empirical method on Laue equivalents.[31] For **2** the data were processed using TEXSAN software.[32] An empirical (on φ-scans) absorption correction was insignificant (T_{min} / T_{max} = 0.89). Crystals of **5** grew as non-merohedral twins related by a 180° rotation around the c^* axis. Their diffraction patterns were deconvoluted and the twinning corrections made, using the GEMINI program.[33] However, the precision of the results is rather low due to a large number of partially overlapping reflections.

The structures were solved by direct methods, and refined by full-matrix least squares on F^2 of all data, using SHELXTL software.[34] All C and F atoms were refined in anisotropic (isotropic for the minor position of the disordered phenanthrene molecule in **3**) approximation, H atoms in isotropic approximation, except for the disordered phenanthrene molecules in **3** and **7**, and in **5**, where they were treating as 'riding'. Thermal motion analysis and bond length correction were made using PLATTON-99 programs.[35]

6.4.3 Theoretical Calculations (performed by Dr Stuart Clarke)

Ab initio psuedopotential calculations within the density functional formalism were performed using the CASTEP code and taking the experimental structure as the starting point.[36] For a given configuration of the unit cell,

expansion of the valence electronic wavefunction in a basis set of plane waves up to an energy cut-off of 400 eV, converged the total energy of the system to better than 1 MeV / cell. The core electrons were described using the psuedopotential approach. The Vanderbilt form for non-local ultrasoft psuedopotentials was used.[37] The Brillouin zone integrations were performed using a k-point set which converged the total energy of the system to less than 1 MeV / cell. The generalised gradient approximation (GGA) was used for the exchange and correlation interactions,[38] as it is generally more accurate at describing molecular systems than convential local density approximation.[39] The total energy of the system was calculated using a preconditioned gradients method.

6.5 References

1. C. R. Patrick and G. S. Prosser, *Nature*, 1960, **187**, 1021.

2. a) E. McLaughlin and C. E. Messer, *J. Chem. Soc. A*, 1966, 1106; b) G. Griffith, P. R. Jackson, E. Kenyon-Blair and K. W. Morcom, *J. Chem. Thermodynamics*, 1983, **15**, 1001.

3. S. Miyagishi, A. Isomi, M. Iwata, T. Asakawa and M. Nishida, *Bull. Soc. Chem. Jpn.*, 1985, **58**, 3643.

4. L. C. T. Shoute and J. P. Mittal, *Proc. Indian Natn. Sci. Acad. Sect. A*, 1988, **54**, 808.

5. A. Misra, R. Dutta, M. Halder and M. Chowdhury, *Chem. Phys. Lett.*, 1997, **281**, 254.

6. J. Potenza and D. Matropaolo, *Acta Crystallogr. Sect B.*, 1975, **31**, 2527.

7. a) F. P. Chen and P. N. Prasad, *J. Chem. Phys.*, 1977, **66**, 4341; b) F. P. Chen, and P. N. Prasad, *Chem. Phys. Lett.*, 1977, **47**, 341; c) S. Degreniers, G. A. Kourouklis, A. Jayaraman, M. L. Kaplan and P. H. Schmidt, *J. Chem. Phys.*, 1985, **83**, 480.

8. K. S. Law and P.N. Prasad, *Chem. Phys. Lett.*, 1978, **59**, 105.

9. a) P. N. Prasad, K. S. Law, J. C. Bellows and A. H. Francis, *J. Luminescence*, 1979, **18/19**, 51; b) F. P. Chen and P. N. Prasad, *Chem. Phys. Lett.*, 1978, **72**, 285.

10. M. Weck, A. R. Dunn, K. Matsumoto, G. W. Coates, E. B. Lobkovsky and R. H. Grubbs, *Angew. Chem. Int. Ed. Engl.*, 1999, **38**, 2741.

11. L. I. Foss, A. Syed and E. D. Stevens, *Acta Crystallogr. Sect C*, 1984, **40**, 272.

12. U. H. F. Bunz and V. Enkelmann, *Chem. Eur. J.*, 1999, **5**, 263.

13. a) J. Burdenuic, R. H. Crabtree, A. L. Rheingold and G. P. A. Yap, *Bull. Chim. Soc. Fr.*, 1997, **134**, 955; b) C. M. Beck, J. Buedenuic, R. H. Crabtree, A. L. Rheingold, G .P. A. Yap, *Inorg. Chim. Acta*, 1998, **270**, 559.

14. J. C. A. Boeyens and F. H. Herbstein, *J. Phys. Chem.*, 1965, **69**, 2153.

15. a) H. Tsuchiya, F. Marumo and Y. Saito, *Acta Crystallogr.*, *Sect. B*, 1972, **28**, 1935; b) D. Wright, K. Yakushi and H. Kuruda, *Acta Crystallogr.*, *Sect. B*, 1978, **34**, 1934.

16. V. Pericek, I. Cisarova, L. Hummel, J. Kroupa and B. Brezina, *Acta Crystallogr.*, *Sect. B*, 1990, **46**, 830.

17. a) C. P. Brock and J. D. Dunitz, *Acta Crystallogr.*, *Sect. B*, 1990, **46**, 795; b) Y. Kai, F. Hama, N. Yasuoka and N. Kasai, *Acta Crystallogr.*, *Sect. B*, 1978, **34**, 1263; c) C. P. Brock and J. D. Dunitz, *Acta Crystallogr.*, *Sect. B*, 1982, **38**, 2218.

18.   A. S. Batsanov and J. C. Collings, *Acta Crystallogr., Sect B*, in press.

19.   a) G. R. Desiraju and A. Gavezzotti, *Acta Crystallogr., Sect. B*, 1989, **45**, 473; b) G. R. Desiraju and A. Gavezzotti, *J. Chem. Soc., Chem. Commun.*, 1989, 621.

20.   L. Shimoni and J. P. Glusker, *Struct. Chem.*, 1994, **5**, 383.

21.   J. A. K. Howard, V. J. Hoy, D. O'Hagan and G. T. Smith, *Tetrahedron*, 1996, **52**, 12613.

22.   V. R. Thalladi, H.-C. Weiss, D. Blaser, R. Boese, A. Nangia and G. R. Desiraju, *J. Am. Chem. Soc.*, 1998, **120**, 8702.

23.   R. S. Rowland and R. Taylor, *J. Phys. Chem.*, 1996, **100**, 7384.

24.   F. H. Allen, O. Kennard, D. G. Watson, L. Brammer, A. G. Orpen and R. J. Taylor, *J. Chem. Soc., Perkin Trans. 2*, 1987, S1.

25.   A. I. Kitaigorodskii, *Mixed Crystals*, Springer-Verlag, Berlin, 1984.

26.   S. Lorenzo, G. R. Lewis and I. Dance, *New J. Chem.*, 2000, **24**, 295.

27.   N. Kurita and H. Sekino, *Chem. Phys. Lett.*, 2001, **384**, 139.

28.   J. Cosier and A. M. Glazer, *J. Appl. Crystallogr.*, 1986, **19**, 105.

29.   R. J. Nelmes, G. M. Meyer and J. E. Tiballis, *J. Phys. C: Solid State Phys.*, 1982, **15**, 59.

30.   *SAINT*, version 6.01, Bruker AXS, Madison, Wisconsin, USA, 1999.

31.   G. M. Sheldrick, *SADABS*, University of Gottingen, Germany, 1998.

32.   *TEXSAN*, version 5.1, MSC, The Woodlands, Texas, USA, 1989.

33.   *GEMINI*, version 1.0, Bruker AXS, Madison, Wisconsin, USA, 1999-2000.

34.   *SHELXTL, An integrated system for solving refining and displaying crystal structures from diffraction data, ver. 5.10*, Bruker Analytical X-ray Systems, Madison, Wisconsin, USA, 1997.

35.   A. L. Speck, *PLATTON-99, A multipurpose tool,* University of Utrecht, The Netherlands, 1980-1999.

36.   CASTEP ver 4.2, Academic version licensed under the UKCP-MSI Agreement, 1999; M. C. Payne, M. P. Teter, D. C. Allan, T. A. Arias and J. D. Joannopolous, *Rev. Mod. Phys.*, 1992, **64**, 1045.

37.   D. Vanderbilt, *Phys. Rev.*, 1990, **B41**, 7892.

38.   J. P. Perdew, *Electronic Structure of Solids*, 1991, eds. P. Ziesche and H. Eschrig, Academie Verlag, Berlin, 1991; J. P. Perdew, J. A. Chevary, S. H. Vosko, K. A. Jackson, M .R. Pederson, D. J. Singh and C. Fiolhais, 1992, **B46**, 6671.

39.   J. P. Perdew and A. Zunger, *Phys. Rev.*, 1981, **B23**, 5048.

Chapter Seven

The Synthesis and Optical Properties of a Series of 4,4'-bis(Phenylethynyl)tolan Oligomers Containing Fluorinated and Non-fluorinated Phenyl Rings

7.1 Introduction

Over recent years our group has been involved in the synthesis of many 1,4-bis(phenylethynyl)benzene (BPEB) derivatives via homogeneous palladium-catalyzed cross-coupling.[1] We have been particularly interested in studying some of the physical properties of these molecules, particularly their optical, structural and liquid crystalline properties. Many of these molecules are highly photo-luminescent, exhibiting large quantum yields. This is due largely to the rigid nature of the conjugated orbitals of the molecules, which hinder the decay of the excited state by alternative means. Although, most BPEB derivatives luminesce in the UV-region, the derivatives of bis(phenylethynyl)anthracene (BPEA) emit in the visible region, and find application as laser dyes, scintillation agents and fluorescers in chemi-luminescent devices such as light sticks.[2]

Many of the molecules show thermotropic liquid crystalline phases. Calamitic mesogens typically consist of a rigid core (which can be a tolan or BPEB unit) and a flexible moiety.[3] However, it has been shown that a flexible moiety is not necessary for the formation of liquid crystal phases. Instead, the axial ratio of a rigid molecule, which is the ratio of its length to diameter, has to be above a certain length to permit the formation of mesophases. This is due to the hard interactions between the molecules. It has recently been demonstrated by Dr C. Viney that the critical axial ratio for nematic phase formation in phenylene-ethynylene molecules is 4.3.[4] It transpires that the axial ratio of the unsubstituted BPEB is large enough to display a nematic phase, and this has been observed experimentally. Many BPEB derivatives also show additional smectic phases with limited positional ordering.

Recently, the group has begun the synthesis of several 1,4-bis(phenylethynyl)benzene (BPEB) derivatives containing perfluorinated and non-fluorinated phenyl rings.[5] The fluorine atom combines the attributes of large electro-negativity with small size, and so it is expected to significantly modify the properties of such molecules. Fluorinated mesogens are often used in liquid crystals to enhance the stability ranges of the liquid crystal phases.[6] The unsubstituted BPEB derivatives 1,4-bis(phenylethynyl)-tetrafluorobenzene, 1,4-(pentafluorophenylethynyl)benzene and 1,4-(pentafluorophenylethynyl)tetrafluorobenzene are shown in Figure **7.1**. Their crystal structures have been solved from X-ray diffraction data. Although the molecular packings of 1,4-bis(phenylethynyl)tetrafluorobenzene and 1,4-bis(pentafluorophenylethynyl)benzene do not show any arene-perfluoroarene stacking motifs, when the two compounds are mixed in a 1:1 ratio a complex is produced which does exhibit arene-perfluoroarene stacking.[7] The packing is shown in Figure **7.2**. Interestingly this complex also shows liquid crystal

phase behaviour that is not present in either of the components. Although the melting point is depressed, as is expected in mixtures, the clearing point is elevated compared to the components. This suggests that the arene-perfluoroarene interaction has a role to play in stabilizing the liquid crystalline phase as well as the solid-state phase, and that possibly the mesogens in the liquid crystal are formed from two or more molecules linked by arene-perfluoroarene stacking.
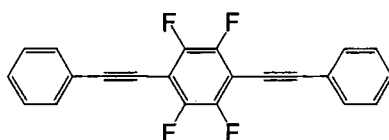
1,4-bis(phenylethynyl)tetrafluorobenzene
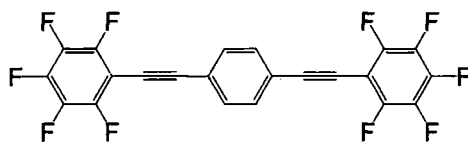
1,4-bis(pentafluorophenylethynyl)benzene
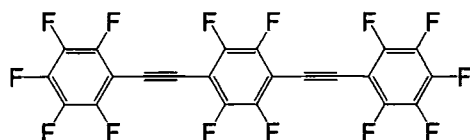
1,4-bis(pentafluorophenylethynyl)tetrafluorobenzene

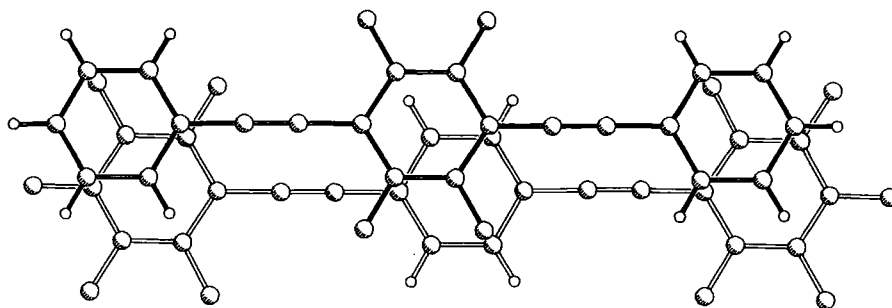Figure **7.1**   Some selectively fluorinated BPEB derivatives

Figure **7.2** Molecular structure of the 1:1 complex of 1,4-bis(phenylethynyl)-
tetrafluorobenzene and 1,4-bis(pentafluorophenylethynyl)benzene

Attempts to grow a crystal of a 1:1 complex between 1,4-
bis(phenylethynyl)benzene and 1,4-bis(pentafluorophenylethynyl)tetrafluoro-
benzene proved problematic. However, a crystal was eventually obtained
from the slow cooling of an equimolar solution of both components in THF.
The crystal structure was solved from X-ray diffraction data and shown to be
of 2:1 1,4-bis(phenylethynyl)benzene : 1,4-bis(pentafluorophenylethynyl)-
tetrafluorobenzene stoichiometry. The molecular packing is made up of
trimers consisting of a 1,4-bis(pentafluorophenylethynyl)tetrafluorobenzene
molecule sandwiched between two approximately parallel 1,4-
bis(phenylethynyl)benzene molecules. These trimers pack in two almost
orthogonal directions. This packing is illustrated in Figure **7.3**. This complex
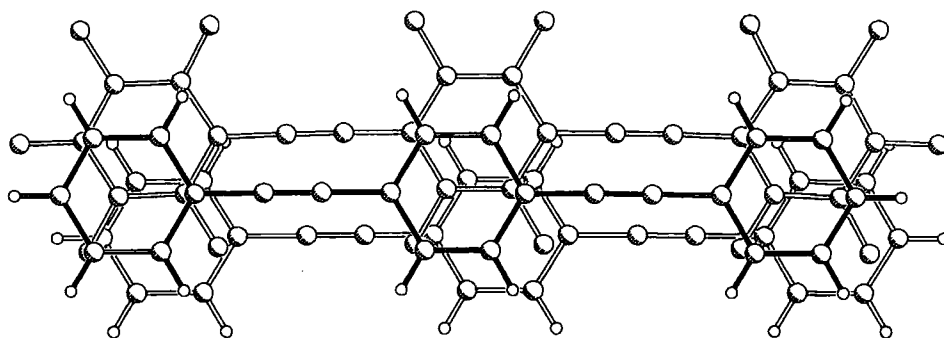represents the first example of a 2:1 arene-perfluoroarene complex.

Figure **7.3**(a) Molecular structure of the trimer of the 2:1 complex of BPEB and 1,4- bis(pentafluorophenylethynyl)tetrafluorobenzene
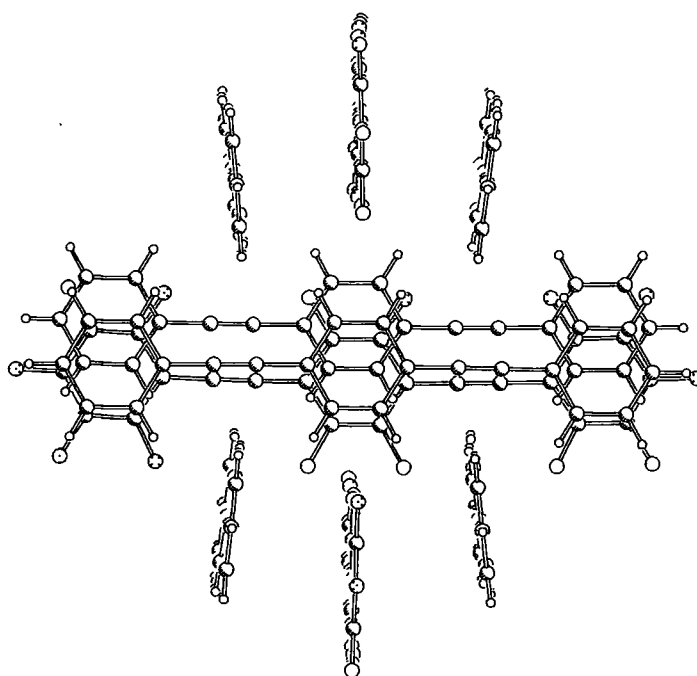

Figure **7.3**(b) Molecular packing of the 2:1 complex of BPEB and 1,4-bis(pentafluorophenylethynyl)tetrafluorobenzene

We are currently in the process of growing crystals of many selectively fluorinated BPEB derivatives and their complexes, with various substituents at the terminal positions, such as methoxy and trifluoromethyl, and then solving their crystal structures from X-ray diffraction data, with the aim of finding out more about the arene-perfluoroarene interaction in their structures. All of the structures obtained thus far belong to one of three structural motifs, some of which show arene-perfluoroarene stacking, and some that do not.[8]

Very recently, there has been a report of the synthesis of 4,4'-bis(pentafluorostyryl)stilbene.[9] Its crystal structure was solved from X-ray diffraction data, and show the molecules to pack in brickwall motif, involving arene-perfluoroarene stacking, as shown in Figure **7.4**. In the solid state, the compound forms a J-aggregate, which is characterised by an intense and narrow absorption band that is red-shifted with respect to the isolated molecule, arising as a result of coherent excitonic coupling between the molecules.
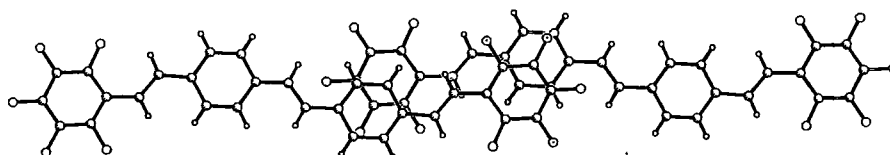

Figure **7.4**(a) Molecular packing of 4,4'-bis(pentafluorostyryl)stilbene viewed perpendicular to the mean plane of the molecules
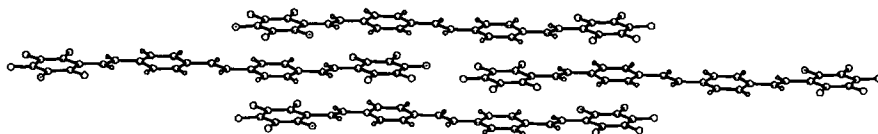
Figure **7.4**(b) Molecular packing of 4,4'-bis(pentafluorostyryl)stilbene showing the brickwall motif

Linear phenylene-ethynylene compounds containing four phenyl rings separated by carbon-carbon triple bonds are are referred to here as 4,4'-bis(phenylethynyl)tolans (BPETs). It was decided to attempt the synthesis of a complete series of unsubstituted BPETs, containing both perfluorinated and non-fluorinated phenyl rings. There are ten members of such a series, none of which are currently known, and which are numbered **1-10** in Figure **7.5**. Once the compounds have been fully characterised, we will be interested in the effect of the particular fluorination pattern upon the optical properties, solid-state properties, and liquid crystal phase behaviour of the compounds

Figure **7.5** The ten combinations of BPETs containing perfluorinated and non-fluorinated rings.

7.2 Results and Discussion

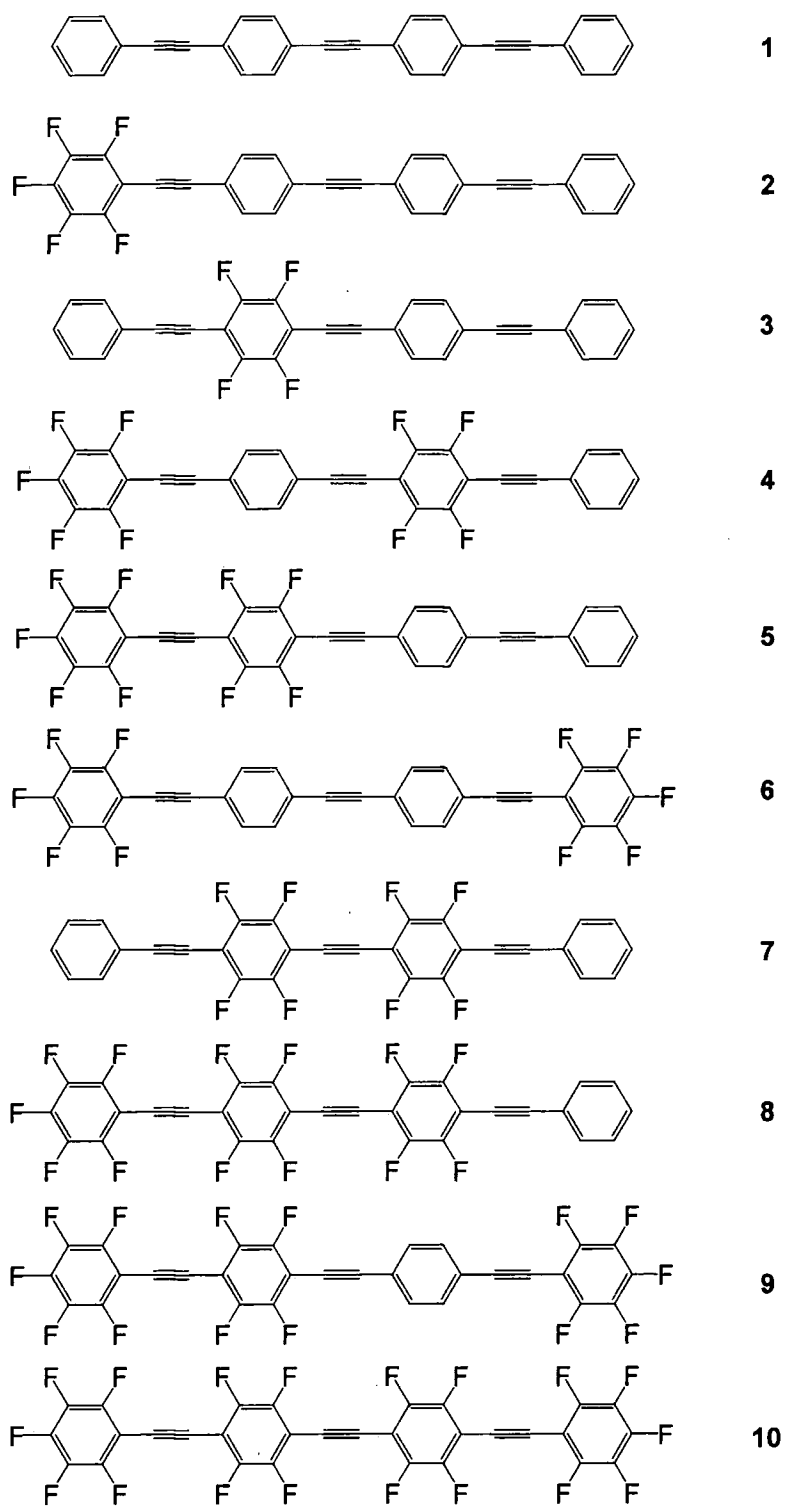### 7.2.1 Synthetic Strategy

It was decided to attempt to the synthesis of all of the BPETs from tolan-based precursors. This involves the coupling of a 1-halogeno-4-(phenylethynyl)benzene derivative with a 1-ethynyl-4-(phenylethynyl)benzene derivative using a palladium-catalyzed cross-coupling approach, based on the Sonogashira reaction.[10] Wherever possible iodo-derivatives were used, even though they are more expensive than aryl bromides, to ensure high yields under mild conditions. The catalyst system used was composed 1 mol % each of bis(triphenylphosphine)palladium(II) dichloride and copper iodide. A slight excess of the terminal alkyne was used in order to compensate for that consumed in the catalyst initiation step, which involves oxidative dimerisation of alkyne as a means to reduce Pd(II) to Pd(0). All reactions were performed in dried amines, with triethylamine being used in preference to diisopropylamine for all reactions involving reagents with a pentafluorophenyl group, in order to avoid possible nucleophilic substitution at the para position by a secondary amine.[11] The progress of the reactions was montitored by GC-MS. This could also detect the formation of any side-products. In most cases, trace quantities of butadiynes were observed, consistent with those amounts expected from the catalyst initiation step.

The preparation of several of the 1-halogeno-4-(phenylethynyl)benzene precursors has been reported in Chapter 5. Those which have not been, are reported in this chapter. These can be prepared via an analogous approach to those in Chapter 5, involving the coupling of a phenylacetylene with a large excess of a 1,4-diiodobenzene. The compound 1-iodo-4-(phenylethynyl)-benzene **11**, has been made this way previously.[12] However, 1-iodo-4-

(pentafluorophenylethynyl)tetrafluorobenzene **12** is a new compound. It was prepared by coupling pentafluorophenylacetylene to an excess of 1,4-diiodotetrafluorobenzene. As with the analogous preparation of 1-iodo-4-(pentafluorophenylethynyl)benzene, it was found that only a low yield of the desired product could be obtained, the major product being the 1,4-bis(pentafluorophenylethynyl)tetrafluorobenzene, even though an excess of the diiodotetrafluorobenzene was used. This was again attributed to the fact that the pentafluorophenylethynyl group is an electron-withdrawing activating group, which makes the product more susceptible to further coupling, compared to the diiodotetrafluorobenzene starting material. The synthesis of these precursors is shown in Scheme **7.1**
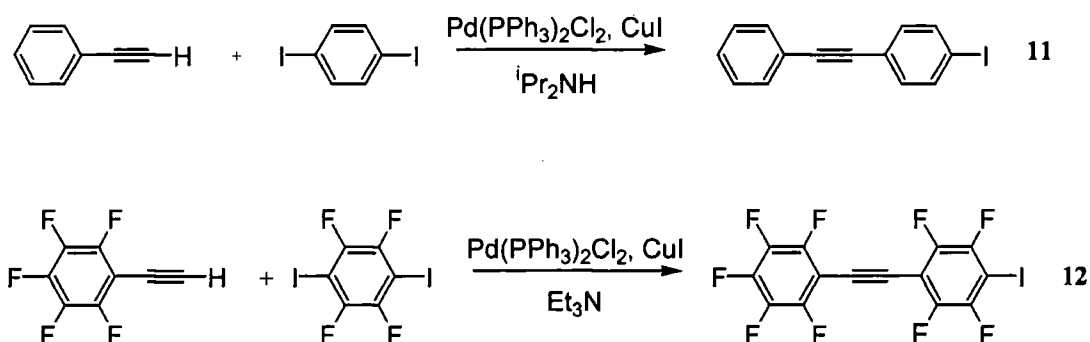
Scheme **7.1**   Synthesis of 1-halogeno-4-(phenylethynyl)benzene derivatives.

It was thought that the 1-ethynyl-4-(phenylethynyl)benzenes could be synthesized in an analogous manner, coupling an iodobenzene derivative with an excess of a 1,4-diethynylbenzene. However, only the parent compound 1-ethynyl-4-(phenylethynyl)benzene could be synthesized in this way. The other reactions resulted either in black, intractable residues, or products that could not be separated from the BPEB derivative side-products either by re-crystallisation or column chromatography. Instead, it was decided that

alternative methods be sought to make these precursors. The method favoured was to synthesize the trimethylsilyl derivatives of these compounds, by coupling trimethylsilylacetylene (TMSA) onto the appropriate 1-halogeno-4-(phenylethynyl)benzene derivative as shown in Scheme **7.2**. Several such derivatives, including 1-trimethylsilylethynyl-4-(phenylethynyl)benzene, have been synthesized previously, using similar methods.[13] Although this could be achieved easily for the coupling of TMSA to 1-iodo-4-(phenylethynyl)benzene to afford 1-trimethylsilylethynyl-4-(phenylethynyl)-benzene **13**, and even to 1-bromo-4-(pentafluorophenylethynyl)benzene to give 1-trimethylsilylethynyl-4-(pentafluorophenylethynyl)benzene **14**, using the more active bis(benzonitrile)palladium(II) dichoride / tri(t-butyl)phosphine based catalyst system, it proved problematic for the reaction of TMSA with 1-iodo-4-(phenylethynyl)tetrafluorobenzene. The product 1-trimethylsilylethynyl-4-(phenylethynyl)tetrafluorobenzene **15** could only be obtained in very low yields, as a mixture with the hydrodehalogenation product, 1-(phenylethynyl)-2,3,5,6-tetrafluorobenzene after prolonged reflux, using either catalyst system. Hydrodehalogenation has been observed previously in these cross couplings, and seems to be particularly prevalent for highly fluorinated aryl halides, although usually only aryl bromides.[14] It is also unusual in view of the fact that the same reagent couples readily with phenylacetylene at room temperature to yield 1,4-bis(phenylethynyl)tetrafluorobenzene.
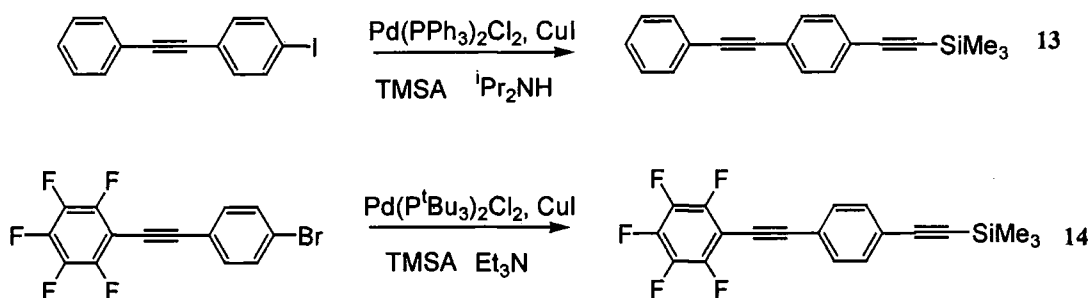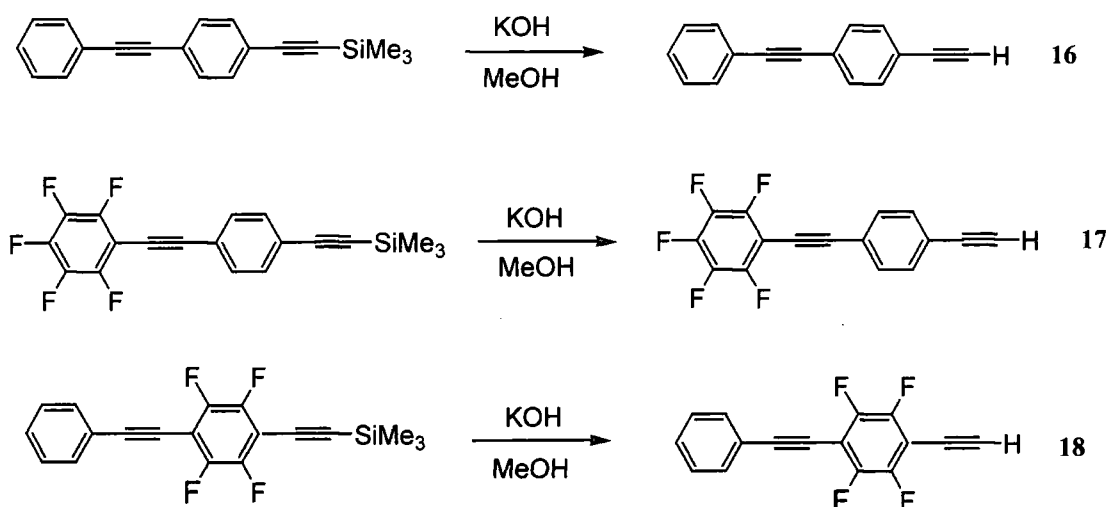

Scheme **7.2** Synthesis of the 1-trimethylsilylethynyl-4-(phenylethynyl)benzenes

Organolithium reagents are known to perform aromatic nucleophilic substitutions of highly fluorinated aromatics, especially at the para position of those activated by electron-withdrawing groups, of which the phenylethynyl group is an example. It was therefore be possible to make the desired trimethylsilyl precursor from the reaction of lithium trimethylsilylacetylide with (phenylethynyl)pentafluorobenzene, which is available in high yields from the palladium catalysed cross-coupling of iodopentafluorobenzene and phenylacetylene.[16] A similar procedure has been used to afford 1,4-bis(triethylsilylethynyl)tetrafluorobenzene.[17] The reaction gave an acceptable yield, and is shown in Scheme 7.3.
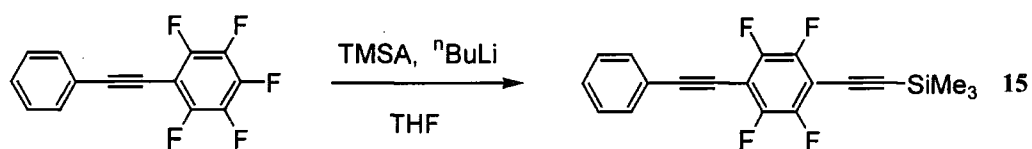
Scheme 7.3. The synthesis of 1-trimethylsilylethynyl-4-(phenylethynyl)-tetrafluorobenzene

1-ethynyl-4-(phenyl-ethynyl)benzene 16 has been prepared from hydrodesilation of 1-trimethylsilylethynyl-4-(phenylethynyl)benzene 13, using catalytic amounts (10 mol %) of potassium hydroxide in methanol / diethyl ether solution at room temperature.[13] Similar methods can be used to prepare 1-ethynyl-4-(pentafluorophenylethynyl)benzene 17, and 1-ethynyl-4-(phenyl-ethynyl)tetrafluorobenzene 18 from their respective 1-trimethyl-silylethynyl-4-(phenylethynyl)benzene derivatives, as shown in Scheme 7.4. However, care had to be taken in the hydrodesilation of 1-trimethylsilylethynyl-4-(pentafluoro-phenylethynyl)benzene to prevent nucleophilic attack at the para position of the pentafluorophenyl ring by a methoxide group.

Scheme **7.4** Hydrodesilations of the 1-trimethylsilylethynyl-4-
(phenylethynyl)benzenes

The coupling of the 1-halogeno-4-(phenylethynyl)benzene derivatives to the 1-ethynyl-4-(phenylethynyl)benzene derivatives to make the BPET compounds can be achieved by homogeneous palladium-catalyzed cross-coupling in an amine solvent. Compounds **1**, **2**, **3**, **4**, **6** and **7** were synthesized in this way as is illustrated in Scheme **7.5**. These reactions were generally achieved at room temperature then with slight heating The products were generally insoluble in the amine and precipitated along with the amine salt. They are also insoluble in most organic solvents, except hot toluene, which was used to extract them. Hot toluene was also used as an eluent when the products were passed down silica columns to remove the catalyst residues. Interestingly, the product tended to remain in solution when the toluene was allowed to cool, but could be precipitated by the addition of hexane, to give analytically pure samples. The yields were acceptable, but there were significant differences in yield. All of the BPETs were characterised by ^{1}H and ^{19}F NMR and mass spectrometry..

Pd(PPh$_3$)$_2$Cl$_2$, CuI

^{i}Pr$_2$NH

Pd(PPh$_3$)$_2$Cl$_2$, CuI

Et$_3$N

F F F F F F

Pd(PPh$_3$)$_2$Cl$_2$ CuI

^{i}Pr$_2$NH

Pd(PPh$_3$)$_2$Cl$_2$ CuI

Et$_3$N
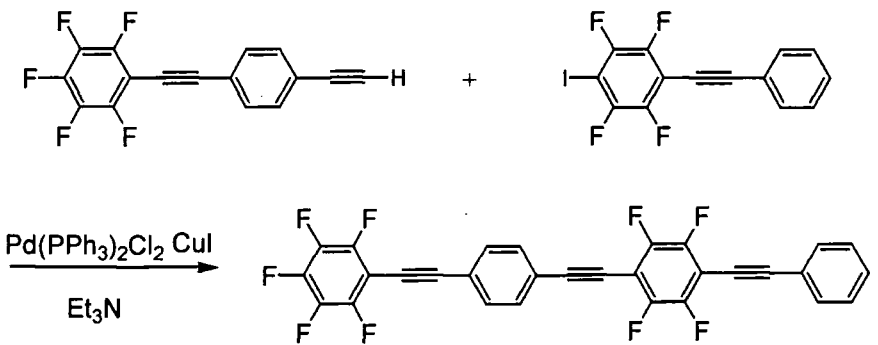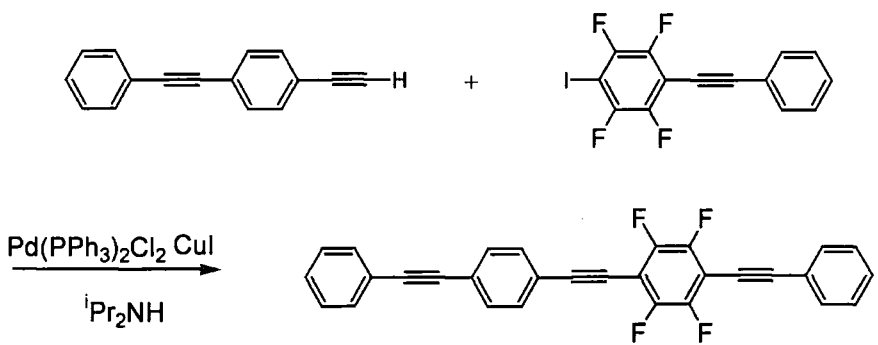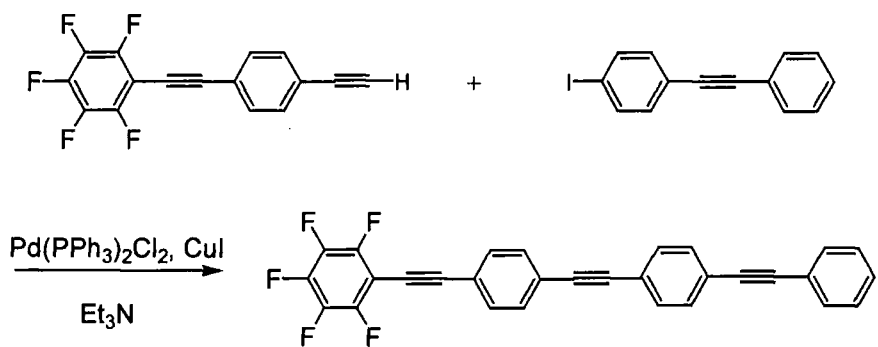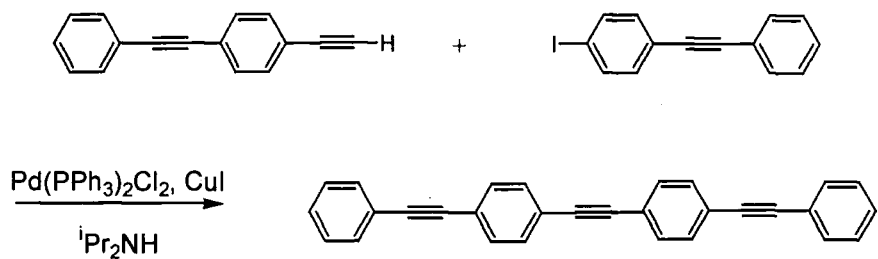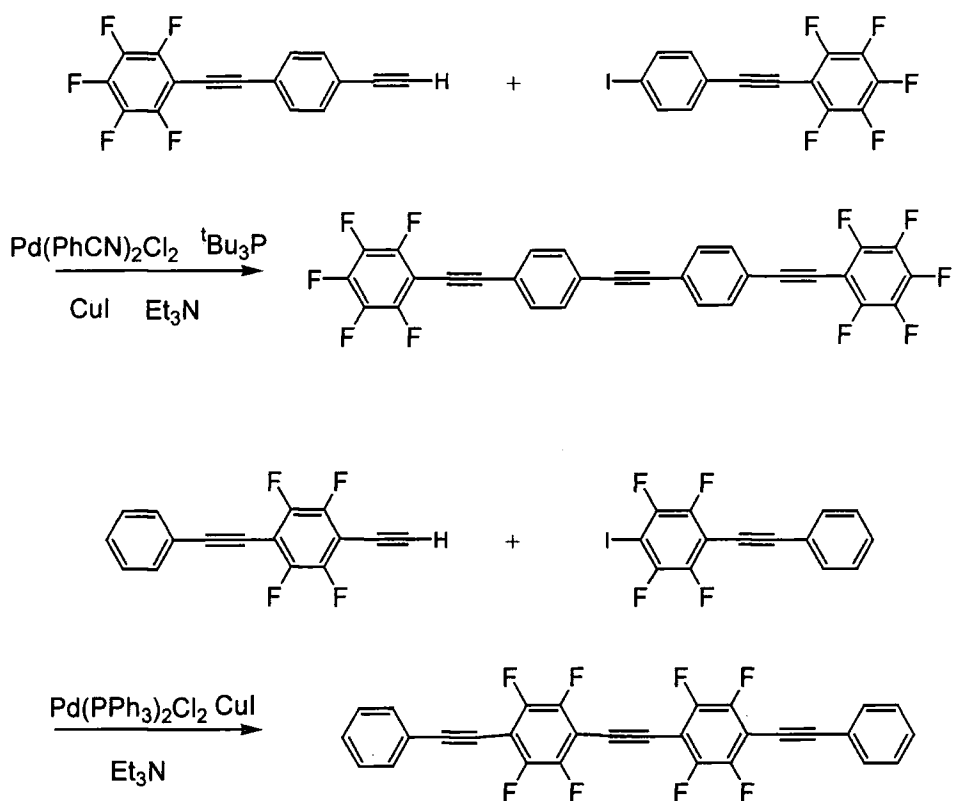
Scheme **7.5** The Synthesis of the BPETs **1**, **2**, **3**, **4**, **6** and **7**

The synthesis of compounds **5**, **8** and **9** was attempted in a similar manner, however the products obtained were not analytically pure. Further analysis of the samples revealed the presence of peaks associated with the butadiyne derivative arising from homo coupling of the terminal alkyne.

7.2.2 Absorption and Fluoresence Studies

The BPET compounds all have strong absorptions in the near UV region. The absorption maxima vary slightly in the range 336 - 342 nm. These values are directly comparable to the BPEB analogues which have maxima in the range 336–340 nm. Their extinction co-efficients are of the order 10^6 dm^2 mol^{-1}. This is an order of magnitude larger than those of the BPEB analogues. The compounds are also observed to fluoresce, when excited near their absoption maxima, even at very low concentrations of the order of 10^{-6} M. The emission maxima are in the blue region of the spectrum in the range 372–420 nm. There appears to be no obvious correlation between the absoprtion and emission maxima and the fluorine substitution. The optical data, including absorption and emission maxima, and extinction co-efficients are given in Table **7.1**.

Table **7.1**   UV-vis absorption and luminescence data for the BPET compounds

Compound	Absorption Maxima (λ, nm) $(\log \varepsilon$ $(dm^2$ $mol^{-1}))$	Fluorescence Maxima (λ, nm), Excitation (λ, nm)
1	336 (5.81)	375 (340)
2	337 (5.52)	377 (340)
3	340 (5.87)	410 (340)
4	338 (5.56)	372 (340)
6	336 (5.95)	376 (340)
7	342 (6.03)	384 (340)
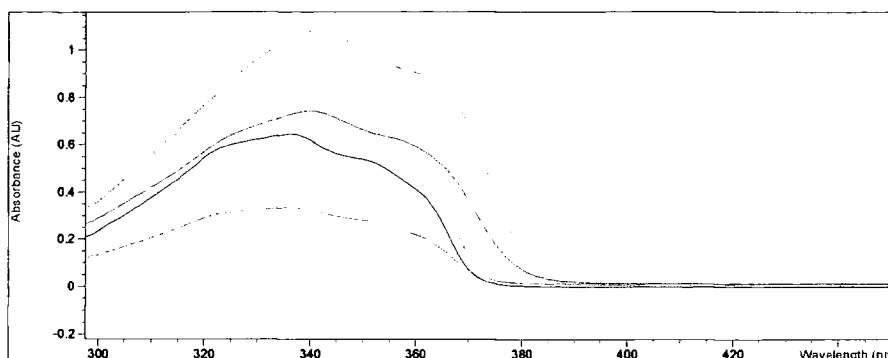
Figure **7.6**   UV-vis absorption spectra of BPET compounds

7.2.3 Attempts at Crystal Growth

The crystal structures of the compounds could reveal much information about the molecular packing of the compounds, particularly in the context of the arene-perfluoroarene interaction. However, all of the BPET compounds are obtained as microcrystalline powders, except for compound **7**, which was obtained as a crystalline solid. This prohibits the growth of crystals suitable for single-crystal diffraction. Several attempts were made to crystallise the compounds from various solvents, but all attempts failed. However, small needles of compound **3** and compound **7**, have been obtained via high temperature sublimation in a sealed tube under *in vacuo*, and evaporation from THF solution respectively. However, these were too small to be suitable for single X-ray diffraction. These compounds may be, however, be suitable for analysis by powder X-ray diffraction, particularly as their rigid rod-like nature should facilitate structure solution by Rietveldt methods.

7.3 Conclusions

A number of selectively fluorinated 4,4'-bis(phenylethynyl)tolan derivatives, have been synthesized from the coupling of selectively fluorinated 1-iodo-4-(phenylethynyl)benzene and 1-ethynyl-4-(phenylethynyl)benzene precursors via homogeneous palladium-catalysed Sonogashira cross-coupling methodology. They are observed to absorb in the UV range 336 – 342 nm. These values are directly comparable to the absorptions for similarly fluorinated 1,4-bis(phenylethynyl)benzene derivatives which suggests that an effective conjugation length (ECL) of 3-4 repeat units is applicable for these phenylene ethynylene systems. However, their extinction co-efficients are an order of magnitude larger than those of the BPEBs.

As expected the bis(phenylethynyl)tolans are observed to be highly fluorescent even in very low concentrations. Their fluorescence maxima are in the UV range 372 – 410 nm, although there is considerable fluorescence in the blue region of the visible spectrum. The emission maxima vary slightly, but there appears to be no obvious correlation between emission maxima with fluorine substitution

7.4 Experimental

7.4.1 Synthesis

All reactions were carried out under a dry nitrogen atmosphere using standard Schlenk techniques for air-sensitive compounds.[8] However, once the reactions were complete further procedures were carried out without any precautions against oxygen. Triethylamine and diisopropylamine were distilled from calcium hydride under nitrogen and THF was distilled over sodium metal under nitrogen, prior to use. All other solvents were GPR grade and used without further purification or drying. Pentafluorophenylacetylene was prepared using a modified literature procedure.[7] All other reagents were obtained from Aldrich and used without further purification, unless otherwise stated. Compound **16** was prepared according to the literature procedure.[13] The palladium complexes bis(triphenylphosphine) palladium(II) dichloride and bis(benzonitrile) palladium(II) dichloride and were made using literature procedures.

^{1}H and ^{19}F NMR experiments were performed on a Varian Mercury spectrometer at 200 MHz and 188 MHz respectively, over an acquisition time of 1 m. The chemical shifts are reported in ppm and referenced to the external standards, tetramethylsilane and trichlorofluoromethane respectively. ^{13}C NMR experiments were performed on a Varian spectrometer at 100 MHz by the departmental service with chemical shifts referenced to tetramethylsilane. All spectra were recorded in dry deuterated chloroform, except for the four ring compounds, which were dissolved in hot d_6-benzene and allowed to cool.

GC-MS analyses were performed on a Hewlett-Packard 5890 Series II gas chromatograph with a 5971A MSD mass selective ion detector and a 12 m

fused silica (5% cross-linked phenylmethylsilicone) capillary column, under the following operating conditions: injector temperature 250 $^{\circ}$C, detector temperature 270 $^{\circ}$C, the oven temperature was ramped from 70 $^{\circ}$C to 270 $^{\circ}$C at the rate 50 $^{\circ}$C /min. UHP helium was used as the carrier gas. Elemental analyses were performed using an Exeter Analytical CE-440 analyzer at the University of Durham by Ms. J. Dostal.

The UV-vis absorption spectra were recorded on a Hewlett-Packard 8453 spectrometer in spectroscopic grade acetonitrile solution. The fluorescence spectra were recorded on a Photon Technologies Inc. MD-5020 spectrometer, with a LPS-200B xenon lamp and a 810 photon detector.

1-Iodo-4-(pentafluorophenylethynyl)tetrafluorobenzene (12)
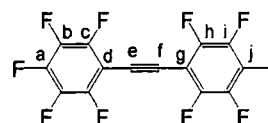
To a 500 ml Schlenk flask were added 1,4-diiodotetrafluorobenzene (12.06 g, 30 mmol), Pd(PPh₃)₂Cl₂ (0.07 g, 0.1 mmol) and CuI (0.02 g, 0.1 mmol), and the flask was evacuated and purged with dry nitrogen three times. Ca. 300 ml of triethylamine was added via cannula under nitrogen, and the mixture allowed to stir. Pentafluorophenylacetylene (2.30 g, 12 mmol) was added dropwise by pipette to the mixture under a nitrogen purge. The reaction mixture was allowed to stir for 4 h at reflux under nitrogen. The reaction mixture was filtered through a coarse sinter funnel and the filtrate evaporated to dryness *in vacuo*. The crude residue was extracted in hexane and filtered through a 3 cm silica pad. The hexane was removed *in vacuo*. The residue was purified via column chromatography using silica with hexane as the eluent, to obtain 5.50 g of recovered diiodotetrafluorobenzene, and 1.02 g (22% yield) of product. The product was re-crystallised from hexane to give colourless plates.

m.p. 114-115 °C.

^{19}F NMR (188 MHz): δ -136.2 (m, 1F), -137.5 (m, 2F), -152.5 (m, 1F), -159.3 (m, 2F), -162.0 (m, 2F).

MS (EI) m/z (rel): 466 (m$^+$, 39), 320 (41), 289 (100), 270 (19), 251 (19), 127 (42).

Anal. Calcd. for C$_{14}$F$_9$I: C 36.05, H 0.0; Found: C 36.13, H 0.0.

1-Trimethylsilylethynyl-4-(phenylethynyl)benzene (13)
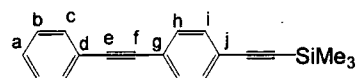
To a 250 ml Schlenk flask were added 1-iodo-4-(phenylethynyl)benzene (1.87 g, 5 mmol), $Pd(PPh_3)_2Cl_2$ (0.04 g, 0.05 mmol) and CuI (0.01 g, 0.05 mmol), and the flask was evacuated and purged with dry nitrogen three times. Ca. 200 ml of diisopropylamine was added via cannula under nitrogen. Trimethylsilylacetylene (Fluorochem) (0.59 g, 6 mmol) was added via pipette to the mixture under a nitrogen purge. The reaction mixture was allowed to stir for 3 h at room temperature under nitrogen. The reaction mixture was filtered through a coarse sinter funnel, and the filtrate evaporated to dryness *in vacuo*. The crude residue was extracted into hexane, and filtered through a 3 cm silica pad. The hexane was removed *in vacuo*. The residue was re-crystallised from hexane (20 ml) to give large colourless crystals.

m.p. 82-84 °C

^{1}H NMR (200 MHz): δ 7.27 (m, 4H), 7.10 (m, 4H), 7.06 (s, 1H), 0.08 (s, 9H).

MS (EI) m/z: 274, 259, 215, 189, 129, 105.

Anal. Calcd. for $C_{19}H_{18}Si$: C 82.90, H 6.55; Found: C 82.97, H 6.57.

1-Trimethylsilylethynyl-4-(pentafluorophenylethynyl)benzene (14)
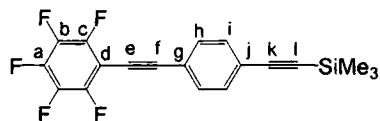

To a 250 ml Schlenk flask was added 1-bromo-4-(pentafluorophenylethynyl)-benzene (1.82 g, 5 mmol), and the flask was evacuated and purged with dry nitrogen three times. Ca. 200 ml of triethylamine was added via cannula under nitrogen. A solution of Pd(PhCN)$_2$Cl$_2$ (0.02 g, 0.05 mmol) and ^{t}Bu$_3$P (Strem) (0.02 g, 0.1 mmol) in ca. 5 ml of toluene under nitrogen was quickly added via pipette to the flask under a purge of nitrogen. Copper iodide (0.01 g, 0.05 mmol) was then added. Trimethylsilylacetylene (Fluorochem) (0.59 g, 6 mmol) was added via pipette to the mixture under a nitrogen purge. The reaction mixture was allowed to stir for 3 h at room temperature under nitrogen. The reaction mixture was filtered through a coarse sinter funnel, and the filtrate evaporated to dryness *in vacuo*. The crude residue was extracted in hexane and filtered through a 3 cm silica pad. The hexane was removed *in vacuo*. The residue was re-crystallised from hexane (20 ml) to give large elongated colourless crystals. Yield 1.39 g, (80 %)

m.p. 137-138 °C.

^{1}H NMR (200 MHz): δ 7.51 (m, 4H, H$_{hi}$), 0.26 (s, 9H, Me).

^{19}F NMR (188 MHz): δ -136.3 (m, 2F, F$_c$), -152.6 (m, 1F, F$_a$) -162.1 (m, 2F, F$_c$).

^{13}C {^{1}H} NMR (125 MHz): δ 147.1 (d, C$_b$, J$_{CF}$ = 250 Hz), 142.1 (d, C$_a$, J$_{CF}$ = 250 Hz), 138.2 (d, C$_c$, J$_{CF}$ = 250 Hz), 132.3 (s, C$_h$), 131.9 (s, C$_i$), 124.7 (s, 121.6, 104.3, 101.4, 97.5, 75.0, 0.1 (s, C$_{Me}$).

MS (EI), m/z (rel): 364 (m$^+$, 27), 349 (100).

Anal. Calcd. for C$_{19}$H$_{13}$F$_5$Si: C 62.63, H 3.60; Found C 62.77, H 3.57.

1-Trimethylsilylethynyl-4-(phenylethynyl)tetrafluorobenzene (15)
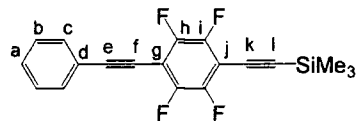
A three-necked 250 ml flask was equipped with a dropping funnel and evacuated and purged with dry nitrogen three times. Ca. 50 ml of dry THF was added via cannula under nitrogen. Trimethylsilylacetylene (Flourochem) (0.98 g, 10 mmol) was added via pipette to the flask under nitrogen purge. A 6.5 ml aliquot of a 1.6 M solution of n-butyl lithium in hexanes (Lancaster) was added via cannula to the dropping funnel under nitrogen. The butyl lithium solution was then added dropwise to the reaction mixture at 0 °C under nitrogen, and the reaction left to stir for 1 h under nitrogen. A sample of (phenylethynyl)pentafluorobenzene (2.68 g, 10 mmol) was added to the reaction mixture at room temperature. The mixture was stirred at 50 °C for 3 h. The reaction mixture was filtered through a 3 cm silica pad with diethyl ether. The filtrate was evaporated *in vacuo*, to leave a dark residue. The residue was extracted in hexane and filtered through another 3 cm silica pad. The hexane was removed *in vacuo* to leave a white residue, which was re-crystallised from hexane to give large crystals. Yield: 1.65 g (48 %)

m.p. 82-84 °C.

^{1}H NMR (200 MHz): δ 7.59 (m, 2H, H_c), 7.38 (m, 3H, H_{ab}), 0.29 (s, 9H, H_{Me})

^{19}F NMR (188 MHz): δ -137.3 (m, 4F, F_{hi}).

^{13}C {^{1}H} NMR (125 MHz): δ 148.2 (d, C_h, J_{CF} = 253 Hz), 146.3 (d, C_i, J_{CF} = 251 Hz), 132.1, 131.8, 131.6, 128.7, 122.0, 111.4, 103.7, 89.2, 0.1 (s, C_{Me}).

MS (EI), m/z (rel): 347 (m$^+$, 19), 346 (65), 332 (26), 331 (100), 269 (31) 267 (24), 264 (24), 262, (28), 249, (43), 245 (20), 244 (77).

Anal. Calcd. for $C_{19}H_{14}F_4Si$: C 65.70, H 4.03; Found: C 65.84, H 4.06.

1-Ethynyl-4-(pentafluorophenylethynyl)benzene (17)
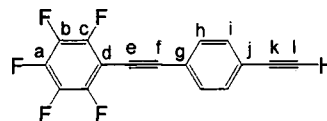
1-Trimethylsilylethynyl-4-(pentafluorophenylethynyl)benzene (0.365 g, 1 mmol) was dissolved in ca. 100 ml of a methanol / diethyl ether solution (1:1 v/v) in a 250 ml Schlenk flask with a nitrogen purge. A 1.5 ml aliquot of a 0.1 M solution of potassium hydroxide (Lancaster) in distilled water was added via Pasteur pipette. After 2 h a sample was taken for GC/MS analysis and the reaction was shown to be complete. Ca. 100 ml of diethyl ether was added to the reaction mixture, and the organic layer was washed with distilled water (100 ml x 3), 0.1 M aqueous hydrochloric acid (100 ml x 3), and then distilled water (100 ml x 3). The ethereal solution was dried over magnesium sulphate, and then evaporated to dryness *in vacuo*. The crude residue was extracted in hexane, filtered through a 3 cm silica pad, and the hexane removed *in vacuo*. The residue was re-crystallised from hexane to give a white crystalline solid. Yield: 0.25 g (86%)

m.p. 116-117 °C.

^{1}H NMR (200 MHz): δ 7.54 (m, 4H, H_{hi}) 3.22 (s, 1H, H_l).

^{19}F NMR (188 MHz): δ -136.2 (m, 2F, F_b) -152.6 (m, 1F, F_a) -162.1 (m, 2F, F_c).

^{13}C {^{1}H} NMR (125 MHz): δ 147.1 (d, C_b, J_{CF} = 250 Hz), 142.1 (d, C_a, J_{CF} = 250 Hz), 138.2 (d, C_c, J_{CF} = 250 Hz), 132.4, 132.0, 123.6, 122.1, 101.0, 83.1, 80.0, 75.1.

Anal. Calcd. for $C_{16}H_5F_5$: C 65.77, H 1.71; Found: C 65.57, H 1.68.

1-Ethynyl-4-(phenylethynyl)tetrafluorobenzene (18)
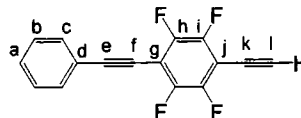
1-Trimethylsilylethynyl-4-(phenylethynyl)tetrafluorobenzene (0.347 g, 1 mmol) was dissolved in ca. 100 ml of a methanol / diethyl ether solution (1:1 v/v) in a 250 ml Schlenk flask with a nitrogen purge. A 1.5 ml aliquot of a 0.1 M solution of potassium hydroxide (Lancaster) in distilled water was added from a Pasteur pipette. After 2 h, a sample was taken for GC-MS analysis and the reaction was shown to be complete. Ca. 100 ml of diethyl ether was added to the reaction mixture, which was then washed with distilled water (100 ml x 3), 0.1 M aqueous hydrochloric acid (100 ml x 3), and then distilled water again (100 ml x 3). The ethereal solution was dried over magnesium sulphate, and evaporated to dryness *in vacuo*. The crude residue was extracted in hexane and filtered through a 3 cm silica pad. The hexane was then removed *in vacuo*, and the residue re-crystallised from hexane to give a white crystalline solid. (Yield: 0.21 g 77%)

m.p. 98-99 °C.

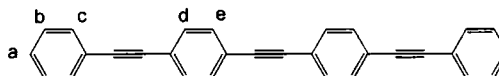^{1}H NMR (200 MHz): δ 7.59 (m, 2H), 7.38 (m, 3H,), 3.69 (s, 1H).

^{19}F NMR (188 MHz): δ -137.3 (m, 4F).

^{13}C NMR (125 MHz): 148.2 (d, C_h, J_{CF} = 253 Hz), 146.3 (d, C_i, J_{CF} = 251 Hz), 132.0, 129.8, 128.5, 121.4, 103.7, 90.9, (s, C_l), 74.2.

MS (EI), m/z (rel): 275 (25), 274 (m+, 100), 223 (21), 222 (20).

Anal. Calcd. for $C_{16}H_6F_4$: C 65.70, H 4.03; Found: C 65.84, H 4.06.

1-Phenylethynyl-4-(4-phenylethynyl-phenylethynyl)benzene (1)

To a 250 ml Schlenk flask were added 1-iodo-4-(phenylethynyl)benzene (0.30 g, 1 mmol), 1-ethynyl-4-(phenylethynyl)benzene (0.24 g, 1.2 mmol), $Pd(PPh_3)_2Cl_2$ (0.007 g, 0.01 mmol) and CuI (0.002 g, 0.01 mmol), and the flask was evacuated and purged with dry nitrogen three times. Ca. 100 ml of diisopropylamine was added via cannula under nitrogen, and the mixture allowed to stir for 4 h at room temperature, and then heated to reflux for 10 min. The reaction mixture was allowed to cool and then filtered through a coarse sinter funnel. The scinter residue was washed with several portions of hot toluene, which was then removed *in vacuo*. The crude residue was extracted in hot toluene and filtered through a 3 cm silica pad whilst hot. The toluene was removed *in vacuo*. The residue was dissolved in a small volume of hot toluene and precipitated by addition of a similar volume of hexane to the cooled toluene solution. The precipitate was filtered off to give the product as a white powder. (Yield: 0.18 g, 33%)
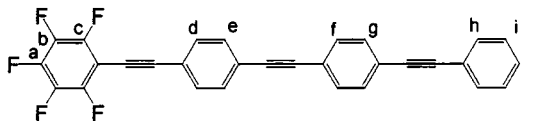
m.p. 266-267°C.

^{1}H NMR (200 MHz): δ 7.22 (m, 4H, H_c), 7.05 (s, 8H, H_{de}), 6.76 (m, 6H, H_{ab}),

MS (EI)

Anal. Calcd. for $C_{30}H_{18}$: C 95.23, H 4.76; Found: C 94.97, H 4.84.

[4-(4-Phenylethynyl-phenylethynyl)-phenylethynyl]-pentafluorobenzene (2)

To a 250 ml Schlenk flask were added 1-iodo-4-(phenylethynyl)benzene (0.30 g, 1 mmol), 1-ethynyl-4-(pentafluorophenylethynyl)benzene (0.34 g, 1.2 mmol), $Pd(PPh_3)_2Cl_2$ (0.007 g, 0.01 mmol) and CuI (0.002 g 0.01 mmol), and the flask was evacuated and purged with dry nitrogen three times. Ca. 100 ml of diisopropylamine was added via cannula under nitrogen, and the mixture allowed to stir for 4 h at room temperature, and then heated to reflux for 10 min. The reaction mixture was allowed to cool and then filtered through a coarse sinter funnel. The residue was washed with several portions of hot toluene, which was then removed *in vacuo*. The crude residue was extracted in hot toluene filtered through a 3 cm silica pad, and the toluene was removed *in vacuo*. The residue was dissolved in a small volume of hot toluene and precipitated by addition of a similar volume of hexane to the cooled toluene solution. The precipitate was filtered off to give the product as a yellow powder. (Yield: 0.31 g 66%)

m.p. 242-243 °C.

^{1}H NMR (200 MHz): δ 7.23 (m, 2H, H_d), 7.05 (s 4H, H_{fg}), 6.97 (m, 3H_{ij}), 6.71 (m, 4H, H_{eh}).
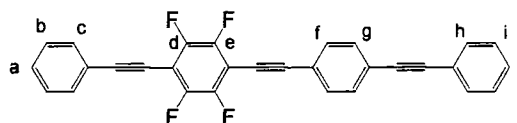
^{19}F NMR (188 MHz): δ -137.5 (m, 2F, F_c) -153.2 (m, 1F, F_a) -162.5 (m, 2F, F_b).

MS (EI) m/z (rel): 470 (6), 469 (33), 468 (m+, 100), 286 (8), 234 (19), 149 (7), 92 (48), 91 (63), 57, (13).

Anal. Calcd. for $C_{30}H_{13}F_5$: C 76.92 H 2.78 Found: C 76.81, H 2.85.

1-Phenylethynyl-4-(4-phenylethynyl-phenylethynyl)-tetrafluorobenzene (3)

To a 250 ml Schlenk flask were added 1-iodo-4-(phenylethynyl)tetrafluorobenzene (0.37 g, 1 mmol), 1-ethynyl-4-(phenyl-ethynyl)benzene (0.24 g, 1.2 mmol), Pd(PPh$_3$)$_2$Cl$_2$ (0.007 g, 0.01 mmol) and CuI (0.002 g, 0.01 mmol), and the flask was evacuated and purged with dry nitrogen three times. Ca. 100 ml of diisopropylamine was added via cannula under nitrogen, and the mixture allowed to stir for 4 h at room temperature, and then heated to reflux for 10 min. The reaction mixture was allowed to cool and then filtered through a coarse sinter funnel. The sinter residue was washed with several portions of hot toluene, which was then removed *in vacuo*. The crude residue was extracted in hot toluene filtered through a 3 cm silica pad whilst hot. The toluene was removed *in vacuo*. The residue was dissolved in a small volume of hot toluene and precipitated by addition of a similar volume of hexane to the cooled toluene solution. The precipitate was filtered off to give the product as a yellow powder. (Yield 0.15 g, 33%)

m.p. 206-207 °C

^{1}H NMR (200 MHz): δ 7.16 (m, 4H, H$_{cf}$), 6.96 (m 4H, H$_{gh}$), 6.67 (m, 6H, H$_{abij}$),

^{19}F NMR (188 MHz): δ -138.0 (m, 4F$_{de}$).

MS (EI) m/z (rel): 452 (7), 451 (34), 450 (m+, 100), 225 (18), 149 (2).

Anal. Calcd. for C$_{30}$H$_{14}$F$_4$: C 80.00 H 3.11, Found C 80.17, H 3.21.

[4-(4-Phenylethynyl-tetrafluorophenylethynyl)-phenylethynyl]-pentafluoro-benzene (4)

To a 250 ml Schlenk flask were added 1-iodo-4-(phenylethynyl)tetrafluorobenzene (0.37 g, 1 mmol), 1-ethynyl-4-(pentafluoro-phenylethynyl)benzene (0.34 g, 1.2 mmol), $Pd(PPh_3)_2Cl_2$ (0.007 g, 0.01 mmol) and CuI (0.002 g, 0.01 mmol), and the flask was evacuated and purged with dry nitrogen three times. Ca. 100 ml of diisopropylamine was added via cannula under nitrogen, and the mixture allowed to stir for 4 h at room temperature, and then heated to reflux for 10 min. The reaction mixture was allowed to cool and then filtered through a coarse sinter funnel. The residue was washed with several portions of hot toluene, which was then removed *in vacuo*. The crude residue was extracted in hot toluene filtered through a 3 cm silica pad, and the toluene was removed *in vacuo*. The residue was dissolved in a small volume of hot toluene and precipitated by addition of a similar volume of hexane to the cooled toluene solution. The precipitate was filtered off to give the product as an off-white powder. (Yield: 0.14 g, 26%)
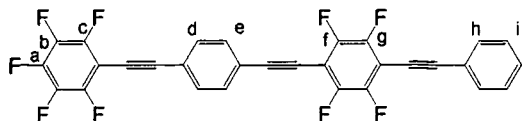
m.p. 236-236 °C

^{1}H NMR (200 MHz): δ 7.12 (m, 2H, H_h), 7.09 (s 4H, H_{de}), 6.64 (m, 3H, H_{ij}).

^{19}F NMR (188 MHz): δ -137.3 (m, 2F, F_c), -137.8 (s, 4F, F_{fg}), -152.8 (m, 1F, F_a), -162.2 (m, 2F, F_b).

MS (EI) m/z (rel): 541 (51), 540 (m+, 100), 350 (6), 270 (27).

Anal. Calcd. for $C_{30}H_9F_9$: C 66.67 H 1.67; Found: C 66.39, H 1.61.

4-(4-Pentafluorophenylethynyl-phenylethynyl)-phenylethynyl]-pentafluoro-benzene (6)
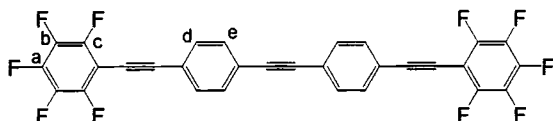
To a 250 ml Schlenk flask were added 1-bromo-4-(pentafluorophenylethynyl)benzene (0.30 g, 1 mmol), 1-ethynyl-4-(pentafluorophenylethynyl)benzene (0.29 g, 1.2 mmol), and CuI (0.002 g, 0.01 mmol), and the flask was evacuated and purged with dry nitrogen three times. Ca. 100 ml of triethylamine was added via cannula under nitrogen. A solution of Pd(PhCN)$_2$Cl$_2$ (0.004 g, 0.01 mmol) and tri(t-butylphosphine) (0.004 g, 0.02 mmol) in ca. 1 ml of toluene, was quickly added via pipette to the flask under nitrogen. The mixture was allowed to stir for 4 h at room temperature, and then heated to reflux for 10 min. The reaction mixture was allowed to cool and then filtered through a coarse sinter funnel. The residue was washed with several portions of hot toluene, which was then removed in vacuo. The crude residue was filtered through a 3 cm silica pad in hot toluene and the toluene was removed *in vacuo*. The residue was dissolved in a small volume of hot toluene and precipitated by addition of a similar volume of hexane to the cooled toluene solution. The precipitate was filtered off to give the product as a yellow powder. (Yield 0.25 g, 48 %)
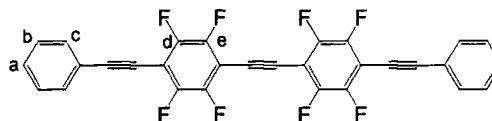
m.p. 246-248 °C.

^{1}H NMR (200 MHz): δ 6.99 (m, 8H, H$_{de}$).

^{19}F NMR (188 MHz): δ -137.4 (m, 4F, F$_c$), -153.1 (m, 2F, F$_a$), -162.4 (m, 4F, F$_b$).

Anal. Calcd. for C$_{30}$H$_8$F$_{10}$: C 64.51 H 1.43; Found: C 64.28, H 1.42.

1-Phenylethynyl-4-(4-phenylethynyl-tetrafluorophenylethynyl)-tetrafluorobenzene (7)

To a 250 ml Schlenk flask were added 1-iodo-4-(phenylethynyl)tetrafluorobenzene (0.37 g, 1 mmol), 1-ethynyl-4-(phenyl-ethynyl)tetrafluorobenzene (0.32 g, 1.2 mmol), Pd(PPh$_3$)$_2$Cl$_2$ (0.007 g, 0.01 mmol) and CuI (0.002 g, 0.01 mmol), and the flask was evacuated and purged with dry nitrogen three times. Ca. 100 ml of diisopropylamine was added via cannula under nitrogen, and the mixture allowed to stir for 4 h at room temperature, and then heated to reflux for a further 10 min. The reaction mixture was allowed to cool and then filtered through a coarse scinter funnel. The residue was washed with several portions of hot toluene, which was then removed *in vacuo*. The crude residue was extracted in hot toluene and filtered through a 3 cm silica pad, and the toluene was removed *in vacuo*. The residue was dissolved in a small volume of hot toluene and precipitated by addition of a similar volume of hexane to the cooled toluene solution. The precipitate was filtered off to give the product as a yellow crystalline solid. (Yield 0.27 g, 51%)

m.p. 268-270 °C:

^{1}H NMR (200 MHz): δ 7.12 (m, 4H, H$_c$), 6.61 (m, 6H, H$_{ab}$).

^{19}F NMR (188 MHz): δ -136.5 (m, 4F, F$_d$), -137.4 (m, 4F, F$_e$).

MS (EI) m/z (rel): 524 (6), 523 (32), 522 (m+, 100), 446 (2), 261 (16).

Anal. Calcd. for C$_{30}$H$_{10}$F$_8$: C 68.97 H 1.19;   Found: C 69.21, H 1.22.

7.5 References

1. a) P. Nguyen, G. Lesley, C. Dai, N. J. Taylor, T. B. Marder, V. Chu, C. Viney, I. Ledoux and J. Zyss, in *Applications of Organometallic Chemistry in the Preparation and Processing of Advanced Materials*, ed. J. F. Harrod and R. M. Laine, Kluwer Academic, Dordrecht, 1995, p. 333; b) P. Nguyen, Z. Yuan, L. Agocs, G. Lesley and T. B. Marder, *Inorg. Chim. Acta*, 1994, **220**, 289; c) P. Nguyen, G. Lesley, T. B. Marder, I. Ledoux and J. Zyss, *Chem. Mater.*, 1997, **9**, 406.

2. S. K. Gill, *Aldrichimica Acta*, 1983, **16**, 59.

3. P. J. Collings, *Liquid Crystals, Nature's Delicate Phase of Matter*, Princeton, University Press, Princeton, 1990.

4. a) C. Viney, R. J. Twieg, C. M. Dannels, M. Y. Chang, *Mol. Cryst. Liq. Cryst.*, 1990, **7**, 147; b) C. Viney, D. J. Brown, C. M. Dannels, R. J. Twieg, *Liq. Cryst.*, 1993, **13**, 95; c) R. J. Twieg, V. Chu, C. Nguyen, C. M. Dannels, C. Viney, *Liq. Cryst.*, 1996, **20**, 287.

5. C. Dai, Ph.D Thesis, University of Waterloo, Ontario, Canada, 1998.

6. a) G .W.Gray, M. Hird, D. Lacey and K. J. Toyne, *J. Chem. Soc., Perkin Trans. 2*, 1989, 2041; b) G. W. Gray, M. Hird, D. Lacey and K. J. Toyne, *Mol. Cryst.Liq. Cryst.*, 1991, **204**, 43.

7.   C. Dai, P. Nguyen, T. B. Marder, A, J, Scott, W. Clegg and C. Viney, *Chem. Commun.*, 1999, 2493.

8.   J. M. Burke, Ph.D. Thesis, University of Durham, UK, Chapter 5. *In preparation.*

9.   W. J. Feast, P. W. Lovenich, H. Puschmann and C. Taliani, *Chem. Commun.*, 2001, 505.

10.   K. Sonogashira, Y. Toda and N. Hagihara, *Tetrahedron Lett.*, 1975, 4467.

11.   P. Tarrant, in *Fluorine Chemistry Reviews*, ed. P. Tarrant, Marcel Dekker, New York, Vol. 7, 1974.

12.   a) J. Kajanus, S. B. van Berlekom, B. Albinsson and J. Martensson, *Synthesis*, 1999, 1155; b) H. Li, D. R. Powell, T. K. Firman and R. West, *Macromolecules*, 1998, **31**, 1093.

13.   O. Lavastre, S. Cabioch, P. H. Dixneuf and J. Vohlidal, *Tetrahedron*, 1997, **53**, 7595.

14.. a) T. X. Neenan and G. M. Whitesides, *J. Org. Chem.*, 1988, **53**, 2489; b) P. Nguyen, Z. Yuan, L. Agocs, G. Lesley and T. B. Marder, *Inorg. Chim. Acta*, 1994, **220**, 289.

15.   P. L. Coe, J. C. Tatlow and R.C. Terrell, *J. Chem. Soc. C.*, 1967, 2626.

16.   Y. Zhang, J. Wen, *Synthesis*, 1990, 727.

17. F. Waugh and D. R. M. Walton, *J. Organomet. Chem.*, 1972, **39**, 275.

18. R. J. Errington, Advanced Practical Inorganic and Metalorganic Chemistry, Blackie A&P, London, 1997.

Chapter Eight

The Synthesis and Crystal Structures of 1,4-diethynyltetrafluorobenzene and 1,4-diethynyl-2,5-difluorobenzene

8.1 Introduction

It is now well established that molecular materials can have many properties, which can fulfil a number of applications. Examples of such are liquid crystal behaviour and non-linear optical properties. These properties are dependant not merely upon the molecular structure, but also upon the supramolecular structure, in other words the arrangement of molecules in the solid state.[1] Structural information can be obtained by a number of diffraction techniques, most notably X-ray diffraction.

The supramolecular structure is dependent on the intermolecular forces. These are often dominated by the specific interactions between particular atoms or groups. Perhaps the best example is the hydrogen bond. Classical hydrogen bonds are largely the result of an electrostatic interaction between the hydrogen atom (called the donor) and an electro-negative atom or group, with lone pairs such as oxygen or nitrogen.[2] It is amongst the strongest of all

intermolecular interactions, with typical hydrogen bond energies are of the order of a few kcal/mol, and hydrogen bond can have a considerable effect on the solid state and thermodynamic properties of the substance.

It was originally thought that only hydrogen atoms bonded to electro-negative such as oxygen and nitrogen, could be sufficiently charged to act as hydrogen bond donors. This was brought into question when, on the basis of several crystal structures, a proposal was put forward that hydrogen atoms bonded to a carbon atom could also act as hydrogen bond donors.[3] Although the conjecture was subject to much dissent, it was subsequently shown by detailed analysis of much crystallographic and spectroscopic data, that these interactions could be described as hydrogen bonds. The energy of such interactions was found from *ab initio* calculations to be weaker than conventional hydrogen bonds being of the order of 5-10 kJ mol^{-1}.[4]

Terminal alkynes are among the best candidates for C-H hydrogen bond donors, as the proton is acidic. A database study of close intermolecular contacts involving $C \equiv CH \cdots O$ motifs has been carried out.[5] This showed a pronounced linearity of the contact and alignment with the lone pairs of the oxygen, which led to the authors to suggest that these were hydrogen bonds. Further evidence for this was obtained from observing the reduction in thermal vibrations of the terminal alkynes in $C-H \cdots X$ contacts.[6] This reduction began at 2.8 Å, which suggests that the hydrogen bonding is a long-range effect. In addition, crystallographic evidence has shown that the carbon-carbon triple bond can act as a hydrogen bond acceptor leading to T-shaped $C \equiv CH \cdots \pi(C \equiv C)$ motifs.[7] This means that terminal alkynes can form co-operative hydrogen bonds, in which the acceptor enhances the effect of the donor. These interactions have been investigated by *ab initio* calculations, and have been shown to have an energy of interaction of about 4 kJ mol^{-1} [8]

Intermolecular interactions often result in well-defined structural motifs. Such motifs can be used to create specific packing arrangements. In this way they are analogous to the molecular synthons used in the creation of molecules in organic synthesis, and hence they are known as supramolecular synthons. A large number of supramolecular synthons have been defined and collated by Desiraju.[9] Many of these are based on classical hydrogen bond interactions. However, some based on other C-H hydrogen bond interactions have recently been proposed as supramolecular synthons, including the terminal alkyne based $C\equiv CH\cdots NC$ and $C\equiv CH\cdots O_2N$ motifs.[10]

The crystal structures of several simple ethynyl arenes have been obtained, including that of 1,4-diethynylbenzene and 1,3,5-triethynylbenzene which were shown to contain close $C\equiv C-H\cdots\pi(C\equiv C)$ contacts.[11] The crystal structures of several para-halogenoethynylbenzenes have also been solved from single-crystal X-ray diffraction data.[12] The structures were very similar containing both close intermolecular halogen$\cdots$halogen and co-operative $C\equiv CH\cdots\pi(C\equiv C)$ motifs, except in the case p-fluorophenylacetylene which displays $C\equiv C-H\cdots X$ close contacts. The crystal structure of 1-fluoro-3,5-diethynylbenzene has also been obtained. It shows no close $C\equiv CH\cdots F$ contacts, which casts doubt on the utility of this motif as a reliable supramolecular synthon.[13] This structure is also very interesting as the protons of terminal alkyne have the possibility of showing some interaction either with the arene rings, the triple bonds or the fluorine atoms.

8.2 Results and Discussion

8.2.1 Synthesis

1,4-diethynyltetrafluorobenzene **1** was synthesized from based-catalyzed hydrodesilation of its trimethylsilyl protected precursor, 1,4-bis(trimethylsilylethynyl)tetrafluorobenzene **2**, obtained from palladium-catalyzed cross-coupling of 1,4-dibromotetrafluorobenzene with trimethylsilylacetylene (TMSA). Both compounds have been synthesized by this route previously.[14] The synthesis of 1,4-diethynyl-2,5-difluorobenzene **3** analogous to that of **1**,. involving palladium-catalyzed coupling of 1,4-dibromo-2,5-difluorobenzene with TMSA, to afford 1,4-bis(trimethylsilylethynyl)-2,5-difluorobenzene **4**, followed by removal of the trimethylsilyl groups with base. Although this compound has been synthesized previously as a precursor to conducting cation radical salts, however, no experimental details or characterisation was given.[15] All the products were obtained in reasonable yields and were fully characterised.

8.2.2 Crystal Growth and Crystallograhic Data

Crystals of 1,4-diethynyltetrafluorobenzene **1,** suitable for X-ray diffraction were grown from the slow evaporation of a DCM solution. Several attempts were made to grow diffraction-quality crystals of **3** from various solutions, however these all resulted in crystals which diffracted poorly. Instead suitable crystals were grown via sublimation *in vacuo* with gentle heating. The crystal structures of **1** and **3** were solved from X-ray diffraction data at low temperatures. Crystallographic data and refinement parameters for both compounds are given in Table **8.1**.

Table 8.1 Crystallographic data and refinement parameters

Compound	1	3
Formula	$C_{10}H_2F_4$	$C_{10}H_4F_2$
Formula weight	198.12	162.13
T (K)	150(2)	120(2)
Crystal system	Monoclinic	Monoclinic
Space group	$P2_1/c$	$P2_1/c$
a (Å)	6.120(1)	3.835(1)
b (Å)	11.474(1)	5.899(1)
c (Å)	5.761(1)	16.236(4)
$\alpha(^o)$	90	90
β $(^o)$	99.37(1)	95.21(1)
γ $(^o)$	90	90
V (Å^3)	399.1(1)	365.8(1)
Z	2	2
ρ_{calcd} (g cm^{-3})	1.648	1.472
$\bar{\lambda}$ (Å)	0.71073	0.71073
μ (mm^{-1})	0.161	0.121
Total reflections	4182	4773
Unique refls.	907	971
R_{int}	0.024	0.019
Refls. ($I > 2\sigma(I)$)		906
R (F, $I > 2\sigma(I)$)	0.031	0.034
wR (F^2, all data)	0.086	0.105

Compound **1** crystallises in space group $P2_1/c$ with Z = 2. This means that the molecular centroid is located on a crystallographic centre of inversion. Compound **3** also crystallises in space group $P2_1/c$ with Z = 2, with the molecular centroid is located on a crystallographic centre of inversion The molecular structures of **1** and **3**, are shown in Figure **8.1** (thermal ellipsoids are plotted at 50 % probability).
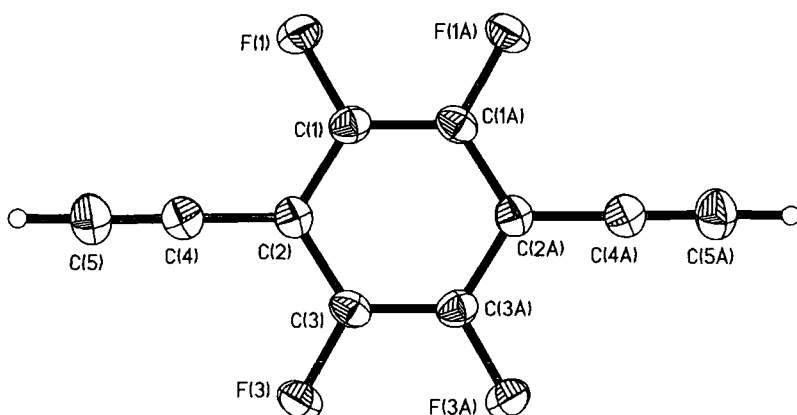

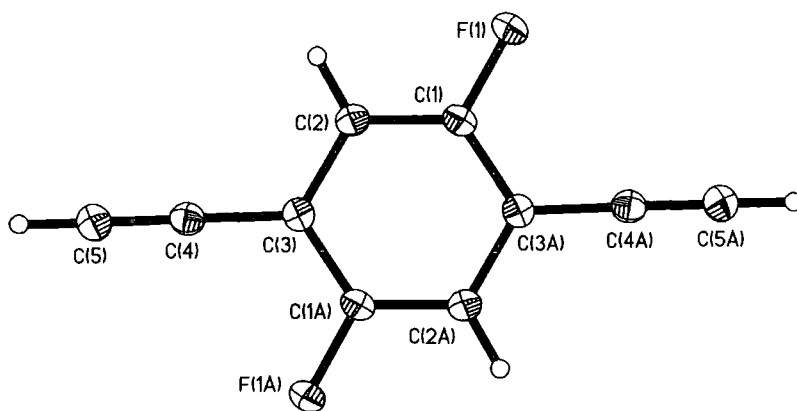Figure **8.1**(a) The molecular structure of 1,4-diethynyltetrafluorobenzene (**1**)

Figure **8.1**(b)   Molecular structure of 1,4-diethynyl-2,5-difluorobenzene (**3**)

8.2.3 Molecular Packing

The packing arrangement of **1** can be described as consisting of infinite stacks of parallel molecules running parallel to the *a*-axis. These columns are arranged in alternating layers of parallel molecules, which are arranged in a herringbone motif. The dihedral angle between the mean planes of molecules in adjacent layers is 41.8°. Within the layers there are close intermolecular contacts between the terminal alkyne groups and two of the fluorine atoms. The packing of 1 is shown in Figure **8.2**. The intermolecular C≡C-H···F distance is 2.45 Å and the C≡C-H···F angle is 132.2°. These values are based on a corrected C-H bond length, obtained from neutron diffraction data.[16] This value is slightly below the sum of the van der Waals radii carbon and hydrogen (2.54 Å).[17] There are also close intermolecular fluorine-fluorine contacts of 2.78 Å, compared to the sum of the van der Waals radii of 2.90 Å. There are no other close intermolecular contacts.
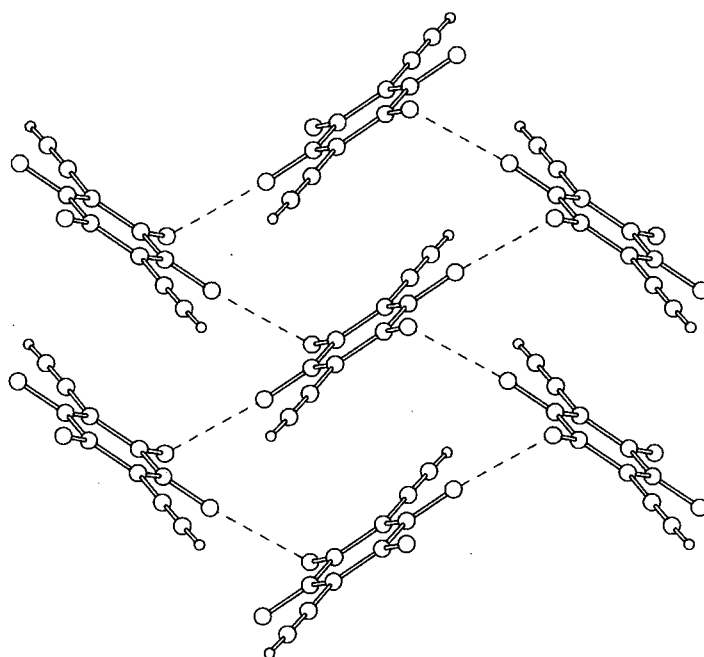
Figure **8.2**(a) The herringbone packing of the layers of molecules of **1**.
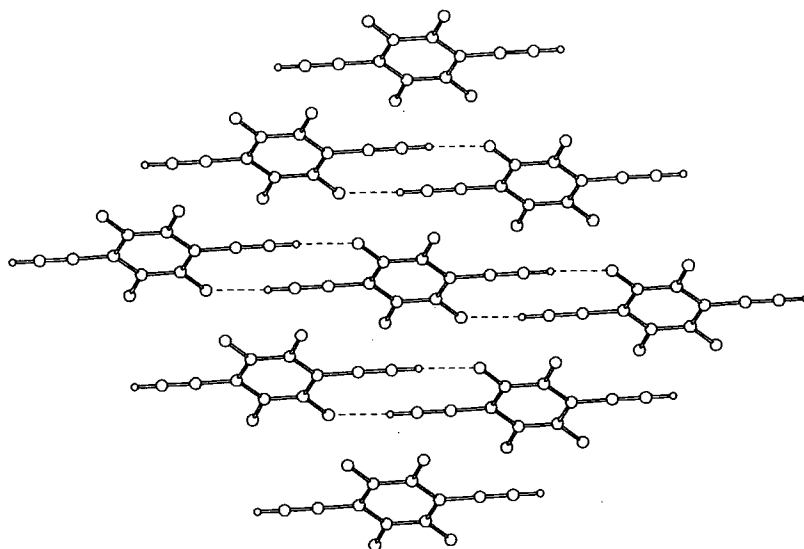
Figure **8.2**(b)   The packing of a layer of molecules of **1** showing the close
$C\equiv CH\cdots F$ contacts

The packing of **1** could be potentially replicated by that of compound **3**. Although this also consists of infinite stacks of parallel molecules in a herringbone arrangement, it is substantially different from that of **1** in that the columns run parallel to the c-axis. The angle between the molecular planes in adjacent layers is 54.3°. This packing arrangement is shown in Figure **8.3**. The intermolecular $C\equiv CH\cdots F$ contact distance is 2.59 Å and the $C\equiv CH\cdots F$ angle of 122.1°. This is above the sum of the van der Waals radii (2.54 Å). Instead there are close $C\equiv CH\cdots\pi(C\equiv C)$ contacts. The structure of **3** is very similar to that of 1,4-diethynylbenzene which also contains close intermolecular T-shaped $C\equiv CH\cdots\pi(C\equiv C)$ contacts.

Figure **8.3**.   The molecular packing arrangement of **3**.

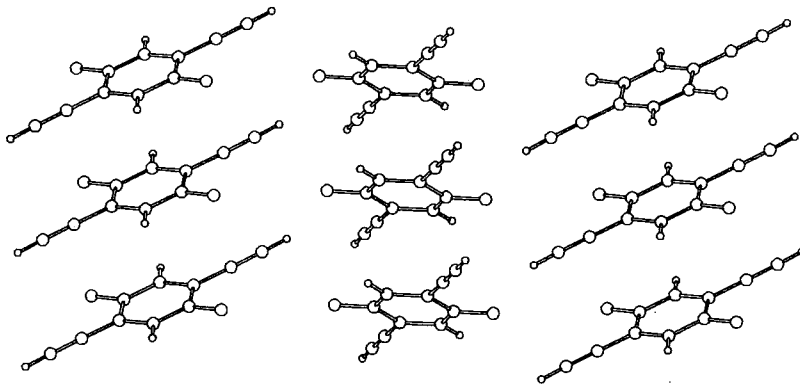## 8.3 Conclusions

The terminal alkynes 1,4-diethynyltetrafluorobenzene and 1,4-diethynyl-2,5-difluorobenzene have been synthesized from hydrodesilylation of their respective 1,4-bis(trimethylsilylethynyl)benzene precursors. The crystal structures of both compounds have been solved from X-ray diffraction data.

The molecular packing of both compounds is observed to be similar with both adopting a herringbone arrangement. However, there are significant differences, particularly with respect to the intermolecular close contacts. The packing of 1,4-diethynyl-tetrafluorobenzene contains C≡CH···F close contacts. Although this packing motif can be potentially replicated by 1,4-diethynyl-2,5-difluorobenzene, it has been found that there are no close C≡CH···F contacts. Instead, there are close T-shaped C≡CH···π(C≡C) contacts, which are very similar to those in the structure of 1,4-diethynylbenzene. This highlights some of the dangers of attempting to predict crystal structures based on interactions between particular atoms or groups, and adds further doubt to the inclusion of C≡CH···F as a reliable supramolecular synthon.

8.4 Experimental

8.4.1 Synthesis

All reactions were carried out under a dry nitrogen atmosphere using standard Schlenk techniques for air-sensitive compounds.[8] However, once the reactions were complete further procedures were carried out without any precautions against oxygen. Diisopropylamine was distilled from calcium hydride under nitrogen, but all other solvents were GPR grade and used without further purification or drying. All the reagents were obtained were used without further purification, unless otherwise stated. The palladium complex bis(triphenylphosphine) palladium(II) dichloride was made using a modified literature procedure.

^{1}H and ^{19}F NMR experiments were performed on a Varian Mercury spectrometer at 200 MHz and 188 MHz respectively. The chemical shifts are reported in ppm and referenced to the external standards, tetramethylsilane and trichlorofluoromethane respectively. All spectra were recorded in dry deuterated chloroform. GC-MS analyses were performed on a Hewlett-Packard 5890 Series II gas chromatograph with a 5971A MSD mass selective ion detector and a 12 m fused silica (5% cross-linked phenylmethylsilicone) capillary column, under the following operating conditions: injector temperature 250 °C, detector temperature 270 °C, the oven temperature was ramped from 70 °C to 270 °C at the rate 20 °C /min. UHP helium was used as the carrier gas. Elemental analyses were performed using an Exeter Analytical CE-440 analyzer at the University of Durham by Ms. J. Dostal.

1,4-bis(trimethylsilylethynyl)-2,5-difluorobenzene (4)

To a 250 ml Schlenk flask were added 1,4-dibromo-2,5-difluorobenzene (2.72 g, 10 mmol), bis(triphenylphosphine)palladium(II) dichloride (0.07 g, 0.1 mmol) and copper(I) iodide (0.02 g, 0.1 mmol), and the flask was evacuated and purged with dry nitrogen three times. Ca. 100 ml of distilled diisopropylamine was added *via* cannula under nitrogen, and then Trimethylsilylacetylene (1.18 g, 12 mmol) was added via pipette under a nitrogen purge. The reaction mixture was heated at reflux for 6 h, after which it was shown to be complete by GC-MS. The reaction mixture was allowed to cool and filtered through a coarse sinter, and evaporated to dryness *in vacuo.* The residue was extracted in hot toluene and filtered through a 3 cm thick silica pad. The toluene was then removed under reduced pressure. The residue was recrystallised from hexane, to afford the product as colourless crystals. Yield 1.81 g

m.p. 101-102 °C.

^{1}H NMR (200 MHz) δ 7.24 (s, 2H), 0.18. (s, 18H). ^{19}F NMR (188 MHz) δ - 148.2 (s, 2F).

MS (EI) m/z (rel): 307 (22), 306 (m$^+$, 78), 292 (28), 291 (100), 165 (12), 138 (17).

Anal. Calc. for $C_{16}H_{20}F_2Si_2$: C 62.74, H 6.53; Found: C 63.05, H 6.59..

1,4-diethynyl-2,5-difluorobenzene (3)

1,4-bis(trimethylsilylethynyl)-2,5-difluorobenzene (0.30 g, 1 mmol) was dissolved in ca. 100 ml methanol in a 100 ml Schlenk flask with a nitrogen purge. A 3 ml aliquot of a 0.1 M solution of potassium hydroxide in distilled water was added via Pasteur pipette. Ca. 100 ml of diethyl ether was added to the reaction mixture, and the organic layer was washed with distilled water (100 ml x 3), 0.1 M aqueous hydrochloric acid (100 ml x 3), and then distilled water again (100 ml x 3). The ethereal solution was dried over magnesium sulphate, and then evaporated to dryness *in vacuo*. The crude residue was extracted with hexane, filtered through a 3 cm silica pad, and the hexane was removed from the filtrate under reduced pressure to leave a white residue, which was re-crystallised from hexane. Yield: 0.14 g (84 %)

m.p. 116-117 $^{\circ}$C

^{1}H NMR (200 MHz) δ 7.24 (s, 2H), 3.41 (s, 2H).

^{19}F NMR (188 MHz) δ −148.1 (s, 2F).

Anal. Calc. for $C_{10}H_4F_2$: C 74.08, H 2.49; Found: C 74.12, H 2.45.

8.4.2 Crystallography

The crystallographic data collection and structure solutions for all the compounds was performed by Dr. Andrei Batsanov. All X-ray diffraction experiments were carried out on a Siemens SMART three-circle diffractomer equipped with a 1K CCD area detector, using graphite-monochromated Mo-K$_{\alpha}$ radiation. The structures were solved by direct methods, and refined by full-matrix least squares on F^2 of all the data, using SHELXTL software All C and F were refined in anisotropic approximation.

8.5 References

1. A. Gavezzotti, *Synlett*, 2002, 201.

2. G. A. Jeffrey and W. Saenger, *Hydrogen bonding in Biological Structures*, Springer, Berlin, 1991.

3.. D. Sutor, *Nature*, 1962, **68**, 195..

4. a) G. R. Desiraju, *Acc. Chem. Res.*, 1991, **24**, 290; b) T. Steiner, *Chem. Commun.*, 1997, 727.

5. G. R. Desiraju, *J. Chem. Soc., Chem. Commun.*, 1990, 454.

6. T. Steiner, *J. Chem. Soc., Chem. Commun.*, 1994, 101.

7. T. Steiner, *J. Chem. Soc., Chem. Commun.*, 1995, 95.

8. D. Philp and J. M. A. Robinson, *J. Chem. Soc., Perkin Trans. 2*, 1998, 1643.

9. G. R. Desiraju, *Angew. Chem. Int. Ed. Engl.*, 1995, **34**, 2311.

10. a) P. J. Langley, J. Hulliger, R. Thaimattam and G. R. Desiraju, *New J. Chem.*, 1998, 1307; b) J. M. A. Robinson, D. Philp, B. M. Kariuki and K. D. M. Harris, *Chem. Commun.*, 1999, 329.

11. H. C. Wiess, D. Blaser, R. Boese, B. M. Doughan and M. M. Haley, *Chem. Commun.*, 1997, 1703.

12. H.-C. Wiess, R. Boese, H. L. Smith and M. M. Haley, *Chem. Commun.*, 1997, 2403.

13. J. M .A. Robinson, B. M. Kariuki, K. D. M. Harris and D. Philp, *J. Chem. Soc., Perkin Trans. 2*, 1998, 2459.

14. T. X. Neenan and G. M. Whitesides, *J. Org. Chem*, 1988, **53**, 2489.

15. a) H. M. Yamamoto, J. Yamarua, and R. Kato, *J. Am. Chem. Soc.*, 1998, **120**, 5905; b) H. M. Yamamoto, R. Maeda, J.-I. Yamaura and R. Kato, *J. Mater. Chem.*, 2001, **11**, 1034.

16. F. H. Allen, O. Kennard, D. G. Watson, L. Brammer, A. G. Orpen and R. J. Taylor, *J. Chem. Soc., Perkin Trans. 2*, 1987, S1.

17. R. S. Rowland and R. Taylor, *J. Phys. Chem.*, 1996, **100**, 7384.

Chapter 9

Conclusions and Suggestions for Further Work

The thesis has presented work concerning the effect of fluorine substitution on the structural and optical properties of several conjugated molecular materials. A series of 1-halogeno-4-(pentafluorophenylethynyl)benzene and 1-halogeno-4-(phenylethynyl)tetrafluorobenzene derivatives have been synthesized, by homogeneous palladium-catalyzed Sonogashira cross-coupling except in the case of 1-chloro-4-(phenylethynyl)tetrafluorobenzene, which was synthesized by organolithium chemistry. The crystal structures of all the compounds except 1-chloro-4-(phenylethynyl)tetrafluorobenzene and 1-fluoro-4-(pentafluorophenylethynyl)benzene have been solved from single-crystal X-ray diffraction data, which revealed them to have a variety of molecular packing arrangements. In most cases, the packing can be largely attributed to intermolecular halogen-halogen interactions or arene-perfluoroarene interactions, as in 1-chloro-4-(pentafluorophenyl-ethynyl)benzene, which is the first crystal structure of a compound that contains a halogen atom other than fluorine, in which arene-perfluoroarene stacking is present. It was not possible to grow crystals of 1-chloro-4-(phenylethynyl)tetrafluorobenzene and 1-fluoro-4-(pentafluorophenyl-ethynyl)benzene suitable for single-crystal X-ray diffraction, although these compounds may be suitable for X-ray powder diffraction and subsequent solution by the Rietveldt method.

It has been shown that both hexafluorobenzene and octafluoronaphthalene can form 1:1 arene-perfluoroarene complexes with several fused-ring polyaromatic hydrocarbons. Their crystal structures have been solved from single-crystal X-ray diffraction data and shown to be composed of infinite columns of alternating, approximately parallel perfluoroarene and polyaromatic molecules. This arrangement is very similar to those observed for other arene-perfluoroarene complexes, and has been attributed to the arene-perfluoroarene interaction. The fact that the perfluoroarenes and the polyaromatics are of substantially different molecular geometries demonstrates the general utility of the arene-perfluoroarene interaction as an intermolecular interaction that appears to be relatively insensitive to molecular geometry. *Ab initio* density functional calculations have been performed on several of the hexafluorobenzene complexes and the minimized energy structures have been shown to be almost identical to the crystal structures. The fact that these calculations do not model van der Waals interactions very well suggests that the energy of interaction must be predominantly due to electrostatics, in contrast to recent reports on similar complexes, which suggested that the arene-perfluoroarene interaction was primarily van der Waals in nature.

It appears from preliminary differential scanning calorimetry measurements that several of the complexes with octafluoronaphthalene show interesting phase behaviour. Samples have been sent to the group of Prof. C. Viney, for analysis by transmission polarised light microscopy, in order to establish the presence of any discotic liquid crystal mesophases. Although not reported in this thesis, similar binary complexes have been obtained between octafluoronaphthalene and 1-fluoronaphthalene, 1,8-diaminonaphthalene, acenaphthene and tetrathiafulvalene, and their crystal structures have also been shown by single crystal X-ray crystallography to consist of infinite columns of alternating molecules. This further demonstrates that the arene-

perfluorarene interaction appears to be fairly insensitive to substituents in these systems. On the basis of these conclusions, it should be possible in theory to obtain binary complexes of octafluoronaphthalene with many other substituted aromatic compounds. It should also be possible to prepare complexes of the known compounds perfluoroanthracene and perfluorotriphenylene with all of these polyaromatic hydrocarbons. It is to be expected that the complexes will all be composed of infinite stacks of alternating perfluoroarene and hydrocarbon components. Although a sample of perfluoroanthracene has been obtained, it requires purification by preperative high-performance liquid chromatography.

A number of compounds belonging to a series of selectively fluorinated bis(phenylethynyl)tolans, containing perfluorinated and non-fluorinated phenyl groups have been synthesized from several tolan-based precursors via palladium-catalyzed Sonogashira cross-coupling methodology. Although attempts were made to synthesize the remaining members of the series, these compounds could not be obtained as analytically pure samples. Further analysis by mass spectrometry revealed the presence of peaks corresponding to the butadiyne derivatives formed from the oxidative homo-coupling of two terminal alkynes. In the absence of air, these can only be formed either during the initiation step of the catalytic cycle or as a by-product of hydrodehalogenation. If it is the former that is responsible, it should be possible to prevent it by using a palladium(0) catalyst.

The compounds are observed to absorb in the UV range 336 - 342nm. These values are directly comparable to the absorptions for similarly fluorinated 1,4-bis(phenylethynyl)benzene derivatives which suggests that an effective conjugation length of 3-4 repeat units is applicable for these phenylene

ethynylene systems. However, their extinction co-efficients are an order of magnitude larger than those of the bis(phenylethynyl)benzenes. As expected, the bis(phenylethynyl)tolans are observed to be highly fluorescent even in very low concentrations. Their fluorescence maxima are in the UV range 372 – 410 nm, although there is considerable fluorescence in the blue region of the visible spectrum. Although the emission maxima do vary slightly, there appears to be no obvious correlation between emission maxima and the fluorine substitution pattern. It would also be of interest to determine the fluorescence lifetimes and quantum yields, for these compounds.

It would be of particular interest if the crystal structures of some of the compounds could be obtained. This could potentially reveal the presence of arene-perfluoroarene stacking, and possibly the formation of brickwall motifs as in 4,4'-bis(pentafluorostyry)stilbene. However, the growth of crystals suitable for single-crystal diffraction has been hampered by the fact that most of them are obtained as microcrystalline powders. Only 1-phenylethynyl-4-(4-phenylethynyltetrafluorophenylethynyl)tetrafluorobenzene shows any degree of crystallinity. However, small needles of 1-phenylethynyl-4-(4-phenylethynyl-phenylethynyl)tetrafluorobenzene have been obtained via sublimation *in vacuo* in a sealed tube at high temperature, although these were also unsuitable for single X-ray diffraction. However, the compounds may be suitable for powder X-ray diffraction particularly as their rigid rod-like nature should facilitate their structure solution by Rietveldt methods. It is to be expected that the compounds will show thermotropic calamatic liquid crystalline mesophases at high temperature as they all have axial ratios in excess of 4.30. Samples are to be submitted to the group of Prof C. Viney for analysis by transmission polarised light microscopy.

Higher-order homologues of these selective fluorinated phenylene ethynylene oligomers could be synthesized via similar methods. However, they would be almost certainly be very insoluble in all solvents and therefore very difficult to separate from the catalyst residues. However, long-chain alkyoxy groups could be used as substituents to impart solubility. It is relatively facile to add these substituents to the para position of terminal perfluorinated phenyl rings, through the use of base catalysed nucleophilic aromatic substitution by long-chain alcohols.

A potentially very interesting project would attempt to combine the two central topics of this thesis through the synthesis and crystal structure solution of several selectively fluorinated phenylene-ethynylene molecules containing polyaromatic moieties. Work has begun in this area with the synthesis of 1-(pentafluorophenyl-ethynyl)naphthalene. The crystal structure of the this compound has been solved from single-crystal X-ray diffraction data, and although it has not yet been fully refined, preliminary indications suggests that it is composed of infinite stacks of parallel molecules in a head-to-tail arrangement, allowing an arene-perfluoroarene stacking motif, similar to that of (phenylethynl)pentafluorobenzene. Attempts are currently being made to grow diffraction quality crystals of 9-(pentafluorophenylethynyl)anthracene and 9,10-bis(pentafluorophenylethynyl)anthracene, in the hope that they will show similar arene-perfluoroarene stacking arrangements.